# Neurocognitive mechanisms of body dysmorphic disorder

Gillian Grennan

A dissertation

submitted in partial fulfillment of the

requirements for the degree of

Doctor of Philosophy

University of Washington

2026

Reading Committee:

Angela Fang, Chair

Sheri J. Y. Mizumori

Scott O. Murray

Program Authorized to Offer Degree:

Neuroscience

University of Washington

**Abstract**

Neurocognitive mechanisms of body dysmorphic disorder

Gillian Grennan

Chair of the Supervisory Committee:

Angela Fang

Department of Psychology

Body dysmorphic disorder (BDD) is a severe psychiatric condition characterized by intrusive preoccupation with perceived appearance flaws, compulsive checking behaviors, and profound functional impairment. Despite its prevalence and clinical burden, the neurocognitive mechanisms that generate and sustain this disorder remain incompletely understood. This dissertation aims to advance the neurobiological model of BDD across three empirical chapters, each targeting a distinct but interrelated level of analysis: neuromodulation of attentional bias, effective connectivity within visual-affective circuits, and early-stage spatial frequency processing. The first chapter utilizes computational modeling methods to discern latent cognitive parameters of decision making during a Modified Posner task. Using drift diffusion modeling, we show distinction between individuals with BDD and healthy controls in measures of attentional bias toward threat. The second chapter highlights a study in which we employed dynamic causal modeling (DCM) of fMRI data acquired during a fearful face viewing paradigm to characterize effective connectivity within BDD's fear-processing network. We identify distinct aberrant connectivities underlying passive-threat viewing in BDD: heightened feedforward connectivity between the amygdala-mOFC, reduced feedback connectivity between the amygdala-pulvinar, and heightened within-FFA connectivity in individuals with BDD compared to healthy controls. These findings implicate amplified secondary affective appraisal of threatening social stimuli, impaired attentional modulation via thalamic feedback, and over-engagement of the ventral visual steam as circuit-level features of BDD's heightened threat sensitivity that underlies symptoms. The third and final chapter attempted to

characterize mechanisms underlying the perceptual distortion that characterizes BDD. We employed a multimodal paradigm spanning both behavioral and neural measures of spatial frequency processing. We found that individuals with BDD showed significantly reduced behavioral contrast sensitivity to low-spatial frequency stimuli and correspondingly reduced activation in bilateral middle temporal (MT) area, relative to healthy controls. These findings provide the first evidence of a bottom-up sensory deficit in magnocellular stream processing in BDD, extending prior accounts of a local-over-global perceptual imbalance beyond top-down attentional mechanisms. Taken together, these findings converge on an integrated neurocognitive model of BDD in which a bottom-up spatial frequency processing deficit, dysregulation of amygdala-centered threat circuit connectivity, and heightened selective attention to threat may be mutually reinforcing to generate and sustain symptoms in BDD.

Table of contents

**Acknowledgements** **7**
**Introduction** **9**
1. Body dysmorphic disorder 9
1.1. Clinical Presentation and Epidemiology. 9
1.2. Nosological position: BDD within the OC-Spectrum 10
2. The Current Neurobiological Model of BDD 11
2.1 Cortico-striato-thalamo-cortical circuitry 11
2.2 Visual processing abnormalities. 12
2.3. Attentional biases, threat processing, and the role of the amygdala. 13
3. Aims and Structure of the Present Dissertation 14
References 16
**Applying a drift diffusion model to test the effect of oxytocin on attentional biases in body dysmorphic disorder** **23**
Foreword 24
Introduction 24
Methods 27
Results 33
Discussion 38
References 42
Supplemental Materials 48
**Effective connectivity in cortical and subcortical visual fear processing networks during fearful face viewing in body dysmorphic disorder** **52**
Foreword 54
Introduction 54
Methods 58
Results 66
Discussion 71
References 76
Supplementary Materials 93
**Aberrant visual processing in body dysmorphic disorder** **99**
Introduction 101
Methods and Materials 104
Results 119
Demographics 119
Behavioral results 121
fMRI results 126
Discussion 132

References 138
**Conclusion** **148**
1. Summary of empirical findings 148
1.1 Chapter one: attentional bias and oxytocinergic modulation 148
1.2 Chapter two: effective connectivity in visual fear-processing networks 149
1.3 Chapter three: low-spatial frequency processing deficits and their significance 150
2. Toward an integrated neurocognitive model of BDD 151
3. Clinical implications 152
4. Limitations and future directions 153
5. Concluding remarks 153
References 155

# Acknowledgements

Thank you to my mentor, Angela Fang, for your help and support over the past 5 years, for championing our ‘no-committee’, and for showcasing the incredible translational science that is possible through collaboration and a steadfast commitment to helping patients get better.

To Drs. Scott Murray, Jamie Feusner, John Pyles, Kelly Chang, and Andrea Stocco, thank you for your countless hours of mentorship. I am still in awe that I got to learn from scientists I admire so much. Your dedication to my education and research, through no obligation of your own, has made this body of work possible.

To the entire CoNNeCT Lab but especially Emily Iannazzi, Yuchen Zhao, Maggie Sarkisova, Randhara Kotuwelle. Thank you for your friendship, solidarity, and for making it possible to go on 8+ vacations a year. I truly couldn’t have done a single part of this program without you.

To my grandparents, Joan and Norman Bounanno, for their fierce belief in the promise of education, which they diligently instilled into my mother, who in turn, instilled the belief into me.

To my dear friends, near and far, thank you for the dinner parties, camping trips, lake days, ski runs, DJ sets, and for flying across the country just to sit on the couch and talk. Because of you all, every day is filled with laughter and joy and I couldn’t be luckier.

To my partner, Jaz, thank you for building us such a magical life. Every day is a good day because I get to spend it with you. Also, thank you for letting me adopt a puppy while writing this dissertation.

To my family, who I owe everything. Thank you to Patty, for being my first and forever friend, for role-modeling what it’s like to trust your own decisions and abilities. To my dad, for giving me much-needed perspective; somehow everything felt much easier with your voice in my head saying “this isn’t life or death, it’s a conference submission”. To my mom, for sending

me to every science camp the Poulsbo Parks and Recreation had to offer, for somehow managing to take care of two kids, a farm, a full-time job, and still finding time to help me with my science fair poster. You are a complete tour-de-force, and this degree is for you. You three have showcased the self-assurance and fulfillment that comes from working at something you enjoy and trying your very best. One step closer to the family farm-to-table!

# Introduction

## 1. Body dysmorphic disorder

### 1.1. Clinical Presentation and Epidemiology.

Body dysmorphic disorder (BDD) is a severe and debilitating psychiatric condition defined by persistent, intrusive preoccupation with perceived defects or flaws in physical appearance (American Psychiatric Association, 2013). Appearance concerns are absent or negligible to an outside observer but for the patient are associated with marked distress and compulsive repetitive behaviors such as mirror checking, excessive grooming, skin picking, reassurance seeking, or camouflaging. Of note, preoccupation and behaviors associated with the appearance concerns can consume several hours per day and profoundly impair occupational, academic, and interpersonal functioning. Preoccupations most commonly target the skin, hair, and nose, though any body area may become the focus of concern (Bjornsson et al., 2010; Buhlmann et al., 2010).

Epidemiological surveys estimate a point prevalence of approximately 1.7-2.4% in the general adult population, with higher rates observed in dermatology and cosmetic surgery settings (Veale et al., 2016). The disorder typically has its onset in early adolescence and often follows a chronic, unremitting course when left without adequate treatment (Bjornsson et al., 2010; Buhlmann et al., 2010; Krebs et al., 2025; Schieber et al., 2015; Veale et al., 2016). Of note, BDD is associated with markedly elevated rates of suicidal ideation and attempts, among the highest of any psychiatric disorder (Pellegrini et al., 2021; PHILLIPS & DIAZ, 1997; Rautio et al., 2024). Despite this burden, BDD remains widely underdiagnosed, in large part because patients conceal their symptoms due to shame and fear of being regarded as vain (Jassi & Krebs, 2023). Understanding

the neurocognitive mechanisms that initiate and sustain this disorder is both a scientific and clinical imperative.

### 1.2. Nosological position: BDD within the OC-Spectrum

DSM-5 and its text revision locate BDD within the Obsessive-Compulsive and Related Disorders (OCRD) chapter, reflecting its phenomenological, neurobiological, and treatment-response overlap with obsessive-compulsive disorder (OCD) (American Psychiatric Association, 2013; Phillips et al., 2010). Like OCD, BDD is characterized by intrusive, ego-dystonic cognitions that are temporarily relieved, but ultimately maintained, by compulsive behaviors. Both disorders show preferential response to serotonin reuptake inhibitors (SRIs) and cognitive-behavioral therapy (Castle et al., 2021; National Collaborating Centre for Mental Health (UK), 2006; Phillips & Hollander, 2008; Pittenger & Bloch, 2014). Neurobiologically, both disorders implicate dysregulation within cortico-striato-thalamo-cortical (CSTC) circuits, particularly orbitofrontal cortex (OFC)-striatal loops, and show overlapping structural and functional neuroimaging abnormalities. Shared endophenotypes including cognitive inflexibility, inhibitory control deficits, and elevated experiential avoidance further support a common neurobiological substrate (Chamberlain et al., 2005; Wilson et al., 2014).

Nevertheless, BDD is distinguished from OCD by several features that point to additional or partially distinct neural mechanisms. Most notably, BDD is uniquely characterized by profound disturbances in visual perception, particularly in the processing of appearance-relevant information (Diaz-Fong & Feusner, 2024; Virgili et al., 2024). This has prompted researchers to propose that, superimposed upon CSTC dysregulation, BDD involves specific aberrations in visual processing pathways that generate distorted internal representations of physical appearance, a neurobiological

signature that differentiates BDD from other OCRDs and that is elaborated on throughout the present dissertation.

BDD also exhibits clinically meaningful overlap with anorexia nervosa (AN), a disorder similarly defined by distorted body image and appearance-driven compulsive behaviors (Hartmann et al., 2013). Both disorders share a predominant onset in adolescence, a female preponderance in clinical samples, severely impaired quality of life, high chronicity, and resistance to standard treatments (Grant & Phillips, 2004; Hartmann et al., 2013). Neurobiologically, AN and BDD show convergent abnormalities in visual processing, including altered spatial frequency use and atypical face perception, as well as overlapping fronto-striatal circuit dysfunction (Li et al., 2015). This convergence suggests that distorted body image across these disorders may share common perceptual and neural mechanisms, and that findings from BDD may have broader relevance to the neuroscience of body image psychopathology.

## 2. The Current Neurobiological Model of BDD

### 2.1 Cortico-striato-thalamo-cortical circuitry

The prevailing neurobiological model of BDD implicates dysfunction within two interacting neural systems: the CSTC circuits, mediating repetitive behavior and cognitive rigidity, and the visual processing network, mediating the perception of appearance-relevant stimuli (Grace et al., 2017; Virgili et al., 2024). The CSTC circuits link prefrontal cortex, particularly the OFC and dorsolateral prefrontal cortex (dlPFC), with the caudate nucleus, putamen, globus pallidus, and thalamus via direct (excitatory) and indirect (inhibitory) pathways. In OCD and related disorders, hyperactivity of the OCD-striatal direct pathway projections is thought to generate intrusive ideation and stereotyped behavioral responses that resist suppression by the indirect pathway

(Menzies et al., 2008). Structural neuroimaging in BDD has identified volume reductions in bilateral OFC and thalamus (Atmaca et al., 2010; Buchanan et al., 2014); although increases in left caudate nucleus volumes have also been identified (Rauch et al., 2003). Increased activity in the OFC and caudate have similarly been associated with BDD symptom severity (Feusner, Moody, et al., 2010). Only one study has investigated the dopaminergic system in individuals with BDD, observing significantly reduced dopamine receptor availability in striatal regions such as the caudate nucleus and putamen (Vulink et al., 2016). The therapeutic efficacy of SRIs in BDD, paralleling OCD, further implicates serotonergic modulation of dopamine systems within fronto-striatal circuits (Ipser et al., 2009; Pittenger & Bloch, 2014).

2.2 Visual processing abnormalities.

BDD is characterized by the presence of visual distortions, where patients focus on minor or perceived flaws in their appearance that are not noticeable to others (Monzani et al., 2013). This perceptual distortion is thought to be caused by deficits in visual information processing in BDD, a theory underscored by both behavioral and functional imaging findings (Virgili et al., 2024). Behaviorally, individuals with BDD display a selective recall of details compared to global features in both face and object processing (Deckersbach et al., 2000; Feusner, Moller, et al., 2010; Hanes, 1998; Jefferies et al., 2012; Monzani et al., 2013). Behavioral imbalances in global versus local processing may indicate imbalances in early visual systems in processing low-spatial frequency (LSF) versus high-spatial frequency (HSF) information. Indeed, prior research has shown that for images filtered to convey LSF information, individuals with BDD show hypoactivity within early visual regions such as the V1 (primary visual cortex) when compared to healthy controls ((Feusner et al., 2011; Feusner, Moody, et al., 2010). If LSF-mediated global processing is underutilized or underdeveloped in BDD, this could cause the overreliance on high-

detailed information and serve as a potential mechanistic driver of the perceptual distortion in BDD. It is yet unclear, however, if this is a mechanistic deficit underlying BDD neurobiology or if this is a downstream consequence of image evaluation from higher-order regions.

### 2.3. Attentional biases, threat processing, and the role of the amygdala.

A further component of BDD's neurocognitive profile concerns the selective allocation of attention to appearance-relevant and threatening stimuli. Eye-tracking studies demonstrate that individuals with BDD fixate preferentially on self-identified appearance defects and exhibit slower disengagement from appearance-related threat cues relative to healthy controls (Greenberg et al., 2014), although these findings are mixed (Kollei et al., 2017). These attentional biases are consistent with the broader theoretical model in which selective attention towards threat serves to maintain anxious preoccupation, as elaborated in cognitive models of anxiety disorders (Cisler & Koster, 2010; Mogg & Bradley, 2016). In BDD, however, attentional biases appear to interact specifically with the disorder's perceptual abnormalities: heightened attention to small facial details may both reflect and reinforce the HSF processing bias, as individuals selectively sample the fine-grained information that confirms their distorted appearance precepts.

Alongside visual processing deficits, BDD is characterized by heightened sensitivity to social threat, manifesting biases in the recognition of facial emotional expressions, particularly faces conveying negative emotions such as contempt, disgust, and anger (Buhlmann et al., 2004, 2011; Feusner, Bystritsky, et al., 2010; Grace et al., 2019; Jefferies et al., 2012; Toh et al., 2015, 2017). Few studies have examined emotional processing dysfunction in BDD using neuroimaging but findings have shown aberrations in the amygdala and prefrontal cortex (Borgers et al., 2022; Rangaprakash et al., 2018). This pattern is consistent with hyperactivity of amygdala-centered fear networks, which in anxiety disorders is thought to lower the threshold for detecting and responding

to social threat signals (Shin & Liberzon, 2010). In BDD specifically, the social-cognitive consequences of amygdala hyperreactivity are likely to reinforce appearance-related preoccupation and avoidance, creating a self-sustaining cycle of distress. However, the degree to which amygdala reactivity reflects intrinsic hyperexcitability versus inadequate top-down prefrontal regulation, or an aberrant weighting of visual input properties, remains an open question. Clarifying the directionality and strength of effective connectivity between subcortical threat-detection regions and visual and prefrontal areas during affective face processing is critical to specify the circuit-level architecture of threat sensitivity in BDD.

## 3. Aims and Structure of the Present Dissertation

This dissertation aims to advance the neurobiological model of BDD by investigating three interrelated neurocognitive mechanisms that the existing literature has implicated but not fully characterized. Each chapter addresses a distinct level of the model, from pharmacological modulation of attentional bias, to circuit-level visual-affective connectivity, to the fundamental perceptual processing of spatial frequency information. The dissertation serves to collectively illuminate how these mechanisms interact to maintain and perpetuate BDD symptoms.

The first empirical chapter investigates the role of attentional biases in BDD and their susceptibility to oxytonergic modulation. By decomposing behavioral responses into latent cognitive parameters, this work aims to disentangle subtle effects of attentional bias underlying emotional processing in BDD, ultimately highlighting novel methods to investigate this phenomenon.

The second empirical chapter examines effective connectivity within cortical and subcortical visual-affective networks during fearful face processing in BDD. By characterizing the directed flow of information between the amygdala, pulvinar, fusiform gyrus, and orbitofrontal cortex, this

chapter directly addresses the circuit-level organization of threat processing in BDD. Specifically, we test whether abnormalities reflect bottom-up amygdala hyperreactivity, impaired top-down prefrontal regulation, or a combination.

The third and final empirical chapter builds on this investigation into cortical organization in BDD but targeted in visual processing of low versus high spatial frequency information, ultimately trying to address where in the brain does BDD's characteristic perceptual distortion originate. By isolating the contributions of LSF and HSF information to visual processing at early and later stages of perceptual analysis, this chapter tests the hypothesis that BDD's detail-focused perceptual style reflects a fundamental bias in how visual information is sampled and weighted.

Together, these three chapters provide a multi-level mechanistic account of BDD that bridges neuromodulatory circuitry and perceptual levels of analysis. In doing so, they advance a more comprehensive neurobiological model of the disorder, clarify points of convergence and divergence with related disorders, and identify candidate mechanisms for targeted intervention.

# References

American Psychiatric Association. (2013). *Diagnostic and Statistical Manual of Mental Disorders* (Fifth Edition). American Psychiatric Association. https://doi.org/10.1176/appi.books.9780890425596

Atmaca, M., Bingol, I., Aydin, A., Yildirim, H., Okur, I., Yildirim, M. A., Mermi, O., & Gurok, M. G. (2010). Brain morphology of patients with body dysmorphic disorder. *Journal of Affective Disorders*, *123*(1–3), 258–263. https://doi.org/10.1016/j.jad.2009.08.012

Bjornsson, A. S., Didie, E. R., & Phillips, K. A. (2010). Body dysmorphic disorder. *Dialogues in Clinical Neuroscience*, *12*(2), 221–232. https://doi.org/10.31887/DCNS.2010.12.2/abjornsson

Borgers, T., Kürten, M., Kappelhoff, A., Enneking, V., Möllmann, A., Schulte, J., Klug, M., Leehr, E. J., Dohm, K., Grotegerd, D., Krause, P., Zwiky, E., Dannlowski, U., Buhlmann, U., & Redlich, R. (2022). Brain functional correlates of emotional face processing in body dysmorphic disorder. *Journal of Psychiatric Research*, *147*, 103–110. https://doi.org/10.1016/j.jpsychires.2022.01.007

Buchanan, B., Rossell, S., Maller, J. J., Toh, W. L., Brennan, S., & Castle, D. (2014). Regional brain volumes in body dysmorphic disorder compared to controls. *Australian & New Zealand Journal of Psychiatry*, *48*(7), 654–662. https://doi.org/10.1177/0004867413520253

Buhlmann, U., Glaesmer, H., Mewes, R., Fama, J. M., Wilhelm, S., Brähler, E., & Rief, W. (2010). Updates on the prevalence of body dysmorphic disorder: A population-based survey. *Psychiatry Research*, *178*(1), 171–175. https://doi.org/10.1016/j.psychres.2009.05.002

Buhlmann, U., Gleiß, M. J. L., Rupf, L., Zschenderlein, K., & Kathmann, N. (2011). Modifying emotion recognition deficits in body dysmorphic disorder: An experimental investigation. *Depression and Anxiety*, *28*(10), 924–931. https://doi.org/10.1002/da.20887

Buhlmann, U., McNally, R. J., Etcoff, N. L., Tuschen-Caffier, B., & Wilhelm, S. (2004). Emotion recognition deficits in body dysmorphic disorder. *Journal of Psychiatric Research*, *38*(2), 201–206. https://doi.org/10.1016/S0022-3956(03)00107-9

Castle, D., Beilharz, F., Phillips, K. A., Brakoulias, V., Drummond, L. M., Hollander, E., Ioannidis, K., Pallanti, S., Chamberlain, S. R., Rossell, S. L., Veale, D., Wilhelm, S., Van Ameringen, M., Dell'Osso, B., Menchon, J. M., & Fineberg, N. A. (2021). Body dysmorphic disorder: A treatment synthesis and consensus on behalf of the International College of Obsessive-Compulsive Spectrum Disorders and the Obsessive Compulsive and Related Disorders Network of the European College of Neuropsychopharmacology. *International Clinical Psychopharmacology*, *36*(2), 61–75. https://doi.org/10.1097/YIC.0000000000000342

Chamberlain, S. R., Blackwell, A. D., Fineberg, N. A., Robbins, T. W., & Sahakian, B. J. (2005). The neuropsychology of obsessive compulsive disorder: The importance of failures in cognitive and behavioural inhibition as candidate endophenotypic markers. *Neuroscience & Biobehavioral Reviews*, *29*(3), 399–419. https://doi.org/10.1016/j.neubiorev.2004.11.006

Cisler, J. M., & Koster, E. H. W. (2010). Mechanisms of attentional biases towards threat in anxiety disorders: An integrative review. *Clinical Psychology Review*, *30*(2), 203–216. https://doi.org/10.1016/j.cpr.2009.11.003

Deckersbach, T., Savage, C. R., Phillips, K. A., Wilhelm, S., Buhlmann, U., Rauch, S. L., Baer, L., & Jenike, M. A. (2000). Characteristics of memory dysfunction in body dysmorphic disorder. *Journal of the International Neuropsychological Society*, *6*(6), 673–681. https://doi.org/10.1017/S1355617700666055

Diaz-Fong, J. P., & Feusner, J. D. (2024). *Visual Perceptual Processing Abnormalities in Body Dysmorphic Disorder*. Springer Berlin Heidelberg. https://doi.org/10.1007/7854_2024_472

Feusner, J. D., Bystritsky, A., Hellemann, G., & Bookheimer, S. (2010). Impaired identity recognition of faces with emotional expressions in body dysmorphic disorder. *Psychiatry Research*, *179*(3), 318–323. https://doi.org/10.1016/j.psychres.2009.01.016

Feusner, J. D., Hembacher, E., Moller, H., & Moody, T. D. (2011). Abnormalities of object visual processing in body dysmorphic disorder. *Psychological Medicine*, *41*(11), 2385–2397. https://doi.org/10.1017/S0033291711000572

Feusner, J. D., Moller, H., Altstein, L., Sugar, C., Bookheimer, S., Yoon, J., & Hembacher, E. (2010). Inverted face processing in body dysmorphic disorder. *Journal of Psychiatric Research*, *44*(15), 1088–1094. https://doi.org/10.1016/j.jpsychires.2010.03.015

Feusner, J. D., Moody, T., Hembacher, E., Townsend, J., McKinley, M., Moller, H., & Bookheimer, S. (2010). Abnormalities of Visual Processing and Frontostriatal Systems in Body Dysmorphic Disorder. *Archives of General Psychiatry*, *67*(2), 197. https://doi.org/10.1001/archgenpsychiatry.2009.190

Grace, S. A., Labuschagne, I., Kaplan, R. A., & Rossell, S. L. (2017). The neurobiology of body dysmorphic disorder: A systematic review and theoretical model. *Neuroscience & Biobehavioral Reviews*, *83*, 83–96. https://doi.org/10.1016/j.neubiorev.2017.10.003

Grace, S. A., Toh, W. L., Buchanan, B., Castle, D. J., & Rossell, S. L. (2019). Impaired Recognition of Negative Facial Emotions in Body Dysmorphic Disorder. *Journal of the International Neuropsychological Society*, *25*(08), 884–889. https://doi.org/10.1017/S1355617719000419

Grant, J. E., & Phillips, K. A. (2004). Is anorexia nervosa a subtype of body dysmorphic disorder? Probably not, but read on. *Harvard Review of Psychiatry*, *12*(2), 123–126. https://doi.org/10.1080/10673220490447236

Greenberg, J. L., Reuman, L., Hartmann, A. S., Kasarskis, I., & Wilhelm, S. (2014). Visual hot spots: An eye tracking study of attention bias in body dysmorphic disorder. *Journal of Psychiatric Research*, *57*, 125–132. https://doi.org/10.1016/j.jpsychires.2014.06.015

Hanes, K. R. (1998). Neuropsychological performance in body dysmorphic disorder. *Journal of the International Neuropsychological Society*, *4*(2), 167–171. https://doi.org/10.1017/S1355617798001672

Hartmann, A. S., Greenberg, J. L., & Wilhelm, S. (2013). The relationship between anorexia nervosa and body dysmorphic disorder. *Clinical Psychology Review*, *33*(5), 675–685. https://doi.org/10.1016/j.cpr.2013.04.002

Ipser, J. C., Sander, C., & Stein, D. J. (2009). Pharmacotherapy and psychotherapy for body dysmorphic disorder. *Cochrane Database of Systematic Reviews*. https://doi.org/10.1002/14651858.CD005332.pub2

Jassi, A., & Krebs, G. (2023). Body Dysmorphic Disorder. *Psychiatric Clinics of North America*, *46*(1), 197–209. https://doi.org/10.1016/j.psc.2022.10.005

Jefferies, K., Laws, K. R., & Fineberg, N. A. (2012). Superior face recognition in Body Dysmorphic Disorder. *Journal of Obsessive-Compulsive and Related Disorders*, *1*(3), 175–179. https://doi.org/10.1016/j.jocrd.2012.03.002

Kollei, I., Horndasch, S., Erim, Y., & Martin, A. (2017). Visual selective attention in body dysmorphic disorder, bulimia nervosa and healthy controls. *Journal of Psychosomatic Research*, *92*, 26–33. https://doi.org/10.1016/j.jpsychores.2016.11.008

Krebs, G., Clark, B. R., Ford, T. J., & Stringaris, A. (2025). Epidemiology of Body Dysmorphic Disorder and Appearance Preoccupation in Youth: Prevalence, Comorbidity and Psychosocial Impairment. *Journal of the American Academy of Child & Adolescent Psychiatry*, *64*(1), 30–40. https://doi.org/10.1016/j.jaac.2024.01.017

Li, W., Lai, T. M., Bohon, C., Loo, S. K., McCurdy, D., Strober, M., Bookheimer, S., & Feusner, J. (2015). Anorexia nervosa and body dysmorphic disorder are associated with abnormalities in processing visual information. *Psychological Medicine*, *45*(10), 2111–2122. https://doi.org/10.1017/S0033291715000045

Menzies, L., Chamberlain, S. R., Laird, A. R., Thelen, S. M., Sahakian, B. J., & Bullmore, E. T. (2008). Integrating evidence from neuroimaging and neuropsychological studies of obsessive-compulsive disorder: The orbitofronto-striatal model revisited. *Neuroscience & Biobehavioral Reviews*, *32*(3), 525–549. https://doi.org/10.1016/j.neubiorev.2007.09.005

Mogg, K., & Bradley, B. P. (2016). Anxiety and attention to threat: Cognitive mechanisms and treatment with attention bias modification. *Behaviour Research and Therapy*, *87*, 76–108. https://doi.org/10.1016/j.brat.2016.08.001

Monzani, B., Krebs, G., Anson, M., Veale, D., & Mataix-Cols, D. (2013). Holistic versus detailed visual processing in body dysmorphic disorder: Testing the inversion, composite and global precedence effects. *Psychiatry Research*, *210*(3), 994–999. https://doi.org/10.1016/j.psychres.2013.08.009

National Collaborating Centre for Mental Health (UK). (2006). *Obsessive-Compulsive Disorder: Core Interventions in the Treatment of Obsessive-Compulsive Disorder and Body Dysmorphic Disorder*. British Psychological Society (UK). http://www.ncbi.nlm.nih.gov/books/NBK56458/

Pellegrini, L., Maietti, E., Rucci, P., Burato, S., Menchetti, M., Berardi, D., Maina, G., Fineberg, N. A., & Albert, U. (2021). Suicidality in patients with obsessive-compulsive and related disorders (OCRDs): A meta-analysis. *Comprehensive Psychiatry*, *108*, 152246. https://doi.org/10.1016/j.comppsych.2021.152246

PHILLIPS, K. A., & DIAZ, S. F. (1997). Gender Differences in Body Dysmorphic Disorder. *The Journal of Nervous and Mental Disease*, *185*(9). https://journals.lww.com/jonmd/Fulltext/1997/09000/Gender_Differences_in_Body_Dysmorphic_Disorder.6.aspx

Phillips, K. A., & Hollander, E. (2008). Treating body dysmorphic disorder with medication: Evidence, misconceptions, and a suggested approach. *Body Image*, *5*(1), 13–27. https://doi.org/10.1016/j.bodyim.2007.12.003

Phillips, K. A., Wilhelm, S., Koran, L. M., Didie, E. R., Fallon, B. A., Feusner, J., & Stein, D. J. (2010). Body dysmorphic disorder: Some key issues for DSM-V. *Depression and Anxiety*, *27*(6), 573–591. https://doi.org/10.1002/da.20709

Pittenger, C., & Bloch, M. H. (2014). Pharmacological Treatment of Obsessive-Compulsive Disorder. *Psychiatric Clinics of North America*, *37*(3), 375–391. https://doi.org/10.1016/j.psc.2014.05.006

Rangaprakash, D., Bohon, C., Lawrence, K. E., Moody, T., Morfini, F., Khalsa, S. S., Strober, M., & Feusner, J. D. (2018). Aberrant Dynamic Connectivity for Fear Processing in Anorexia Nervosa and Body Dysmorphic Disorder. *Frontiers in Psychiatry*, *9*, 273. https://doi.org/10.3389/fpsyt.2018.00273

Rauch, S. L., Phillips, K. A., Segal, E., Makris, N., Shin, L. M., Whalen, P. J., Jenike, M. A., Caviness, V. S., Jr, & Kennedy, D. N. (2003). A preliminary morphometric magnetic resonance imaging study of regional brain volumes in body dysmorphic disorder. *Psychiatry Research: Neuroimaging*, *122*(1), 13–19. https://doi.org/10.1016/S0925-4927(02)00117-8

Rautio, D., Isomura, K., Bjureberg, J., Rück, C., Lichtenstein, P., Larsson, H., Kuja-Halkola, R., Chang, Z., D'Onofrio, B. M., Brikell, I., Sidorchuk, A., Mataix-Cols, D., & Fernández De La Cruz, L. (2024). Intentional Self-Harm and Death by Suicide in Body Dysmorphic Disorder: A Nationwide Cohort Study. *Biological Psychiatry*, *96*(11), 868–875. https://doi.org/10.1016/j.biopsych.2024.05.006

Schieber, K., Kollei, I., De Zwaan, M., & Martin, A. (2015). Classification of body dysmorphic disorder—What is the advantage of the new DSM-5 criteria? *Journal of Psychosomatic Research*, *78*(3), 223–227. https://doi.org/10.1016/j.jpsychores.2015.01.002

Shin, L. M., & Liberzon, I. (2010). The neurocircuitry of fear, stress, and anxiety disorders. *Neuropsychopharmacology: Official Publication of the American College of Neuropsychopharmacology*, *35*(1), 169–191. https://doi.org/10.1038/npp.2009.83

Toh, W. L., Castle, D. J., & Rossell, S. L. (2015). Facial affect recognition in body dysmorphic disorder versus obsessive-compulsive disorder: An eye-tracking study. *Journal of Anxiety Disorders*, *35*, 49–59. https://doi.org/10.1016/j.janxdis.2015.08.003

Toh, W. L., Castle, D. J., & Rossell, S. L. (2017). Attentional biases in body dysmorphic disorder (BDD): Eye-tracking using the emotional Stroop task. *Comprehensive Psychiatry*, *74*, 151–161. https://doi.org/10.1016/j.comppsych.2017.01.014

Veale, D., Gledhill, L. J., Christodoulou, P., & Hodsoll, J. (2016). Body dysmorphic disorder in different settings: A systematic review and estimated weighted prevalence. *Body Image*, *18*, 168–186. https://doi.org/10.1016/j.bodyim.2016.07.003

Virgili, G., Neill, E., Enticott, P., Castle, D., & Rossell, S. L. (2024). A systematic review of visual processing in body dysmorphic disorder (BDD). *Psychiatry Research*, *339*, 116013. https://doi.org/10.1016/j.psychres.2024.116013

Vulink, N. C., Planting, R. S., Figee, M., Booij, J., & Denys, D. (2016). Reduced striatal dopamine D 2/3 receptor availability in Body Dysmorphic Disorder. *European Neuropsychopharmacology*, *26*(2), 350–356. https://doi.org/10.1016/j.euroneuro.2015.11.018

Wilson, A. C., Wilhelm, S., & Hartmann, A. S. (2014). Experiential avoidance in body dysmorphic disorder. *Body Image*, *11*(4), 380–383. https://doi.org/10.1016/j.bodyim.2014.06.006

# Applying a drift diffusion model to test the effect of oxytocin on attentional biases in body dysmorphic disorder

Gillian Grennan[1], Yuchen Zhao[1], Angela Fang[1]

[1]Department of Psychology, University of Washington

**Individuals with body dysmorphic disorder (BDD) display selective attentional biases to threat. Oxytocin is an endogenous neuropeptide proposed to modulate attentional salience in social contexts. We conducted a secondary analysis applying drift diffusion modeling (DDM) to test whether individuals with BDD would display an attentional bias to threat, and whether oxytocin would modulate this bias. Eighteen participants with BDD and 15 healthy controls received an oxytocin or placebo nasal spray during two study visits, in randomized order, and completed a modified spatial cueing paradigm. DDM successfully parsed distinct task components demonstrating a selective attentional bias to disgust versus neutral faces in BDD compared to controls in the placebo condition, and a main effect of oxytocin on exacerbating this bias across participants. There were no effects using mean reaction time measures. DDM may reveal insights about attentional biases by utilizing trial-wise information. Oxytocin may exacerbate attentional biases to threat in BDD.**

# Foreword

The following manuscript was published in the Journal of Obsessive Compulsive and Related Disorders on October 2, 2023. The full published works can be found via doi: 10.1016/j.jocrd.2023.100841

# Introduction

Body dysmorphic disorder (BDD) affects approximately 2 in every 100 individuals in the general population (Buhlmann et al., 2010; Koran et al., 2008) and is greatly understudied compared to disorders of equal prevalence. BDD is marked by excessive concerns with perceived flaws or abnormalities in one's appearance (APA, 2013). By definition, these flaws, typically centered on the nose, skin or hair, are generally not noticeable by others. Due to time-consuming intrusive thoughts about one's appearance, individuals with BDD often engage in compulsive rituals such as mirror checking, grooming, and comparing. According to cognitive behavioral models, these rituals negatively reinforce BDD symptoms and are linked with several cognitive and emotional processing mechanisms (Fang & Wilhelm, 2015). Selective attentional biases, in particular, have been a focus of research in BDD for the past two decades (Buhlmann et al., 2002a; Fang et al., 2022; Feusner et al., 2010; Greenberg et al., 2014; Grocholewski et al., 2012; Johnson et al., 2018; Kerwin et al., 2014). For example, eye-tracking studies utilizing depictions of the participant's own face have shown that individuals with BDD displayed heightened selective attention toward imagined defects on their own faces compared to healthy controls (Greenberg et al., 2014; Grocholewski et al., 2012), although another study found comparable attention to positive and negative features in one's own face in BDD versus controls (Kollei et al., 2017). Furthermore, studies using the Emotional Stroop Task have found that individuals with BDD displayed stronger Stroop interference for BDD-related negative words, compared to healthy controls (Toh et al., 2017), and for both positive and negative words in a non-threat-specific manner (Buhlmann et al., 2002a). Although studies have begun to show disrupted attentional mechanisms in BDD, more research is needed to better

understand the nature of these attentional biases and ways they can be manipulated. Modulating how information is attended to may have important implications for mitigating other cognitive biases occurring in later stages of processing, such as interpretive and memory biases, which have also been documented in BDD (Johnson et al., 2018).

One candidate pharmacologic approach for modulating attentional biases in BDD is intranasal oxytocin. Oxytocin is an endogenous neuropeptide, which has been examined as a promising treatment for psychiatric disorders characterized by deficits in social cognition, such as emotion recognition and social approach avoidance behavior (Guastella et al., 2009; Quintana et al., 2020). Oxytocin acts across a diverse array of brain regions, including higher order cortical areas, the limbic system, basal ganglia, and brainstem. Specifically, oxytocin has been shown to reduce amygdala activity in response to fearful faces in healthy males (Domes et al., 2007; Kirsch et al., 2005), although results differ in females (Domes et al., 2010). In social anxiety disorder (SAD), which has many shared features as BDD, oxytocin has also been shown to normalize hyperactive amygdala responses to fear (Labuschagne et al., 2010). The social salience theory of oxytocin proposes that its central effects (when delivered intranasally) are exerted through modulation of attention to social cues (Shamay-Tsoory & Abu-Akel, 2016). This effect is typically observed in response to threatening or negative social cues, but has similarly been observed for emotional cues in general, especially when the stimuli presented are unfamiliar to the participant (Leknes et al., 2013; Marieke et al., 2013). Thus, for a disorder like BDD which is characterized by selective attentional biases to social stimuli (e.g., faces), oxytocin may have clear therapeutic potential.

We previously examined attentional biases to social threat cues in BDD using a modified spatial cueing paradigm as part of a larger study testing the effect of intranasal oxytocin on modulating social cognition (Fang et al., 2019). Based on the literature on attentional biases in anxiety disorders (Amir et al., 2003; Bar Haim et al., 2007), which are closely related to BDD, we expected that in the placebo condition, individuals with BDD would show an attentional bias toward disgust faces (as these faces would be perceived as threatening), as well as a disengagement bias from disgust faces (which would be reflected in longer reaction times in trials requiring disengaging attention from disgust faces). Based on previous

literature on oxytocin's effects on attention in clinical samples (Fang et al., 2014; Kim et al., 2014), we also expected that oxytocin would modulate these biases in BDD compared to healthy controls. Contrary to these hypotheses, our previous analysis using mean reaction times for calculating attentional bias scores yielded non-significant differences between how individuals with BDD and healthy controls responded to threat and no effect of oxytocin (Beatty et al., 2019). A limitation of our approach was the use of group averaged reaction time measures, which may not be sensitive to trial-by-trial variability in responses.

To address this limitation, we turned to computational models, which aim to parse apart different components of a cognitive process by exploiting intra-individual variability in reaction times and have been recently applied to examine attentional biases in clinical disorders (Haller et al., 2021; Price et al., 2019). Specifically, drift diffusion models have been recently popularized as a way to discern different psychophysical components that underlie binary decision tasks in the cognitive bias literature (Bowen et al., 2016; Dietel et al., 2021; Jublie et al., 2022; Klaur et al., 2007; Myers et al., 2022; Price et al., 2019; Thompson et al., 2020; van Ravenzwaaij et al., 2012; White et al., 2017). A drift diffusion model (DDM) models a binary choice task decision through the continuous random walk process, assuming that the participant, when presented with two choices, will accumulate information continuously until one of two decision thresholds is met. Within psychological paradigms, DDMs are useful for separating the binary decision process into distinct parameters with cognitive interpretations. A DDM utilizes an individual's trial-level distribution of reaction times and accuracies to specify a set of parameters that provides an optimal fit to an individual's empirical reaction time/accuracy distribution. These parameters include: (1) *v*, or "drift rate", which represents a participant's cognitive speed or efficiency, and the quality of information being accumulated during the decision process; (2) *z*, or "decision starting point", which represents starting bias towards one of the two possible decisions; (3) *a*, or "decisional threshold", which serves as a measure of the amount of information needed to make a decision; (4) *t0*, or "extradecisional component", which is representative of the time taken by all processes not directly related to the decision-making process, such as stimulus encoding, preparing and executing a motor response, or orienting to the

presented target (Voss et al., 2004). Typically, DDM analyses are applied to understand decision-related parameters such as drift, decision starting point, or decisional threshold. For attentional bias paradigms, since the decision itself is incidental to the attentional orienting processes of interest, the strength of DDM in this context is the ability to separate these decision-related parameters from the extradecisional component, *t0*, to potentially expose a purer behavioral measure of attention (Price et al., 2019). This can be done by calculating the extradecisional component separately for emotionally evocative versus neutral cues to derive a cleaner index of attentional bias that removes cognitive processes related to decision-making.

We therefore sought to conduct a secondary analysis of the oxytocin dataset to examine whether DDM would provide more precise and sensitive measures of attentional bias. We hypothesized that in the placebo condition, individuals with BDD would show an attentional bias to disgust versus neutral faces based on the *t0* parameter. As oxytocin has been shown to modulate attentional biases, we also hypothesized that oxytocin would mitigate any group differences in *t0* compared to placebo.

# Methods

**Participants**

Adult healthy controls and participants with BDD according to DSM-IV-TR criteria were recruited using advertisements within the local community and online. Participants with BDD were additionally recruited from a BDD specialty outpatient program. All participants were excluded if they reported a history of nasal pathology (recurrent nosebleeds, hypophysectomy, atrophic rhinitis), frequent cigarette smoking (≥15 cigarettes per day), active suicidal or homicidal ideation, endocrine diseases such as untreated thyroid disease and diabetes, systemic steroid

or hormone use (except oral contraception), pregnancy, or serious medical illnesses such as cardiovascular disease, seizures, etc. Participants were similarly excluded if they met diagnostic criteria for schizophrenia, psychotic disorder, bipolar disorder, or substance dependence/abuse. Participants with BDD were deemed eligible if they met criteria for principal BDD based on the Structured Clinical Interview for DSM-IV (SCID; First et al., 2002). Healthy control participants did not have any current psychiatric illness. Female participants were deemed eligible if they were taking low-dose oral contraception (<50 mcg daily dose of ethinyl estradiol) and eligible women attended drug administration visits only during the active phase of their oral contraceptive (i.e., not during the placebo week). Female participants using multiphasic contraceptives ($n$ = 4, 31% of female participants) were on the same dose of ethinyl estradiol for drug administration visits. These conditions served to mitigate possible confounds such as an effect of estrogen on endogenous oxytocin or differences in oxytocin levels based on menstrual phase (Salonia et al., 2005). All participants provided written informed consent prior to any study procedures. The original study protocol was approved by the Partners Human Research Committee and registered through Clinicaltrials.gov (NCT02671266).

**Measures**

**Clinical Characterization of BDD.** In addition to the SCID interview, the Yale-Brown Obsessive-Compulsive Scale Modified for BDD (BDD-YBOCS; Phillips et al., 1997) and Brown Assessment of Beliefs Scale (BABS; Eisen et al., 1998) were administered by a PhD psychologist or doctoral candidate with expertise in BDD to assess BDD symptom severity and insight, respectively. Participants also completed the self-report Depression Anxiety and Stress Scale (DASS; Lovibond & Lovibond, 1995). In

the current sample, the reliability of the BDD-YBOCS and BABS in BDD participants were acceptable (BDD-YBOCS Cronbach's  = 0.61; BABS Cronbach's  = 0.72). The DASS Depression subscale had strong internal consistency (Cronbach's  = 0.87 for the full sample).

**Modified Posner Task.** The Modified Posner Task (Posner, 1980; Posner et al., 1980) was used to assess attentional biases to emotionally salient cues (e.g., face stimuli depicting disgust, neutral, or happy expressions). The Posner Task is a spatial cueing paradigm, which included 360 trials in total over the course of 10 minutes. On each trial, participants were presented with a fixation cross in the center of a computer screen for 500 ms with two white frames on the top and bottom. Participants were instructed to direct their attention to the fixation cross. Next, a face cue was presented inside one of the white frames (either top or bottom) while the other frame remained empty. The face cue remained on screen for 500 ms and was immediately followed by a target letter "E" or "F" presented in the center of one of the frames. Trials in which the target letter appeared in the same frame as the face cue reflecting attentional "engagement" mechanisms were deemed "validly-cued" trials, while trials in which the target letter appeared in the opposite frame as the face cue reflecting attentional "disengagement" mechanisms were labeled "invalidly-cued" trials. Participants were instructed to indicate as quickly and accurately as possible by clicking the left/right mouse button whether the displayed target was an "E" or an "F". The face cue presented prior to presentation of the target letter consisted of equal numbers (64 trials) of neutral, disgust, and happy facial expressions. All faces used as cues were selected from the Ekman standardized face set. Similarly, there were equal numbers of valid and invalidly-cued trials (180 trials). Trial types (both face cue type and valid or invalidly-cued trial types) were pseudo-randomized with equal number of valid/invalid trial types for each face cue (32 trials) and this stimulus presentation order was kept consistent across subjects. See Figure 1 for visualization of task paradigm.

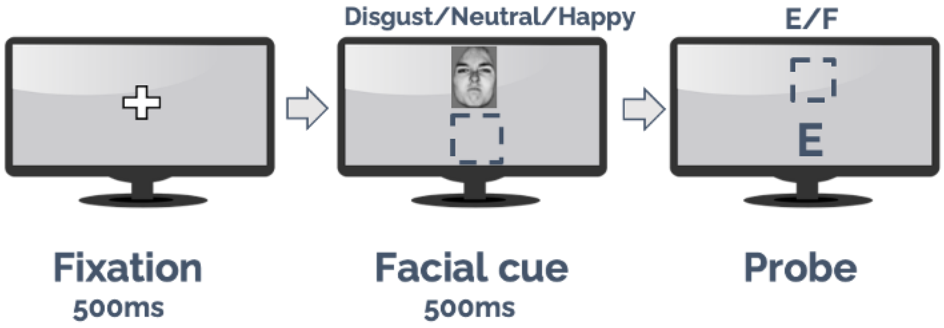


Figure 1. Example trial within the Modified Posner Task (Posner, 1980; Posner et al., 1980). In a given trial, participants were presented with a fixation cross in the center of a computer screen for 500 ms with two white frames on the top and bottom with instructions to fixate on the center cue. A face cue was then presented in either the top or bottom half of the screen for 500 ms while the opposite half remained empty. The face cue immediately followed by a target letter "E" or "F" presented in the center of one of the frames and the participant was instructed to indicate whether the target letter was an "E" or an "F" as quickly as possible. The above schematic represents an invalidly-cued disgust trial, in which the target letter appeared in the opposite frame as the disgust face cue, while a validly-cued trial (not pictured) consists of target letters appearing in the same frame as the previously displayed facial cue. The facial cues consisted of pseudo-randomized emotion types: disgust, neutral, and happy faces.

**Procedure**

Participants underwent three study visits. Urine pregnancy tests were administered to all female participants at the beginning of each study visit to confirm absence of pregnancy and assessment of eligibility. During visit one, participants were further screened for diagnostic and medical eligibility. Each participant similarly partook in a history and physical examination conducted by a study nurse at the Translational Clinical Research Center to assess medical exclusion criteria.

Participants underwent a randomized, double-blind, placebo-controlled, within-subjects crossover design for their two drug administration visits. These visits were separated by a minimum 1-week washout

period and eligible participants were instructed to avoid alcohol, caffeine, and nicotine for 24 hours leading up to the study visit. Each of the drug administration visits began with assessment of vital signs conducted by a nurse. Oxytocin (24 IU) and placebo were self-administered in metered dose spray bottles by the participant in the presence of a nurse. Using a standardized administration protocol, participants were instructed to inhale three sprays per nostril (4 IU oxytocin per spray) which represents the typical dosage in single-session experimental studies that utilize intranasal oxytocin (Quintana et al., 2021). The nasal sprays (Syntocinon® nasal spray; Novartis, Basel, Switzerland) and matched placebo sprays (containing the same ingredients minus the active peptide) were purchased from a pharmacy in Switzerland under an Investigational New Drug (#124112) application from the Food and Drug Administration. Participants were assessed approximately 20 minutes after administration for adverse events using a symptom checklist. Those who experienced adverse events were monitored and symptoms were confirmed to have resolved before the visit ended. The MGH Research Pharmacy randomized the order of nasal sprays allowing study staff and participants to be blind to the drug condition. After completing all experimental procedures, participants were asked to report whether they believed they received the active drug or placebo, the degree of certainty they had to this belief and reasons why. Approximately 45 minutes after administration, participants began the experimental tasks including the Modified Posner Task. Results for several of these tasks, as well as drug-related adverse events and assessment of the blind, have been reported elsewhere (Fang et al., 2019). In brief, adverse events were equally likely to be reported for oxytocin and placebo, and participants were not able to distinguish between oxytocin and placebo nasal sprays.

**Data Preparation and Analysis Overview**

**Drift Diffusion Model.** Each participant's individual reaction time/accuracy distribution was fitted with a DDM to parse apart distinct components of task performance. Models were fitted to the data using the *fast-dm-v30.2* software (Voss & Voss, 2007) and model fits were verified through the Kolmogorov-Smirnov method; commands used and data preparation steps are detailed in the supplementary materials.

Trials were separated by stimulus type (happy, neutral, or disgust face) and cue type (invalid or valid) prior to model fitting. Outlier trials with reaction times greater than three standard deviations from the mean reaction time across subjects were removed prior to model fitting (1.19% of trials removed). With this, a stimulus- and cue-specific DDM was created for each individual, outputting optimized DDM parameters: extradecisional time (*t0*), drift rate (*v*), and decisional separation (*a*). Inter-trial variability in extradecisional time (*st0*), drift rate (*sv*), and starting point (*sz*) were all set to 0. Voss and colleagues suggest setting decisional starting point (*zr*) to 0.5 (0.5**a* or halfway between the two decisional thresholds), assuming no intrinsic decisional bias towards a correct/incorrect response as we can assume that the participants will display no starting bias towards a correct (upper decisional threshold) or incorrect (lower decisional threshold) decision (Lerche & Voss, 2016; Voss & Voss, 2007). Percentage of contaminants was set to 0. Simulations (see Supplement) verified that the DDM was able to accurately reproduce realistic reaction time/accuracy distributions given the estimated parameters with the current number of trials per condition and relative error rates.

**Bias Scores.** Reaction time (RT) bias was calculated using the following calculation: RT bias = [(mean RT of invalid – valid disgust trials) – (mean RT of invalid – valid neutral trials)]. In contrast to other indices commonly drawn from the Posner task which treat engagement and disengagement scores separately and assume that differences in RT between threat trials and neutral trials stem only from attentional allocation to visuospatial information, this reflects a summative attentional bias measure that takes into account the confound of RT slowing in response to threat for anxious individuals (Clarke et al., 2013; Mogg et al., 2008). In other words, a delay in RT in response to disgust faces on valid trials (relative to neutral faces) may obscure a real bias involving faster detection of threat (e.g., an attentional engagement bias toward disgust cues) and a delay in RT in response to disgust faces on invalid trials (relative to neutral faces) may appear to amplify a disengagement bias that is not actually present. By including both engagement and disengagement scores in a single measure of attentional bias, we are able to account for RT slowing in response to disgust faces and avoid the assumption that valid and invalid trials provide pure measures of attentional allocation. Accordingly, DDM parameters were derived using

the same approach of calculating a summative bias index. The extradecisional time parameter (*t0*) from each stimulus condition (happy, neutral, or disgust faces) was used to generate attentional bias scores (*t0* bias) for disgust compared to neutral trials using the following calculation: *t0* bias = [(*t0*_invalid – *t0*_valid disgust) – (*t0*_invalid – *t0* valid neutral). The equivalent *t0* bias metric was calculated for happy trials. Drift bias (*v* bias) and bias of decisional separation (*a* bias) were similarly calculated. Greater *t0* bias scores reflected a greater attentional preference for disgust compared to neutral faces.

**Statistical Analyses.** All bias indices (RT bias, *t0* bias, *v* bias, and *a* bias) were analyzed with separate linear mixed models using maximum likelihood. For Aim 1, participant group (BDD or healthy control) was entered as a fixed effect in the placebo condition only, with visit as a repeated random effect and visit order as a covariate, and *t0* bias (for disgust versus neutral) as the dependent variable. For Aim 2, drug condition (oxytocin or placebo) as well as a group*drug interaction term were additionally entered as fixed effects in the model with *t0* bias (for disgust versus neutral) as the dependent variable. Results are reported based on a compound symmetry variance-covariance structure. *A priori* hypotheses regarding effects on *t0* bias for disgust cues only were tested at alpha = 0.05, whereas exploratory analyses regarding effects of oxytocin on *t0* bias (for happy faces only) and on *v* bias and *a* bias (for disgust and happy cues) were tested at alpha = 0.05/5 tests = 0.01. All analyses were conducted in SPSS 24.

# Results

### Demographic and Clinical Characteristics

Table 1 displays demographic and clinical characteristics of the sample.

| | **BDD Patients (n = 18)** | **Healthy Controls (n = 15)** | ***p*-value** |
|---|---|---|---|
| Age (SD) | 25.44 (4.18) | 27.75 (10.52) | 0.40 |

| | | | |
|---|---|---|---|
| Sex (% Female) | 38.90% | 37.50% | 0.93 |
| Race (% Caucasian) | 66.66% | 62.50% | 0.64 |
| Ethnicity (% Hispanic) | 88.89% | 93.75% | 0.62 |
| Highest Education Level Completed | | | 0.85 |
| College Graduate (%) | 33.33% | 37.50% | |
| Post-graduate/Professional Degree (%) | 16.67% | 25.00% | |
| BDD-YBOCS (Mean, SD) | 25.00 (4.28) | NA | NA |
| BABS (Mean, SD) | 12.56 (4.09) | NA | NA |
| DASS-21 Depression Subscale (SD) | 4.94 (4.22) | 1.07 (1.49) | **p < 0.001** |

**Table 1.** *Participant Demographic and Clinical Characteristics*

**Model Fitting**

We observed a reasonably good fit of DDM to each participant's datasets across stimulus and cue types (Kolmogorov-Smirnov $p$ for all stimulus types: BDD group mean $p = 0.94 \pm 0.08$; HC group mean $p = 0.94 \pm 0.07$). We further verified model fit through visual inspection (See Supplementary Figure 2).

**Group Differences in Attentional Bias**

We initially investigated group differences in attentional bias by comparing differences in reaction time (i.e., RT bias) during invalidly-cued versus validly-cued disgust relative to invalidly-cued versus validly-cued neutral trials across participants in the placebo condition alone. Consistent with Beatty et al. (2019), we found no significant effects of participant group in RT bias ($F = 0.12$, $p = 0.73$). Calculated RT bias of disgust versus neutral trials for both participant groups can be seen in Figure 2A. Median accuracy

differences were not statistically tested across all participants, as we observed no change in median accuracy across patient groups, trial types, or drug conditions (all median accuracies = 1.0 ± 0.00). These results were sustained in comparing RT bias for happy versus neutral trials ($F = 0.52$, $p = 0.48$).

We utilized the optimized DDM parameters fit individually to each participant, trial type, and drug condition to parse components related to attentional orienting and decision-related processes. Our main hypothesis was regarding group differences in attentional bias to disgust versus neutral trials, which we tested in the placebo condition. We observed a significant difference in the *t0* bias between participants with BDD and healthy controls on disgust versus neutral trials ($F(1,31) = 5.89$, $p = 0.02$) with individuals with BDD displaying a higher *t0* bias (mean *t0* bias = 0.003 ± 0.04, 95% CI: [-0.07, 0.08]) compared to healthy controls (mean *t0* bias = -0.14 ± 0.04, 95% CI: [-0.23, -0.05]). Healthy controls displayed an attentional preference to neutral over disgust facial stimuli as represented by the negative summative *t0* bias measure, whereas participants with BDD displayed a slight attentional bias towards disgust over neutral, as represented by the positive summative *t0* bias measure. Calculated *t0* bias for disgust versus neutral trials for both participant groups can be seen in Figure 2B.

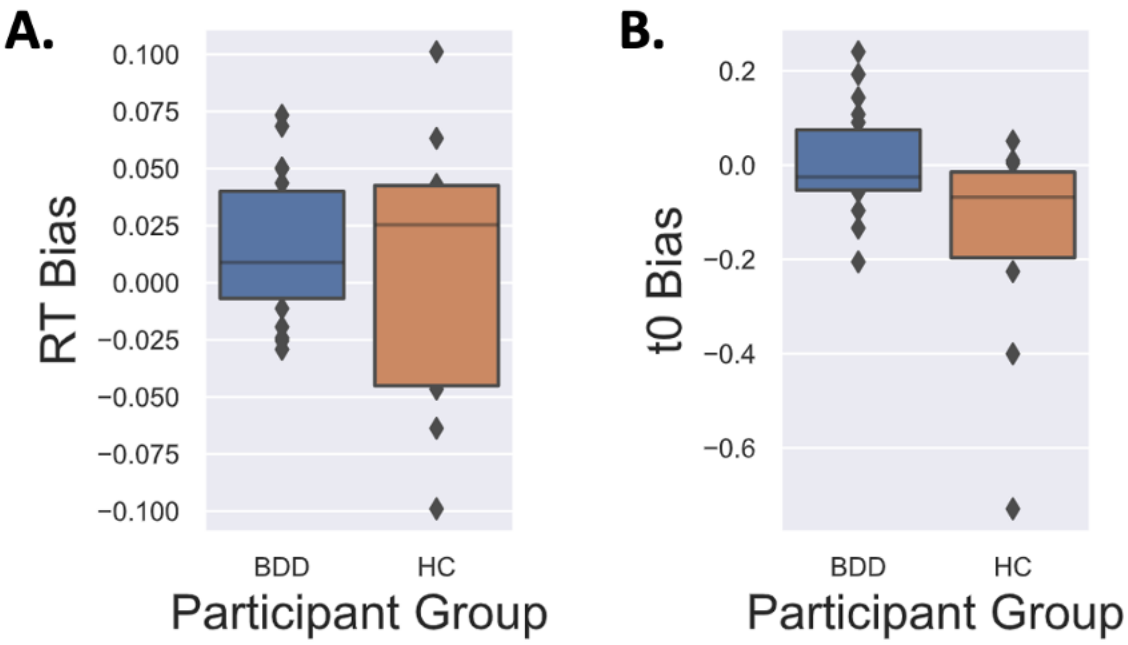

Figure 2. Mean RT bias for participants with BDD (in blue) and healthy controls (in orange) during disgust versus neutral trials (Figure 2A, left panel). Using mean reaction time to create our bias metric, we did not observe a significant main effect of group ($F = 0.122$, $p = 0.729$). Calculated *t0* bias for disgust versus neutral trials for participants with BDD (in blue) and healthy controls (in orange); we observed a significant main effect of group when comparing *t0* bias ($F = 5.893$, $p = 0.021$) with participants with BDD showing greater *t0* bias compared to healthy controls on disgust relative to neutral trials (Figure 2B, right panel).

**Effects of Oxytocin on Attentional Biases**

With regard to effects of oxytocin on attentional biases for disgust based on *t0*, we tested whether there was a significant interaction between participant group and drug condition in *t0* bias of disgust versus neutral trials. Our hypothesis was that oxytocin compared to placebo would mitigate group differences in attentional biases towards disgust by reducing the attentional bias for disgust in the BDD group. Contrary to our hypothesis, we did not observe a significant interaction of drug condition by participant group ($F(1,33.44) = 0.03$, $p = 0.86$). However, we did observe a significant main effect of group ($F(1,33.52) = 11.56$, $p = 0.002$) and a significant main effect of drug ($F(1,33.44) = 4.81$, $p = 0.04$). Participants with BDD displayed a higher *t0* bias for disgust versus neutral (mean *t0* bias = 0.04 ± 0.03, 95% CI: [-0.01, 0.09]), as compared to controls (mean *t0* bias = -0.09 ± 0.03, 95% CI: [-0.15, -0.03]), and those receiving oxytocin displayed a higher *t0* bias for disgust versus neutral (mean *t0* bias = 0.02 ± 0.03, 95% CI: [-0.04, 0.07]) relative to those receiving placebo (mean *t0* bias = -0.07 ± 0.03, 95% CI: [-0.12, -0.01]) across all participants.

**Exploratory Analyses**

We conducted exploratory analyses to examine effects of oxytocin on *t0* bias for happy versus neutral faces. There was no significant drug by participant group interaction ($F(1,32.78) = 2.43$, $p = 0.13$); however, there were marginal main effects of both participant group ($F(1,33.68) = 3.78$, $p = 0.06$) and

main effect of drug ($F(1,32.78) = 3.65$, $p = 0.07$). As in the comparison of disgust versus neutral trials, participants with BDD displayed increased *t0* bias preferentially towards happy versus neutral faces (in the placebo condition), an effect that was increased in both BDD and healthy control groups when receiving oxytocin compared to placebo.

We explored effects of oxytocin on other bias metrics (*a*, *v*) for all face types. For happy versus neutral trials, we did not observe a significant drug by participant group interaction (all $p$'s > 0.45). There were also no significant effects of group or drug in the *a* or *v* bias metrics (all $p$'s > 0.27). For disgust versus neutral faces, there was no significant drug by group interaction for *a* or *v* (all $p$'s > 0.66). There was a significant effect of group in the *a* metric ($F(1,33.35)= 7.48$, $p = 0.01$), driven by a lower *a* bias on disgust-neutral trials in BDD, as compared to healthy controls, although this effect was unexpected and did not survive corrections for multiple comparisons.

**Association Between Decisional Style Differences and BDD Symptom Severity**

As an exploratory analysis, we examined correlations between the calculated *t0* bias during disgust versus neutral trials in the placebo condition and the clinician-rated BDD-YBOCS as an indicator of symptom severity. We observed a significant positive association between *t0* bias of disgust versus neutral trials and BDD-YBOCS scores in patients with BDD using DASS depression scores as a covariate (Spearman r = 0.52, $p = 0.03$). A larger *t0* bias was associated with greater BDD symptom severity, as shown in Figure 3. In other words, the attentional bias towards disgust relative to neutral faces increases as symptom severity of BDD increases in individuals with BDD.

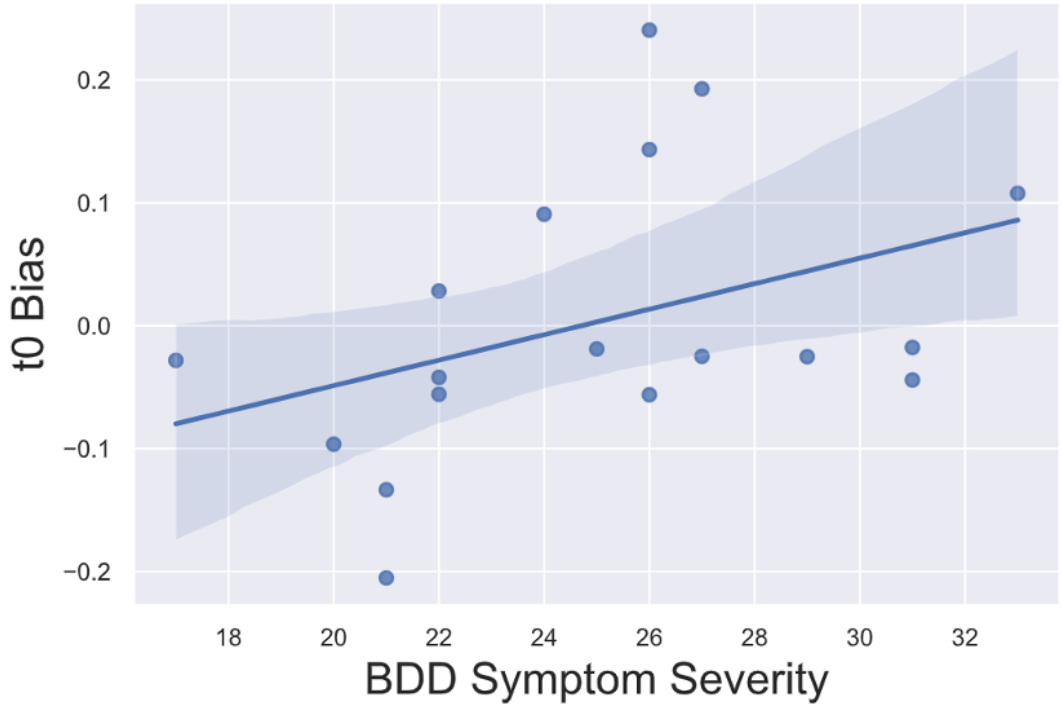


Figure 3. Linear regression plot with 95% confidence intervals showing the significant relationship between greater *t0* bias on disgust versus neutral trials during the placebo study visit and increasing patient symptom severity on the clinician-rated BDD-YBOCS with DASS depression scores as a covariate (Spearman $r = 0.52$, $p = 0.03$).

## Discussion

This secondary analysis of 18 participants with BDD and 15 healthy controls examined the effects of oxytocin on a DDM-derived attentional bias measure known as *t0* using a Modified Posner Task. In DDM, *t0* refers to an extradecisional parameter that includes attentional orienting to a target and is modeled separately from irrelevant decision-related features of task performance (e.g., determining whether the target was an "E" or an "F"). We therefore expected that *t0* would yield a cleaner behavioral measure of attentional bias to threat compared to average reaction time measures. We found that individuals with BDD and healthy controls displayed distinguishable *t0* patterns in the placebo condition.

Whereas healthy controls displayed an attentional preference for neutral versus disgust stimuli, those with BDD displayed the opposite pattern. Oxytocin modulated attentional biases, but in an unexpected manner, by increasing *t0* biases across both groups, rather than specifically for those with BDD. Thus, oxytocin did not appear to normalize attentional bias patterns for those with BDD, but rather worsened attentional biases to disgust faces for all participants.

This is the first study to apply DDM to examine cognitive mechanisms in BDD following several studies showing how DDM can isolate attention from decision-related components of widely-used task paradigms for measuring attentional bias (Naim et al., 2022; Price et al., 2019). Using DDM, we found that there was a significant group difference in the *t0* parameter within the placebo condition between individuals with BDD and healthy controls, driven by a preference for neutral stimuli (relative to disgust) in controls and a slight preference for disgust stimuli (relative to neutral) in BDD. Exploratory analyses with happy versus neutral faces revealed a similar pattern showing that individuals with BDD also displayed a small preference for happy faces. These findings join a larger growing body of research demonstrating selective attentional biases in BDD, even for face stimuli that do not include one's own face as has been typically investigated (Greenberg et al., 2014; Grocholewski et al., 2012; Kollei et al., 2017), although the current study did not test differences in attentional allocation to own versus others' faces. To calculate attentional bias, we used a summative measure including both attentional engagement and attentional disengagement processes given previous research showing that threat cues may be associated with reaction time delays and that engagement and disengagement measures from the Posner task are confounded by these threat-related delays (Clarke et al., 2013; Mogg et al., 2008). Thus, a strength of this measure was its ability to capture non-attentional responses to threat stimuli such as reaction time delays caused by behavioral freezing in anxious individuals. Based on cognitive theories of BDD, attentional biases for threat may act like a filter for making problematic interpretations of ambiguous social scenarios. They are also proposed to contribute to negative emotions and reliance on dysfunctional self-defeating coping strategies, such as excessive rituals and avoidance behavior (Buhlmann et al., 2002b; Wilhelm et al., 2010). Our findings therefore support a model of disgust (and

potentially happy) faces as being particularly salient for those with BDD and being linked to severity of symptoms.

Contrary to our hypothesis, intranasal oxytocin did not specifically modulate attentional biases for the BDD group, compared to healthy controls, by normalizing the bias for disgust that was found in the placebo condition. Rather, oxytocin elicited a main effect across all participants in a manner that exacerbated *t0* bias scores and worsened attentional bias to disgust across BDD and healthy control groups. This is consistent with studies showing that oxytocin may amplify maladaptive tendencies in clinical populations (for a review, see Olff et al., 2013), including BDD (Fang et al., 2019). However, our findings contrast with results from a meta-analysis examining effects of single dose oxytocin on threat processing, which found that oxytocin did not significantly impact attentional bias toward social or disorder-specific threat in healthy or clinical populations (Leppanen et al., 2018). Most of the studies included in the meta-analysis used the dot probe task to assess attentional bias and no studies applied computational modeling to examine task performance. It is possible that the application of DDM in combination with a within-subject design maximized power in the study to detect a main effect of drug, as low power and small sample sizes have been identified as major translational barriers for advancing oxytocin as a candidate therapeutic (Quintana et al., 2021; Walum et al., 2016). Our study needs to be replicated in much larger samples to confirm these findings and determine whether attachment or symptom severity may moderate the effects of oxytocin, as has been shown in previous studies. Although we caution the use of intranasal oxytocin in patients with BDD due to our observed effects, demonstration of moderated effects would suggest that there may be subgroups of individuals with BDD who may still benefit from oxytocin (Bartz et al., 2011; Fang et al., 2014; Fang et al., 2017). Conversely, recent work has explored social salience modulation due to administered oxytocin. Although some studies have indicated that oxytocin modulates attention biases towards positive emotional stimuli when compared against negative or neutral stimuli, several studies have found that administered oxytocin increases attention to emotional stimuli, regardless of valence (Leknes et al., 2013; Marieke et al., 2013; Shamay-Tsoory & Abu-Akel, 2016), especially when the stimuli are novel to the participant. This could explain

our finding of increased bias towards positive, as well as threatening, stimuli; however, these observed effects were only moderately significant. Further work is needed to explore bias differences across a greater range of emotional stimuli to confirm this effect. Additionally, exploring the effect of oxytocin on attention biases to emotional cues in BDD in concert with neuroimaging may elucidate the neurobiological mechanisms that oxytocin is acting upon. Future research may also examine the association between attentional biases and endogenous oxytocin in BDD, as one study reported greater endogenous serum oxytocin levels in BDD, which were associated with symptom severity (Fang et al., 2020).

An unexpected exploratory finding was that individuals with BDD, compared to healthy controls, displayed a lower *a* reflecting a lower decisional threshold for disgust-neutral trials. In other words, individuals with BDD needed less information to make a decision about the location of the target when the target was in the opposite location of a disgust or neutral cue. Although exploratory, we note how this differs from studies demonstrating greater conservativeness in decision making in obsessive compulsive disorder (Banca et al., 2015), which is highly comorbid with BDD. More research is needed to examine whether individuals with BDD display decisional impulsivity, which could make them vulnerable to greater suicidal ideation and substance use disorders.

Some limitations warrant mention. First, we elected to use a summative attentional bias measure to account for behavioral reaction time slowing in response to threat, which has been linked to anxious individuals; however, this is an imperfect measure of attentional bias as it assumes that reaction time slowing effects are additive with engagement and disengagement mechanisms (Mogg et al., 2008). Future work could adapt the task to display both threat and neutral cues in each trial (akin to the dot probe task) to account for the presence of threat in each trial, which would be a more ideal approach (Clarke et al., 2013). Computational analytical techniques, such as DDM as used here, could also be used in tandem with naturalistic estimates of attention bias such as with eye-tracking, which would enhance the ecological validity of the task paradigm used and parameters outputted. Second, we had a very modest sample size that limited statistical power in the study. Including a greater number of trials or repeated runs

on the task may enhance the reliability of the estimated parameters outputted by the DDM. Finally, the facial stimuli used in the study were not gender-matched to the participant or validated for attractiveness, which could both affect the way in which individuals with BDD exhibit attentional biases towards or against these faces. The stimuli also consisted entirely of white individuals, which limits the ecological validity of these findings. Future work utilizing facial stimuli in spatial cueing paradigms such as ours should address these confounds to increase the relevance and replicability of their findings.

In summary, this study showcased how computational models can be implemented in common attentional cueing tasks to examine core patterns of psychopathology in clinical populations that may be otherwise undetectable in conventional analyses using mean reaction time. As clinical research studies can often fall detriment to recruitment sparsity, easily implemented computational models, such as DDMs, allow us to optimally utilize all available data collected from niche patient samples and have large implications for replicability within the field.

# References

American Psychiatric Association. (2013). Diagnostic and statistical manual of mental disorders (5th ed.). Washington, DC: Author.

Amir, N., Elias, J., Klumpp, H., & Przeworski, A. (2003). Attentional bias to threat in social phobia: facilitated processing of threat or difficulty disengaging attention from threat? *Behav Res Ther, 41*(11), 1325-1335.

Banca, P., Vestergaard, M. D., Rankov, V., Baek, K., Mitchell, S., Lapa, T.,…Voon, V. (2015). Evidence accumulation in obsessive-compulsive disorder: the role of uncertainty and monetary reward on perceptual decision-making thresholds. *Neuropsychopharmacology 40*(5), 1192-1202.

Bar-Haim, Y., Lamy, D., Pergamin, L., Bakermans-Kranenburg, M. J., & van, I. M. H. (2007). Threat-related attentional bias in anxious and nonanxious individuals: a meta-analytic study. *Psychol Bull, 133*(1), 1-24.

Bartz, J., Simeon, D., Hamilton, H., Kim, S., Crystal, S., Braun, A.,…Hollander, E. (2011). Oxytocin can hinder trust and cooperation in borderline personality disorder. *Social Cognitive Affective Neuroscience, 6*(5), 556-563.

Beatty, C. C., Hoeppner, S., Smilansky, H., Lawson, E. A., Wilhelm, S., & Fang, A. (2019, November). Effect of intranasal oxytocin on modulating attentional bias in body dysmorphic disorder. Poster presented at the annual meeting of the Association for Behavioral and Cognitive Therapies, Atlanta, GA.

Bowen HJ, Spaniol J, Patel R, Voss A (2016) A Diffusion Model Analysis of Decision Biases Affecting Delayed Recognition of Emotional Stimuli. PLoS ONE 11(1): e0146769. https://doi.org/10.1371/journal.pone.0146769

Buhlmann, U., Glaesmer, H., Mewes, R., Fama, J. M., Wilhelm, S., Brahler, E., & Rief, W. (2010). Updates on the prevalence of body dysmorphic disorder: a population-based survey. *Psychiatry Research, 178*(1), 171-175.

Buhlmann, U., McNally, R. J., Wilhelm, S., & Florin, I. (2002a). Selective processing of emotional information in body dysmorphic disorder. *Journal of Anxiety Disorders, 16,* 289-298.

Buhlmann, U., Wilhelm, S., McNally, R. J., Tuschen-Caffier, B., Baer, L., & Jenike, M. A. (2002b). Interpretive biases for ambiguous information in body dysmorphic disorder. *CNS Spectrums, 7,* 435-443.

Clark, P. J. F., MacLeod, C., & Guastella, A. J. (2013). Assessing the role of spatial engagement and disengagement of attention in anxiety-linked attentional bias: a critique of current paradigms and suggestions for future research directions. *Anxiety, Stress, & Coping, 26,* 1-19.

Dietel, F.A., Möllmann, A., Bürkner, PC. *et al.* (2021). Interpretation Bias Across Body Dysmorphic, Social Anxiety and Generalized Anxiety Disorder—A Multilevel, Diffusion Model Account. *Cogn Ther Res* **45**, 715–729.

Domes, G., Heinrichs, M., Glascher, J., Buchel, C., Braus, D. F., & Herpertz, S. C. (2007). Oxytocin attenuates amygdala responses to emotional faces regardless of valence. *Biological Psychiatry* *62*(10), 1187-1190.

Domes, G., Lischke, A., Berger, C., Grossmann, A., Hauenstein, K., Heinrichs, M., & Herpertz, S. C. (2010). Effects of intranasal oxytocin on emotional face processing in women. Psychoneuroendocrinology, 35, 83-93.

Eisen, J. L., Phillips, K. A., Baer, L., Beer, D. A., Atala, K. D., & Rasmussen, S. A. (1998). The brown assessment of beliefs scale: Reliability and validity. *American Journal of Psychiatry*, *155*(1), 102–108.

Fang, A., Baran, B., Beatty, C. C., Mosley, J., Feusner, J. D., Phan, K. L., Wilhelm, S., & Manoach, D. S. (2022). Maladaptive self-focused attention and default mode network connectivity: A transdiagnostic investigation across social anxiety disorder and body dysmorphic disorder. *Social Cognitive and Affective Neuroscience, 17*(7), 645-654.

Fang, A., Hoge, E. A., Heinrichs, M., & Hofmann, S. G. (2014). Attachment style moderates the effects of oxytocin on social behavior and cognition during social rejection: Applying an RDoC framework to social anxiety disorder. *Clinical Psychological Science, 2,* 740-747.

Fang, A., Jacoby, R. J., Beatty, C., Germine, L., Plessow, F., Wilhelm, S., & Lawson, E. A. (2020). Serum oxytocin levels are elevated in body dysmorphic disorder and related to severity of psychopathology. *Psychoneuroendocrinology, 113*, 104541.

Fang, A., Lawson, E. A., & Wilhelm, S. (2019). Intranasal oxytocin modulates higher-order social cognition in body dysmorphic disorder. *Depression and Anxiety, 36,* 153-161.

Fang, A., Treadway, M.T., & Hofmann, S. G. (2017). Working hard for oneself or others: Effects of oxytocin on reward motivation in social anxiety disorder. *Biol Psychology, 127,* 157-162.

Fang, A., & Wilhelm, S. (2015). Clinical features, cognitive biases, and treatment of body dysmorphic disorder. *Annual Review of Clinical Psychology, 11,* 187-212.

Feusner, J. D., Moller, H., Altstein, L., Sugar, C., Bookheimer, S., Yoon, J., & Hembacher, E. (2010). Inverted face processing in body dysmorphic disorder. *Journal of Psychiatric Research, 44,* 1088-1094.

First, M. B., Spitzer, R. L., Gibbon, M., & Williams, J. B. W. (2002). *Structured clinical interview for DSM-IV-TR Axis I Disorders, Research Version, Patient Edition (SCID-I/P)*. New York, NY: Biometrics Research.

Greenberg, J. L., Reuman, L., Hartmann, A. S., Kasarskis, I., & Wilhelm, S. (2014). Visual hot spots: an eye tracking study of attention bias in body dysmorphic disorder. *Journal of Psychiatric Research, 57,* 125-132.

Grocholewski, A., Kliem, S., & Heinrichs, N. (2012). Selective attention to imagined facial ugliness is specific to body dysmorphic disorder. *Body Image, 9,* 261-269.

Haller, S. P., Stoddard, J., Pagliaccio, D., Bui, H., MacGillivray, C., Jones, M., & Brotman, M. A. (2021). Computational modeling of attentional impairments in disruptive mood dysregulation and attention deficit/hyperactivity disorder. *Journal of the American Academy of Child and Adolescent Psychiatry, 60*, 637-645.

Jublie, A., & Kumar, D. (2022). Attentional Bias for Self-Face: Investigation using Drift Diffusion Modelling. *Proceedings of the Annual Meeting of the Cognitive Science Society*, 44. Retrieved from https://escholarship.org/uc/item/4596x01f

Kerwin, L., Hovav, S., Helleman, G., & Feusner, J. D. (2014). Impairment in local and global processing and set-shifting in body dysmorphic disorder. *Journal of Psychiatric Research, 57,* 41-50.

Kim, Y. R., Kim, C. H., Park, J. H., Pyo, J., & Treasure, J. (2014). The impact of intranasal oxytocin on attention to social emotional stimuli in patients with anorexia nervosa: a double blind within-subject cross-over experiment. *PLoS One, 9*(6), e90721.

Klauer, K. C., Voss, A., Schmitz, F., & Teige-Mocigemba, S. (2007). Process components of the implicit association test: a diffusion-model analysis. *Journal of Personality and Social Psychology, 93*(3), 353–368.

Kollei, I., Horndasch, S., Erim, Y., & Martin, A. (2017). Visual selective attention in body dysmorphic disorder, bulimiar nervosa and healthy controls. *Journal of Psychosomatic Research, 92,* 26-33.

Koran, L. M., Abujaoude, E., Large, M. D., & Serpe, R. T. (2008). The prevalence of body dysmorphic disorder in the United States adult population. *CNS Spectrums, 13*(4), 316-322.

Leknes, S., Wessberg, J., Ellingsen, D. M., Chelnokova, O., Olausson, H., & Laeng, B. (2013). Oxytocin enhances pupil dilation and sensitivity to 'hidden' emotional expressions. *Social cognitive and affective neuroscience*, *8*(7), 741–749. https://doi.org/10.1093/scan/nss062

Leppanen, J., Ng, K. W., Kim, Y. R., Tchanturia, K., & Treasure, J. (2018). Meta-analytic review of the effects of a single dose of intranasal oxytocin on threat processing in humans. *Journal of Affective Disorders, 225,* 167-179.

Lerche, V., & Voss, A. (2016). Model complexity in diffusion modeling: Benefits of making the model more parsimonious. *Frontiers in Psychology, 7,* 1324.

Lovibond, S.H. & Lovibond, P.F. (1995). *Manual for the Depression Anxiety Stress Scales*. (2nd. Ed.) Sydney: Psychology Foundation.

Marieke S. Tollenaar, Michaela Chatzimanoli, Nic J.A. van der Wee, Peter Putman. (2013). Enhanced orienting of attention in response to emotional gaze cues after oxytocin administration in healthy young men. *Psychoneuroendocrinology*, 38(9), 1797-1802.

Mogg, K., Holmes, A., Garner, M., & Bradley, B. P. (2008). Effects of threat cues on attentional shifting, disengagement and response slowing in anxious individuals. *Behaviour Research and Therapy, 46*(5), 656-667.

Myers, C. E., Interian, A., & Moustafa, A. A. (2022). A practical introduction to using the drift diffusion model of decision-making in cognitive psychology, neuroscience, and health sciences. *Frontiers in psychology*, *13*, 1039172. https://doi.org/10.3389/fpsyg.2022.1039172

Naim, R., Haller, S., Linke, J. O., Jaffe, A., Stoddard, J., Jones, M.,…Brotman, M. A. (2022). Context-dependent amygdala-prefrontal connectivity during the dot-probe task varies by irritability and attentional bias to angry faces. *Neuropsychopharmacology, 47,* 2283-2291.

Olff, M., Frijling, J. L., Kubzansky, L. D., Bradley, B., Ellenbogen, M. A., Cardoso, C.,… van Zuiden, M. (2013). The role of oxytocin in social bonding, stress regulation and mental health: an update on the moderating effects of context and interindividual differences. *Psychoneuroendocrinology, 38*(9), 1883-1894.

Phillips, K. A., Hollander, E., Rasmussen, S. A., Aronowitz, B. R., DeCaria, C., & Goodman, W. K. (1997). A severity rating scale for body dysmorphic dis- order: Development, reliability, and validity of a modified version of the Yale-Brown Obsessive Compulsive Scale. *Psychopharmacology Bulletin*, *33*(1), 17–22.

Price, R. B., Brown, V., & Siegle, G. J. (2019). Computational modeling applied to the dot-probe task yields improved reliability and mechanistic insights. *Biological Psychiatry, 85*, 606-612.

Quintana, D. S., Lischke, A., Grace, S., Scheele, D., Ma, Y., & Becker, B. (2021). Advances in the field of intranasal oxytocin research: lessons learned and future directions for clinical research. *Molecular Psychiatry, 26,* 80-91.

Salonia, A., Nappi, R. E., Pontillo, M., Daverio, R., Smeraldi, A., Briganti, A., Fabbri, F., Zanni, G., Rigatti, P., & Montorsi, F. (2005). Menstrual cycle-related changes in plasma oxytocin are relevant to normal sexual function in healthy women. *Hormones and Behavior, 47*(2), 164-169.

Thompson, A. and Steinbeis, N. (2021), Computational modelling of attentional bias towards threat in paediatric anxiety. Dev. Sci., 24: e13055.

Toh, W. L., Castle, D. J., & Rossell, S. L. (2017). Attentional biases in body dysmorphic disorder (BDD): Eye-tracking using the emotional Stroop task. *Comprehensive Psychiatry, 74*, 151-161.

van Ravenzwaaij, D., van der Maas, H. L. J., & Wagenmakers, E.-J. (2012). Optimal decision making in neural inhibition models. *Psychological Review, 119*(1), 201–215.

Voss, A., & Voss, J. (2007). Fast-dm: A free program for efficient diffusion model analysis. *Behavior Research Methods, 39,* 767-775.

Voss, A., Rothermund, K., & Voss, J. (2004). Interpreting the parameters of the diffusion model: An empirical validation. *Memory and Cognition, 32,* 1206-1220.

Walum, H., Waldman, I. D., & Young, L. J. (2016). Statistical and Methodological Considerations for the Interpretation of Intranasal Oxytocin Studies. *Biological Psychiatry, 79*(3), 251-257.

White, C.N., Servant, M. & Logan, G.D. (2018). Testing the validity of conflict drift-diffusion models for use in estimating cognitive processes: A parameter-recovery study. *Psychon Bull Rev* **25**, 286–301.

# Supplemental Materials

**Modified Posner Task Reliability Checks.**

We first aimed to verify the presence of exogenous attention effects during the modified Posner task, specifically whether the validity of the facial cue relative to the target letter location caused changes within reaction time. We isolated reaction time recorded from trials during the placebo condition for healthy control subjects. We found that as expected on all emotion types healthy controls showed on average longer RT on invalid compared to validly-cued trials (mean happy invalid-valid RT = 0.012 seconds +/- 0.004; mean neutral invalid-valid RT = 0.002 +/- 0.004, mean disgust invalid-valid RT = 0.013 +/- 0.004), although for each emotion type, we did not observe significant differences between invalid and validly-cued RT lengths (all $p$'s > 0.40). Further, we aimed to verify the split-half reliability

of the task across both participant groups, trial types and drug conditions. We observed a significant correlation between the first and second half trials of the task (Spearman $r = 0.55$, $p < .0001$) ensuring performance was similar across all participants for the entire duration of the task and could be subsequently used for DDM fitting and statistical analyses.

**Drift Diffusion Model (DDM) Specifications.**

A schematic of a randomly selected participant's estimated distribution provided from the fit DDM overlayed on their empirical response time/accuracy distribution can be seen in Supplementary Figure 1. In the current study, trials with reaction times greater than three standard deviations from the mean reaction time across subjects were removed prior to model fitting. Responses were coded as correct vs. incorrect. Response time distributions for correct and incorrect trials were consolidated for each participant and DDM was fit to each individual's data separately for each stimulus-type (disgust, happy, or neutral faces) and cue-type (invalid vs. validly cued trials). The extradecisional component (*t0*), decisional separation (*a*), drift rate (*v*), and differences in speed of response execution (*d*) were all allowed to fluctuate across trial conditions and were measured at the individual level. Due to low trial sizes per participant, inter-trial variability in extradecisional time (*st0*), drift rate (*sv*), and starting point (*sz*) were all set to 0 for each condition to minimize model assumptions. Decisional starting point (*zr*) was set to 0.5 (0.5**a* or halfway between the two decisional thresholds), assuming no intrinsic decisional bias towards a correct/incorrect response. Kolmogorov-smirnov was used as the estimation procedure. Based on recommendations from Voss and colleagues, the percentage of contaminants (*p*) was set to 0.

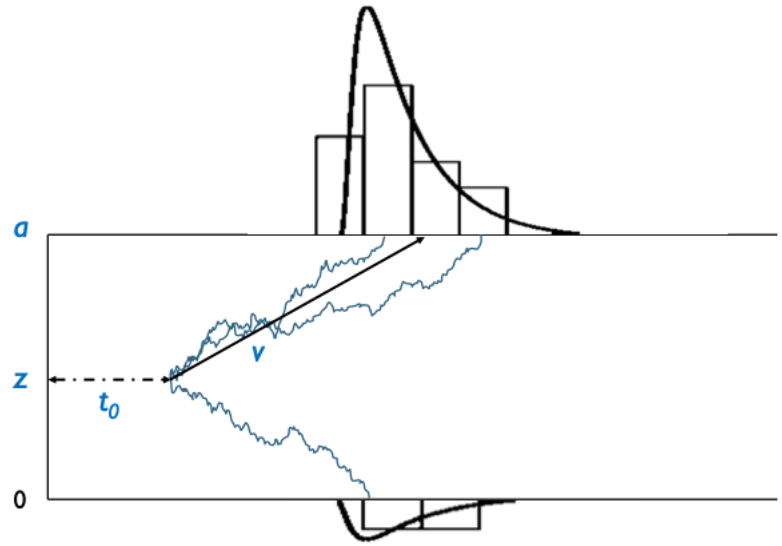


**Supplementary Figure 1.** Estimated DDM fit for a randomly selected participant during the placebo condition; response time distribution for correct trials can be seen above while incorrect trials can be seen below with the fit DDM probability density function overlayed in black. The DDM was fit using invalidly-cued disgust trials. Visual depictions of the outputted parameters (in blue) used for group comparisons can be seen in the prototypical DDM depiction (*a, z, t0, v*). Note, for our DDM fitting, we manually set *z* to 0.5**a* for all trials and subsequently did not perform group analyses on the *z* bias between trial types.

These model preferences were entered into the fast-dm software using the specifications below:

method ks

precision 3

set p 0

set zr 0.5

set sv 0

set szr 0

set st0 0

format RESPONSE TIME

Model fits were verified using the Kolmogorov-Smirnov test statistic and through visual inspection. See Supplementary Figure 2 below for all subjects' DDM fit to their empirical response time/accuracy distributions for invalidly-cued neutral trials during the placebo condition.

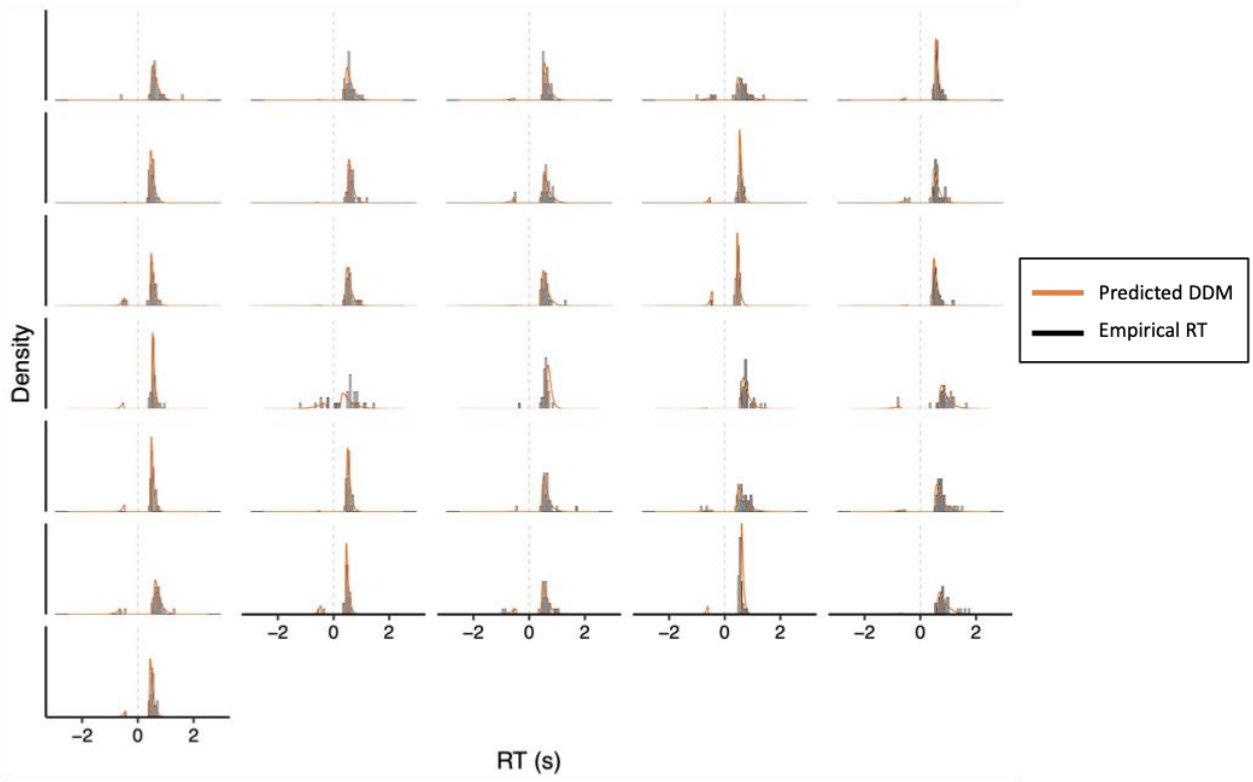


**Supplementary Figure 2.** Optimized DDM fit for all participants for invalidly-cued neutral face trials during the placebo drug condition. Fits estimated using all trial types (happy, disgust, neutral; invalid-cued, valid-cued) and drug conditions all provided statistically reasonable fits determined through Kolmogorov-Smirnov tests and further verified through visual inspection.

# Effective connectivity in cortical and subcortical visual fear processing networks during fearful face viewing in body dysmorphic disorder

Gillian Grennan BS[1], Angela Fang PhD[1], Andrea Stocco PhD[1], Qasim Bukhari PhD[2], Rangaprakash Deshpande PhD[3], Reza Tadayonnejad MD PhD[4-6], Jamie D. Feusner MD[7-9]

[1]Department of Psychology, University of Washington; Seattle WA

[2]McGovern Institute for Brain Research and Department of Brain and Cognitive Sciences, Massachusetts Institute of Technology; Cambridge, MA

[3]Massachusetts General Hospital; Cambridge, MA

[4]TMS Clinical and Research Service, Neuromodulation Division, Semel Institute for Neuroscience and Human Behavior at UCLA; Los Angeles California

[5]Department of Psychiatry and Biobehavioral Sciences, David Geffen School of Medicine at UCLA; Los Angeles, CA

[6]Division of the Humanities and Social Sciences, California Institute of Technology; Pasadena, CA

University of California at Los Angeles; Los Angeles CA

[7]Department of Psychiatry, University of Toronto; Toronto, Canada

[8]Centre for Addiction and Mental Health; Toronto, Canada

[9]Department of Women and Children's Health, Karolinska Hospital, Karolinska Institutet; Stockholm, Sweden

**Individuals with body dysmorphic disorder (BDD) demonstrate emotional processing biases; however, it is unclear whether differences are related to visual threat network dysfunction. Understanding neural connectivity patterns during visual processing**

**of threatening stimuli could provide insights into mechanisms that maintain BDD symptoms. Participants with BDD (n=32) and healthy controls (n=37) completed a fearful face processing task during fMRI. Using dynamic causal modeling, we compared effective connectivity between groups in connections among regions implicated in fearful face processing: the bilateral pulvinar, amygdala, fusiform face area and the medial orbitofrontal cortex (mOFC). We found through Bayesian model selection that both BDD and control groups were fit by the same connectivity model, with driving input of fearful faces to the pulvinar and amygdala and bidirectional connections between each region. Using parametric empirical bayes to test for group differences, we found significantly higher connectivity from the left amygdala to the left mOFC and within the left FFA as well as significantly reduced connectivity from the right amygdala to the right pulvinar in individuals with BDD. However, we observed no significant associations with body dysmorphic symptoms. BDD may be characterized by aberrations in the fearful face viewing network. Future studies could address whether these effects are specific to BDD or may also characterize other disorders with emotional face processing dysfunction.**

## Foreword

The following manuscript has been submitted for consideration at Scientific Reports.

## Introduction

Body dysmorphic disorder (BDD) is a relatively common and debilitating psychiatric disorder characterized by an obsessive focus on misperceived appearance defects that are generally not noticeable to others (1,2). BDD affects approximately 2% of the general population but is understudied compared to disorders of similar prevalence (3–5).

Individuals with BDD show deficits in emotional processing (6–9). Specifically, individuals with BDD misinterpret others' neutral-expression faces as angry, and angry faces as disgusted (7), and show attentional biases to faces with disgust expressions (10) compared with healthy controls. In addition, those with BDD are less accurate in recognizing angry, sad and neutral expressions, and slower in recognizing angry, happy, and neutral expressions than healthy controls (11).

Few studies have examined emotional processing dysfunction in BDD using fMRI, but both studies to date have found aberrations in the amygdala and prefrontal cortex (12,13). The amygdala is a central hub for detecting threat and processing emotionally salient stimuli, with higher responses to fearful stimuli (14,15).

Rangaprakash and colleagues found that during repeated exposure to fearful faces, healthy controls displayed increasingly enhanced connectivity from the amygdala to the medial prefrontal cortex (mPFC), typical of a temporal limbic response to fearful stimuli (16). Notably, this temporal pattern was absent in participants with BDD, implying impaired feedforward frontolimbic connectivity during fear processing (13). In contrast, another study reported increased amygdala-PFC connectivity and greater left amygdala activity in BDD during negative

face viewing (12). Other work has shown right amygdala hyperactivity in response to spatially filtered faces (15), while a similar task found right amygdala hypoconnectivity, reinforcing the amygdala's role in face-processing dysfunction in BDD (16). Further, extensive research on anxiety disorders in general have shown heightened amygdala responses and altered amygdala-PFC coupling during fearful face processing (17,18). Similarly, increased amygdala reactivity to negative stimuli and reduced top-down regulatory influence from the PFC has been shown in depressed individuals (19,20).

More broadly, anxiety has been linked to altered visual processing (21,22) with evidence suggesting that disrupted amygdala-visual cortex connectivity may lead to hypervigilance and heightened responses to emotional stimuli (19,20). Similarly, connectivity between subcortical stimulus processing regions responsible for rapid, coarse visual threat detection such as the pulvinar (23–25) have been shown to have altered connectivity with the PFC in depressed individuals (26). It is yet untested whether emotional processing deficits evident in BDD are mechanistically influenced by interactions between the limbic system and early visual processing regions.

In addition, individuals with BDD show abnormalities in visual processing, particularly a bias toward high-detail over holistic processing. Neuroimaging studies have found increased activity in temporal and ventral visual stream (VVS) regions compared to healthy controls (12,27,28). Notably, greater VVS activity during own-face viewing has been linked to higher anxiety symptoms in BDD (29). Functional specificity of the fusiform face area (FFA), a key VVS region involved in face processing, has been shown to predicted by its structural connectivity to limbic regions such as the amygdala in both humans (30) and non-human primates (31). The FFA has shown increased connectivity with the amygdala (12) and higher-order regions like the

precuneus and posterior cingulate cortex (32) in BDD. It remains unclear whether FFA differences in BDD stem from heightened feedforward input from VVS regions or from intrinsic FFA dysfunction. Additionally, pulvinar hyperconnectivity with higher-order visual areas has been observed in social anxiety disorder (33), suggesting that this bottom-up hyperactivity drives overstimulation in higher-order visual or emotional regulation areas, potentially contributing to altered emotional stimulus processing.

Emotional processing dysfunction in BDD may also involve abnormalities in emotion regulation regions such as the orbitofrontal cortex (OFC). The OFC receives input on emotional salience from the amygdala and VVS, and is associated with emotion regulation involved in stimulus processing by way of feedback connections to the amygdala and pulvinar (34). Connectivity between the amygdala and OFC has been confirmed through structural imaging studies showing both feedforward and feedback connections are conserved across both humans and non-human primates (35–37). The OFC has been implicated in related disorders such as obsessive-compulsive disorder (OCD) (38–42), with OFC hyperactivity (43,44) and amygdala-OFC altered effectivity connectivity (45–47) proposed as mechanisms underlying compulsive behaviors. Additionally, OFC and amygdala volume reductions have been shown in individuals with OCD compared to controls (48). Despite the overlap in compulsive symptoms between OCD and BDD, research on the OFC's role in BDD remains limited. Existing studies have linked OFC self-connectivity to BDD symptom severity (39), and found left OFC hyperactivity during own- versus other-face viewing in BDD (49). However, the specific role of OFC-limbic connectivity in emotion regulation during face processing in BDD is still unknown.

Understanding the influence of fear and anxiety on connectivity patterns during visual processing may provide insights into neural mechanisms that maintain BDD symptoms. Toward

this end, we applied dynamic causal modeling in both BDD participants and healthy controls to investigate differences in effective connectivity between regions involved in fearful face processing, including the pulvinar, amygdala, FFA, and an emotion regulation area, the mOFC (50–52). Our hypotheses regarding individual connections were as follows:

(1) Based on prior evidence, we expected that individuals with BDD would show higher arousal to fearful faces compared to healthy controls (6–8). We hypothesized that heightened arousal would manifest in increased feedforward connectivity from the pulvinar to the amygdala, from the amygdala to the FFA, and bidirectional connectivity between the pulvinar and FFA. This is supported by prior evidence in both humans and animals showing that the pulvinar has a key role in amplifying evoked responses in higher order regions and that this coupling between regions will strengthen in response to the emotional valence of the stimuli (34,53); there has also been evidence of pulvinar overfeeding in social anxiety disorder (33), which is closely related to BDD.

(2) We hypothesized that individuals with BDD would display increased feedback connectivity from the FFA to the amygdala compared to controls, due to prior evidence showing greater reliance of the VVS, which includes the FFA, in BDD (12,27–29), as well as observed hyperconnectivity of the FFA and amygdala during negative face viewing (12).

(3) We hypothesized hyperconnectivity from the amygdala to the mOFC based on prior evidence showing hyperactivity (49) of the OFC in BDD populations in tandem with evidence from OCD studies showing hyperconnectivity of the amygdala and prefrontal cortex (38,39).

(4) We hypothesized hypoconnectivity from the mOFC to the amygdala due to diminished inhibitory function of the mOFC on the amygdala in the BDD group based on prior evidence showing dysfunctional emotion regulation in BDD (7,54,55) and differential feedback connectivity between the mOFC and amygdala in social anxiety disorder (56,57).

(5) We further postulated that all differences in connectivities involving the amygdala would be lateralized to the right side, as the right amygdala has been shown to mediate fear processing (58).

(6) Finally, we hypothesized that observed aberrant effective connectivity estimates in the BDD group would be significantly associated with BDD symptom severity.

## Methods

### Participants

We recruited healthy controls (n = 37) and participants with BDD (n = 32); both groups were comprised of unmedicated, young individuals (aged 15–38 years). The study was approved by the UCLA Institutional Review Board and all research was performed in accordance with relevant guidelines and regulations. Informed consent from all participants ≥18 years old was obtained prior to study procedures, and parental consent plus participant assent was obtained for those under 18. Participants were right-handed as determined by the Edinburgh Handedness Inventory

(59) and were deemed to have normal, or corrected-to-normal, visual acuity as tested with a Snellen eye chart. Participants were recruited from the community as well as through advertisements in outpatient clinics at UCLA and in the greater Los Angeles area.

Participants with BDD were excluded if they met diagnostic criteria for any lifetime psychotic or bipolar disorder, current substance dependence/abuse, and/or if they had active suicidal or homicidal ideation or self-injurious behavior. Participants were similarly excluded if they had a lifetime neurological disorder, current pregnancy, any medical illness that could affect cerebral metabolism, or current treatment with cognitive behavior therapy (CBT). Participants were required to be free from psychoactive medications for at least 8 weeks prior to entering the study. One participant with BDD was undergoing outpatient psychotherapy (although not CBT) at the time of the study.

To enhance generalizability, we allowed current DSM-IV diagnoses of dysthymia, OCD, major depression, panic disorder, generalized anxiety disorder, social anxiety disorder, or agoraphobia. Comorbid diagnoses in the BDD group can be found in Supplementary Table 1. Controls were excluded if they had any lifetime DSM-IV Axis I disorder.

**Measures**

**Clinical Measures.** Participants were telephone screened, followed by a clinical interview with the study physician (JDF). Diagnostic assessments included the Mini International Psychiatric Interview (MINI) (60) and the BDD Diagnostic Module (61) based on the DSM-IV. Anxiety and depression symptom severity were measured using the Hamilton Anxiety Rating Scale (HAMA) (62), and the Montgomery Asberg Depression Rating Scale (MADRS) (63). Delusionality was

assessed using the Brown Assessment of Beliefs Scale (BABS) (64). Participants with BDD were additionally administered the Yale-Brown Obsessive Compulsive Scale Modified for BDD (BDD-YBOCS) to assess BDD symptom severity (65).

**Imaging data acquisition.** Functional MRI data were acquired on a Siemens Trio 3T scanner using a T2*weighted echo planar imaging (EPI) gradient-echo pulse sequence (repetition time/echo time = 2,500/25ms; flip angle = 80°; matrix = 64 x 64; field-of-view = 192 mm; in-plane voxel-size = $3mm^3$; 0.75 mm intervening spaces; 32 total interleaved slices). Higher resolution-matched bandwidth (MBW) T2 and T1-weighted images were collected for coregistration. fMRI data preprocessing methods can be found in the Supplementary Materials.

**fMRI data preprocessing.** fMRI data were preprocessed in the FMRIB Software Library (FSL version 5.0.6). Specifically, data underwent spatial smoothing (5mm full-width-half-maximum Gaussian kernel), high-pass temporal filtering (100s), skull stripping, and were motion corrected using 6 motion parameters. We coregistered participant's functional images to their MBW T2-weighted structural image, which was then registered to the MNI-152 template brain volume. We excluded participants with motion values >2 standard deviations from the group mean as defined by FSL DVARS (66).

**Fearful face task.** Participants viewed blocks of either fearful faces or scrambled shapes while performing a gender-labeling task to ensure vigilance (67) (Figure 1). Face-stimuli were selected from the NimStim dataset which has standardized face images (68). Each block contained 4 stimuli, either faces or scrambled shapes, with equal numbers of male and female faces. Blocks

were presented 10 times per condition across 2 runs, totaling 40 trials per stimulus type. Stimuli were shown for 4 seconds each with a 0.5-second interstimulus interval. During face trials, participants identified gender (male/female); during scrambled trials, they identified shape (circle/oval) by pressing corresponding keys.

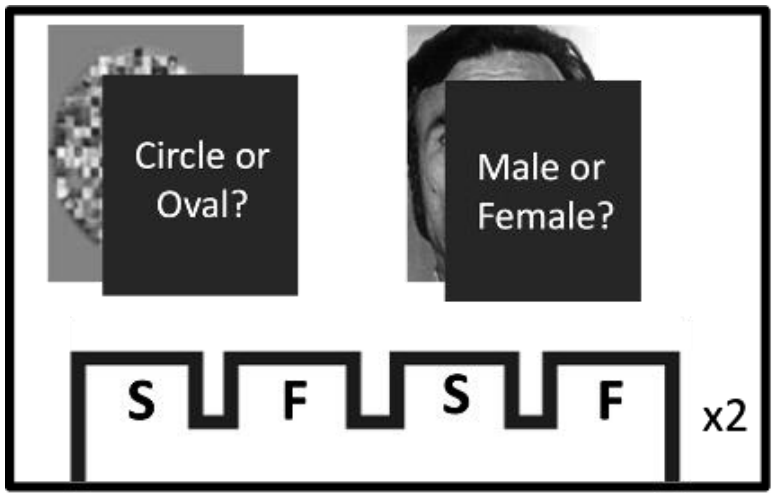


**Figure 1**. Fearful face processing paradigm. During this task, an equal number of male- and female-appearing faces were presented as either scrambled images or unaltered images of fearful faces. Participants were asked to identify the gender of the face to ensure attention.

**Region of Interest (ROI) Parcellation.** We chose regions of interest (ROIs) based on prior structural and functional evidence of these ROIs as central nodes in a visual fearful face processing network as well as because of their implications in BDD (69). Selected ROIs were as follows: bilateral pulvinar, amygdala, fusiform face area (FFA), and medial orbitofrontal cortex (mOFC). The mOFC was included based on previous findings showing abnormal mPFC-amygdala connectivity in BDD patients (13) as well as OFC differences in BDD during own-face processing (49) and studies implicating the OFC as part of an extended face processing network (50,70). Specifically, the medial, rather than lateral, portion of the OFC was selected due to a

greater number of published papers supporting a link between mOFC and fear and human evidence for structural white matter connectivity between the amygdala and mOFC (36,71). Bilateral pulvinar was defined anatomically using the Craddock-200 atlas (72). Bilateral amygdala and mOFC were anatomically defined using Automatic Anatomical Labeling (73). Bilateral FFA was extracted using a functionally-defined Neurosynth reference inference Z map (thresholded at $p<0.05$) (74). We further validated our extracted FFA ROIs with prior work accounting for inter-individual variability in the functionally-defined FFA and ensured the average size of the ROIs was close to prior, more conservative analyses (75). ROIs were selected based on strong a priori anatomical and functional evidence regarding fearful face processing; given the well-established roles of the ROIs selected, we elected to use anatomical derivations of the ROIs rather than mass-univariate activation maps. This is consistent with recommendations in the DCM literature emphasizing biologically motivated model specification (76). ROI locations were defined individually to account for anatomical variability. Bilateral ROIs were kept separate due to known hemispheric differences in BDD and fear processing (12,13,77,78). Although hypotheses involving the amygdala were lateralized to the right side, we opted to include bilateral nodes to ensure that the model captured the full architecture of fearful face processing. As DCM inferences depend on network completeness, omitting left-side connections could bias the estimation of right-sided parameters or obscure meaningful group differences (76,79). Eigenvariate time series from these regions were then extracted using principal component analysis (PCA) to provide a matrix of size *timepoints x trial type* for each ROI and subject individually; each ROI eigenvariate explained at least 80% of the variance across all participants. ROI timeseries were mean-centered through the eigenvariate extraction process prior to use in the DCM analysis. As an exploratory analysis, we examined univariate task

effects using GLM across all ROIs used within the DCM analysis; across all subjects, participants showed greater BOLD fMRI activation across all ROIs in response to fearful versus scrambled stimuli as analyzed via one-sample t-tests (all uncorrected-$p < 0.04$).

**Dynamic causal modeling.** We used dynamic causal modeling (73; DCM) in SPM12 to assess effective connectivity during fearful face processing. Bilinear, non-stochastic DCMs were estimated separately for each subject using eight Regions-of-Interest (ROIs): the left and right pulvinar, amygdala, FFA, and mOFC. An *a priori* model specified the pulvinar as the starting node, which shares connections to both the FFA and amygdala. The FFA similarly connects to the amygdala, which terminally connects to the mOFC (Figure 2). Connections between all nodes were verified to have plausible biophysical basis by examining prior studies showing white matter and functional connectivity between these nodes in humans (34,50,81–84). In total we included 8 feedforward connections, 8 feedback connections, and 8 intra-region connections (Figure 2; 24 connections total). Trial types (scrambled versus fearful) were used as the driving inputs. Importantly, DCM estimates directed connectivity based on a biophysically informed generative model of neural interactions, Thus, the term "directional" reflects the model-based influences of one region on another that are more likely to account for the observed regional timeseries, without directly relying on their observed temporal precedence (which might be affected by regional differences in the hemodynamics response: (76,80). Therefore, our interpretation of DCM results is grounded in this model-based framework, rather than assumptions about temporal causality. Model comparison was conducted using Bayesian random-effects analysis, which accounts for between-subject heterogeneity in the model that provides the best fit to the data. Model comparison was performed within each group separately,

to further account for any underlying heterogeneity that would affect model fit. This procedure yields, for each model, the probability densities that a participant from that group will be best fit by a given model. These distributions were then used to compute the exceedance probability associated with each model, that is, the probability that a given model would fit an individual better than any of the others (85). A DCM model includes different matrices of parameters, which capture different forms of direct and modulatory interactions between ROIs or between experimental stimuli and ROIs. The connectivity parameters discussed throughout the manuscript relate to the A-matrix, or the matrix of direct intrinsic connectivity between ROIs as visualized in Figure 2. We opted to focus on the A-matrix (to represent stable group differences in intrinsic connectivity) and the C-matrix (to represent stable regional differences in responses to specific stimuli) to address our hypotheses. We did not include the B-matrix (which reflects modulatory effects from the experimental stimuli) or the D-matrix (which reflects modulatory effects of one region on the connectivity), as these were not central to addressing our hypotheses. Given this, we decided instead to only include the direct effects of stimuli on different ROIs, and systemically explore the best ways to connect the inputs to the model (see Supplementary Figure 1); we have followed similar procedures in prior work (86,87).

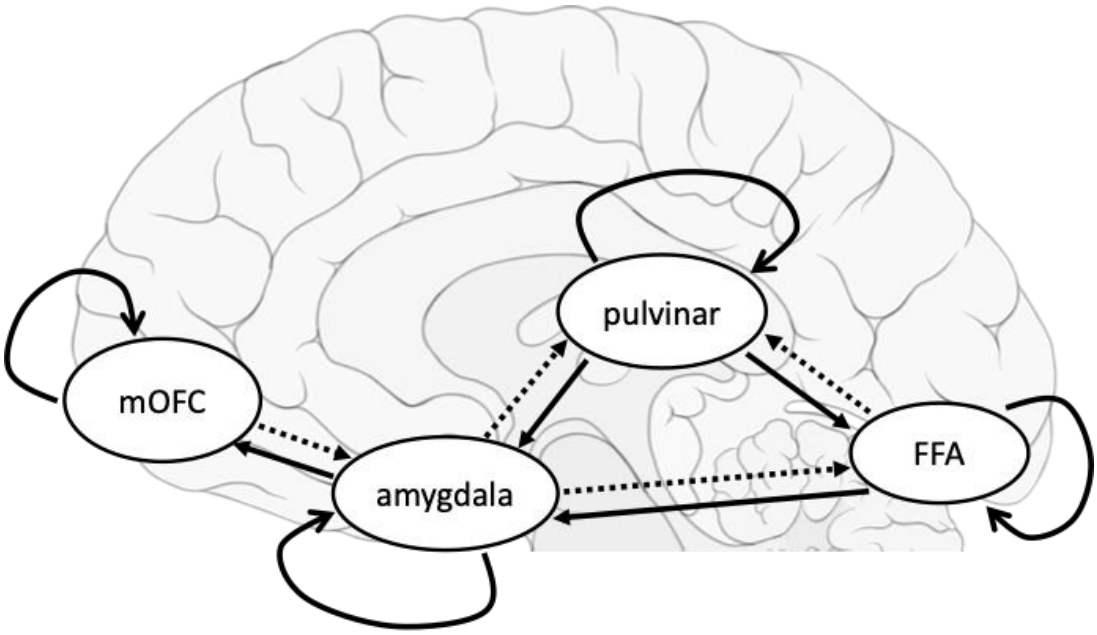


**Figure 2.** The *a priori* DCM with nodes of the bilateral pulvinar, amygdala, FFA and mOFC. We included connections between the pulvinar, FFA, and amygdala as well as connections between the amygdala and mOFC. We also included intra-region self-feeding connections. Feedforward and intra-region connections between regions are displayed as solid lines while feedback connections are displayed as dashed.

**Statistical analysis.** Group-level analyses were conducted using Parametric Empirical Bayes (PEB) within the DCM framework. PEB provides a hierarchical Bayesian approach for estimating between-subject effects by accounting for the uncertainty of individual (first-level) DCM parameters and modeling group-level effects in a single Bayesian framework (88). This approach is the recommended standard for group comparisons in DCM as it enhances sensitivity, avoids circularity, and eliminates the need for traditional multiple-comparison correction applied to pairwise-tests across individual parameters (89,90). To estimate group differences across parameters we used the estimated A-matrix from each participant's DCM. The posterior means

and covariance estimates of all subject-wise parameters also taken forward for the second-level PEB models. We then used Bayesian Model Reduction (BMR), which efficiently searches the model space by pruning parameters that do not contribute to model evidence. The results models were averaged using Bayesian Model Averaging (BMA) to yield robust posterior estimates of group effects, weighted by their evidence. Connectivities with a posterior probability ($Pp$) > 0.95 are considered as having strong evidence for group differences. The full estimated A-matrix as well as the PEB results for each estimated connectivity parameter are reported in Supplementary Table 1.

To test associations between connectivity estimates and symptom severity, we conducted a PEB analysis within individuals with BDD only, looking at the relationship between all 24 connectivity parameters and BDD-YBOCS total scores. We also performed further exploratory analyses using dimensional measures of anxiety and depression symptoms.

# Results

**Demographics**

| Characteristic | BDD group (n = 32) | Control group (n = 37) | Test statistic | P-value |
|---|---|---|---|---|
| Age | 23.50 ± 0.84 | 21.68 ± 0.74 | t = 1.63 | 0.11 |
| Sex (n, %) | | | t = -0.24 | 0.81 |

| | | | | |
|---|---|---|---|---|
| Female | 27 (84.38) | 32 (86.49) | | |
| Male | 5 (15.62) | 5 (13.51) | | |
| Race/ethnicity (n, %) | | | = 2.10 | 0.72 |
| Asian | 9 (28.12) | 9 (24.32) | | |
| African American/Black | 2 (6.25) | 6 (16.22) | | |
| Hispanic | 2 (6.25) | 1 (2.70) | | |
| Mixed race | 3 (9.38) | 3 (8.11) | | |
| White | 16 (50) | 18 (48.65) | | |
| Education (years) | 15.13 ± 0.57 | 13.85 ± 0.45 | t = 1.78 | 0.08 |
| BDD-YBOCS | 29.50 ± 0.97 | NA | | - |
| BABS | 15.19 ± 0.58 | NA | | - |
| MADRS | 15.53 ± 1.40 | 1.22 ± 0.27 | t = 10.70 | **<0.0001** |
| HAMA | 10.06 ± 1.18 | 2.16 ± 0.29 | t = 6.94 | **<0.0001** |
| Comorbid diagnoses (n, %) | | | | - |
| Agoraphobia | 2 (6.25) | | | |
| Dysthymia | 2 (6.25) | | | |

| | | | | |
|---|---|---|---|---|
| Generalized anxiety disorder | 4 (12.5) | | | |
| Major depressive disorder | 10 (31.3) | | | |
| Social anxiety disorder | 4 (12.5) | | | |
| Panic disorder | 1 (3.13) | | | |

**Table 1. Demographic and clinical characteristics of the sample.** P-values are derived from between-groups t-tests or chi-square (marked with *). Comorbidities of the BDD group are also listed here. To enhance generalizability, we allowed current DSM-IV diagnoses of dysthymia, OCD, major depression, panic disorder, generalized anxiety disorder, social anxiety disorder, or agoraphobia. Of note, 5/32 (15.63%) of participants in the BDD group had at least 2 comorbidities.

**Bayesian model selection.** The model space was defined to address: (A) which region in the visual fearful face processing network is the input region for presented stimuli and if this varies depending on whether stimuli were fearful vs scrambled faces, and (B) the directionality of these connections, i.e., whether this network is operating as a feedback, feedforward, or bidirectional system. We conducted a two-stage model comparison to address these questions. First, we compared models that differed by stimulus driving regions, that is, the input regions for the different stimulus types (Supplementary Figure 1A). We compared a model in which (i) both stimulus types (fearful vs scrambled) drove activity in the pulvinar (Pulvinar/Pulvinar model), (ii) fearful faces drive input to both the pulvinar and amygdala, while scrambled faces only drive

activity in the pulvinar (Pulvo-amygdala/Pulvinar model), and (iii) fearful faces drive activity in the amygdala while scrambled faces drive activity in the pulvinar (Pulvinar/Amygdala model). We determined through Bayesian model selection that both groups (BDD and HCs) were best fit by the Pulvo-amygdala/Pulvinar model, in which fearful faces drove regional input activity in the bilateral pulvinar and amygdala while the scrambled faces drove input activity in just the bilateral pulvinar. Using these verified stimulus driving regions, we then tested models with varying directionality of connections using a (i) feedforward model, (ii) feedback model, and (iii) bidirectional model, in which all connections between nodes were reciprocal (Supplementary Figure 1B). Again, using Bayesian model selection, we observed that both groups were fit by the model with bidirectional connectivity between all ROIs, providing evidence for both feedforward and feedback connections utilized within this network. Exceedance probabilities for each model within each group can be seen in Supplementary Figure 1C. The distribution of the exceedance probabilities for each model can be seen in Supplementary Figure 2.

**Group differences in effective connectivity**

As described above, both groups were fit by the same structural model in which scrambled faces drove input to the pulvinar, fearful faces to the pulvinar and amygdala, with bidirectional connections between all nodes. Modeling only ipsilateral and self-connections, the final model included 24 connections. Using Parametric Empirical Bayes (PEB), we investigated group differences across the estimated connectivity parameters (see Figure 3, Supplementary Table 1). We observed significant greater connectivity from the left amygdala to the left mOFC ($\beta = 0.09$, $Pp = 0.96$) and greater connectivity within the left FFA ($\beta = 0.12$, $Pp = 0.96$), in individuals with BDD compared to controls. Additionally, individuals with BDD showed significantly reduced

connectivity from the right amygdala to the right pulvinar ($\beta$ = -0.11, *Pp* = 0.98). No other connectivity parameter yielded significant differences (all other *Pp* < 0.81).

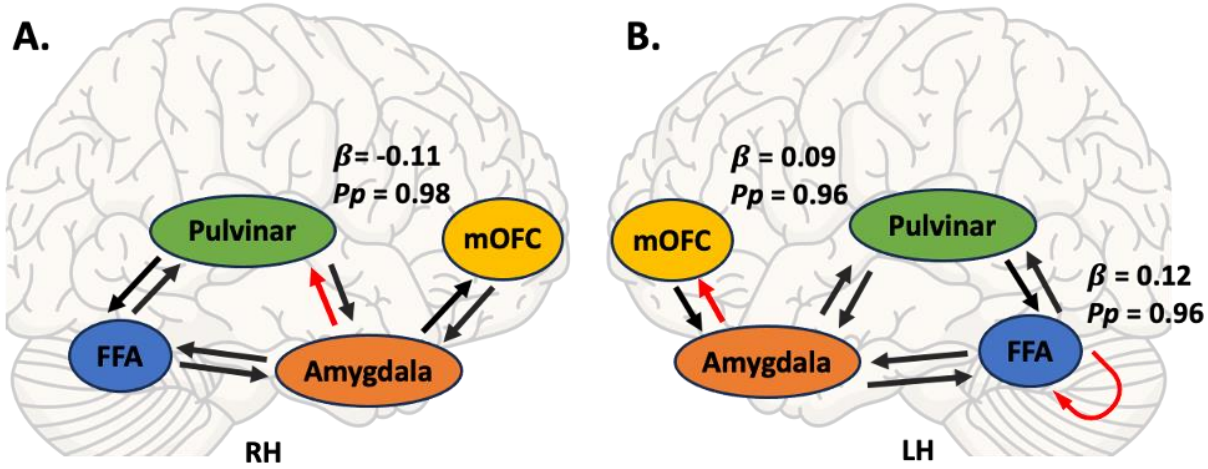


**Figure 3.** PEB analysis yielded three significantly different effective connectivity estimates between individuals with BDD and HCs. A) effective connectivity from the right amygdala to the right pulvinar ( = -0.11, *Pp* = 0.98) was significantly reduced in individuals with BDD compared to HCs. B) effectivity connectivity from the left amygdala to the left mOFC ( = 0.09, *Pp* = 0.96) as well as connectivity within the left FFA ( = 0.12, *Pp* = 0.96) was significantly greater in individuals with BDD compared to controls. RH = right hemisphere; LH = left hemisphere; BDD=body dysmorphic disorder; HC=healthy controls; mOFC=medial orbitofrontal cortex; FFA=fusiform face area

**Associations with body dysmorphic symptoms**

There were no significant associations with body dysmorphic symptoms within the BDD group across all estimated connectivities, however we did observe a marginal association with

symptom severity and connectivity within the left pulvinar ($\beta$ = -0.01, $Pp$ = 0.94) and from the right pulvinar to the right FFA ($\beta$ = 0.01, $Pp$ = 0.94).

**Exploratory associations with depression and anxiety symptoms**

Within the BDD group, we observed a significant association between the connectivity estimate from the left amygdala to the left mOFC and anxiety symptoms ($\beta$ = 0.01, $Pp$ = 0.97), such that higher connectivity was associated with increased anxiety symptoms; this connectivity was marginally associated with depression symptoms in the same direction ($\beta$ = 0.01, $Pp$ = 0.93). Reduced connectivity within the left pulvinar was significantly associated with increased depression symptoms ($\beta$ = -0.01, $Pp$ = 0.97), an effect that was marginal for anxiety symptoms ($\beta$ = -0.01, $Pp$ = 0.94). We observed marginal associations with anxiety symptoms and the connectivities from the left FFA to the left amygdala ($\beta$ = -0.01, $Pp$ = 0.94), and from the left pulvinar to the left FFA ($\beta$ = 0.01, $Pp$ = 0.93). Similarly, we observed marginal associations with depression and the connectivities from the left pulvinar to the left FFA ($\beta$ = 0.01, $Pp$ = 0.92) and from the right FFA to the right amygdala ($\beta$ = -0.01, $Pp$ = 0.93).

# Discussion

This study examined effective connectivity involved in fearful face processing in individuals with BDD and HCs. We observed significantly higher connectivity from the left amygdala to the left mOFC and within the left FFA as well as significantly reduced connectivity from the right amygdala to the right pulvinar in individuals with BDD compared to healthy controls. While aberrant connectivity from the left amygdala to the left mOFC was positively associated with anxiety and depression symptoms in individuals with BDD, these effects were not

significant when correcting for multiple comparisons and we observed no significant associations with BDD symptoms across all connectivity parameters. Additionally, no single hypothesized connection showed significant group differences.

Feedforward connectivity from the left amygdala to the left mOFC was significantly different between patients and controls with connectivity heightened in BDD compared with HC. We hypothesized that there would be increased amygdala-to-mOFC connectivity in BDD, lateralized to the right hemisphere, given the right amygdala's role in fear processing (58), which was not confirmed. However, the left amygdala has been associated more generally with emotional processing (78,91). Further, while the right amygdala is involved in the rapid detection of emotional/ threatening stimuli, the left amygdala is responsible for more detailed stimulus evaluation deriving from stimuli-induced arousal fluctuations (92,93). Thus, we speculate that the current findings could possibly reflect deficits in emotional processing for individuals with BDD, arising during a secondary process of stimulus evaluation.

Several studies have reported distinct amygdala-prefrontal connectivity patterns in BDD compared to HCs, both during task and at rest (12,13,94). In the same participants as the current study, a self-emotion labeling task revealed impaired feedforward amygdala-mPFC connectivity in BDD; unlike HCs, individuals with BDD showed no increase in connectivity across experimental blocks (13). Another study found increased left amygdala-prefrontal connectivity and hyperactivity in the left amygdala during negative face viewing in BDD (12). Similarly, amygdala hyperactivity, particularly on the right, was observed in response to emotionally neutral, spatial frequency-filtered faces (27). At rest, BDD participants also showed greater left amygdala-frontal connectivity compared to HCs (94).

These findings support disrupted frontolimbic connectivity in BDD, especially during emotional face perception (13). Notably, similar frontolimbic hyperconnectivity has been reported in social anxiety disorder (95), a condition that shares features with BDD, such as heightened social rejection sensitivity and self-focused attention (6,7,96–99). Differences in OFC activity (100) and connectivity (39,47,101) has been observed in OCD compared with HC, and linked to emotion regulation during stimulus appraisal as well as compulsive sub-types of OCD. Future work, potentially in a transdiagnostic sample of BDD, social anxiety disorder, and OCD, could potentially help elucidate shared and unique phenotypes and any potential associations between altered frontolimbic connectivity and cross-cutting symptom domains.

Moreover, connectivity from the right amygdala to the right pulvinar significantly contributed to distinguishing BDD from HC, with reduced connectivity in BDD compared with HC. Although outside of our hypotheses, one speculative possibility is that this might reflect diminished attention modulation in response to threat in individuals with BDD. The pulvinar, a core region of the thalamus, is thought to provide salience-dependent stimulus information to areas such as the amygdala and OFC via feedforward connections. The pulvinar also receives a wide array of feedback input from the cortex and integrates this multimodal information to redirect processing towards salient stimuli (34,53). Diminished amygdala-pulvinar feedback connectivity could possibly be related to symptoms of attentional bias previously seen in individuals with BDD (10,102–104). However, this remains speculative until directly tested since this connection, to the best of our knowledge, has not been previously probed in those with BDD.

Further, we observed significantly higher connectivity within the left FFA in individuals with BDD compared to HCs. Prior research on FFA activation and connectivity differences in BDD are mixed, with some showing higher overall FFA activity (28) and connectivity (12) in BDD

compared with HC, and other studies showing no differences in FFA activation level in response to neutral faces in BDD (12,27). Our results converge on growing evidence showing face processing differences, specifically negative emotional face processing, in BDD centered around deficits in the FFA (12,77). Contrary to our hypotheses, we did not observe aberrant FFA connectivity within other regions such as FFA-amygdala or FFA-pulvinar connectivity in the BDD group compared to controls. Hyperactivity and hyperconnectivity of the FFA in BDD has been interpreted as an overreliance on the VVS, or high-detail visual processing, compared to HC (28,77). It is possible that we did not observe FFA connectivity differences with regions such as the amygdala due to the specific task design. The task of gender labeling, although of low task difficulty but requiring facial characteristic identification, could have potentially required both groups to rely on detail processing by highly engaging the VVS (105) and its connections with the pulvinar and amygdala, making inherent connectivity differences in VVS regions such as the FFA too subtle for accurate group distinction (i.e., a ceiling effect).

Notably, Bayesian model selection revealed that both groups were best fit by the same structural connectivity model, with bidirectional connections between regions of the pulvinar, amygdala, FFA, and mOFC. This indicates that individuals with BDD display a comparable combination of feedforward and feedback influence during fearful face processing as is typical in HC (106–108).

Several limitations should be noted. While significant, group differences showed modest effect sizes and aberrant connectivities were not significantly associated with symptom severity in BDD. However, our sample showed relatively low variance in BDD symptoms, likely due to the small sample size. Null symptom-brain associations are not uncommon in clinical connectivity studies, particularly in relatively small samples with restricted symptom variance (109,110); this emphasizes the need for larger samples to enable us to capture sufficient symptom heterogeneity

within our clinical sample. Further, we utilized scrambled images as our control condition rather than neutral faces, given prior evidence that face—baseline contrasts are more reliable (111–115). However, this limits the ability to disentangle the effects of fearful expressions from general face processing. Future studies should include neutral and other emotional expressions as well as incorporate retest reliability to enhance validity. Additionally, the task used in this study was an implicit face processing paradigm, which limits the generalizability of our findings to ethological BDD symptoms. As participants were not explicitly instructed to evaluate the emotional content of the faces, the extent to which the observed effects reflect deliberate emotional appraisal versus automatic perceptual or attentional processes remains unclear. Finally, we constrained our regions and connections of interest for this study to ones we believed to be implicated in BDD and important for fearful face processing, but there could exist relevant regions outside of this network.

The BDD sample included many individuals with comorbidities (n=17/32, see Table 1) to allow for a more generalizable sample, given the high rate of psychiatric comorbidities in the general BDD population (116,117). As some connections showed significant associations with anxiety and depression symptoms in the BDD group, there may still be latent factors related to comorbidities that drove our group differences, which is an inherent limitation in case-control studies. Finally, both groups were comprised of majority female participants. As BDD has been shown to occur at almost equal rates across genders (2), this limits the generalizability of our findings.

This study is part of a growing effort to investigate the neural mechanisms underlying emotion and face processing in individuals with BDD. We found that during fearful face viewing, differential connectivity between the amygdala and mOFC, within the FFA, and between the

amygdala and pulvinar were significantly different between individuals with BDD from HC. Of note, none of our hypothesized connections were significant. Clinically, this network-level characterization may help guide future interventions aimed at reducing perceptual threat bias or through strengthening regulatory prefrontal feedback. For instance, connectivity-informed targets could be leveraged in neuromodulation augmentation approaches (i.e., TMS, neurofeedback) or used to evaluate mechanisms of change across existing treatments such as cognitive-behavioral therapy. Our findings add to the current theoretical model of BDD, further implicating the amygdala and FFA, and their connections, as regions with key differences compared to neurotypical individuals. Future work should investigate the role these regions play in the etiology or in the maintenance of BDD. Future research is warranted to better understand if and how aberrant fearful face viewing is linked to specific symptoms, including utilizing transdiagnostic samples that could potentially overlap in symptom dimensions and neural phenotypes.

## References


1. Phillips KA, Menard W, Fay C, Weisberg R. Demographic Characteristics, Phenomenology, Comorbidity, and Family History in 200 Individuals With Body Dysmorphic Disorder. Psychosomatics. 2005 Jul;46(4):317–25. doi:10.1176/appi.psy.46.4.317
2. American Psychiatric Association. Diagnostic and Statistical Manual of Mental Disorders [Internet]. Fifth Edition. American Psychiatric Association; 2013 [cited 2022 May 4]. Available from:

https://psychiatryonline.org/doi/book/10.1176/appi.books.9780890425596 doi:10.1176/appi.books.9780890425596

3. Buhlmann U, Glaesmer H, Mewes R, Fama JM, Wilhelm S, Brähler E, et al. Updates on the prevalence of body dysmorphic disorder: A population-based survey. Psychiatry Research. 2010 Jun;178(1):171–5. doi:10.1016/j.psychres.2009.05.002
4. Koran LM, Abujaoude E, Large MD, Serpe RT. The Prevalence of Body Dysmorphic Disorder in the United States Adult Population. CNS spectr. 2008 Apr;13(4):316–22. doi:10.1017/S1092852900016436
5. Rief W, Buhlmann U, Wilhelm S, Borkenhagen A, Brähler E. The prevalence of body dysmorphic disorder: a population-based survey. Psychol Med. 2006 Jun;36(6):877–85. doi:10.1017/S0033291706007264
6. Buhlmann U, McNally RJ, Etcoff NL, Tuschen-Caffier B, Wilhelm S. Emotion recognition deficits in body dysmorphic disorder. Journal of Psychiatric Research. 2004 Mar;38(2):201–6. doi:10.1016/S0022-3956(03)00107-9
7. Buhlmann U, Etcoff N, Wilhelm S. Emotion recognition bias for contempt and anger in body dysmorphic disorder. Journal of Psychiatric Research. 2006 Mar;40(2):105–11. doi:10.1016/j.jpsychires.2005.03.006
8. Toh WL, Castle DJ, Rossell SL. Facial affect recognition in body dysmorphic disorder versus obsessive-compulsive disorder: An eye-tracking study. Journal of Anxiety Disorders. 2015 Oct;35:49–59. doi:10.1016/j.janxdis.2015.08.003
9. Feusner JD, Bystritsky A, Hellemann G, Bookheimer S. Impaired identity recognition of faces with emotional expressions in body dysmorphic disorder. Psychiatry Research. 2010 Oct;179(3):318–23. doi:10.1016/j.psychres.2009.01.016

10. Grennan G, Zhao Y, Fang A. Applying a drift diffusion model to test the effect of oxytocin on attentional biases in body dysmorphic disorder. Journal of Obsessive-Compulsive and Related Disorders. 2023 Oct;39:100841. doi:10.1016/j.jocrd.2023.100841

11. Grace SA, Toh WL, Buchanan B, Castle DJ, Rossell SL. Impaired Recognition of Negative Facial Emotions in Body Dysmorphic Disorder. J Int Neuropsychol Soc. 2019 Sep;25(08):884–9. doi:10.1017/S1355617719000419

12. Borgers T, Kürten M, Kappelhoff A, Enneking V, Möllmann A, Schulte J, et al. Brain functional correlates of emotional face processing in body dysmorphic disorder. Journal of Psychiatric Research. 2022 Mar;147:103–10. doi:10.1016/j.jpsychires.2022.01.007

13. Rangaprakash D, Bohon C, Lawrence KE, Moody T, Morfini F, Khalsa SS, et al. Aberrant Dynamic Connectivity for Fear Processing in Anorexia Nervosa and Body Dysmorphic Disorder. Front Psychiatry. 2018 Jun 26;9:273. doi:10.3389/fpsyt.2018.00273

14. Adolphs R, Spezio M. Role of the amygdala in processing visual social stimuli. In: Progress in Brain Research [Internet]. Elsevier; 2006 [cited 2025 Dec 10]. p. 363–78. Available from: https://linkinghub.elsevier.com/retrieve/pii/S0079612306560200 doi:10.1016/S0079-6123(06)56020-0

15. Davis M. Neurobiology of fear responses: the role of the amygdala. JNP. 1997 Aug 1;9(3):382–402. doi:10.1176/jnp.9.3.382

16. Gross J. Handbook of Emotion Regulation. 2nd ed. The Guilford Press; 2014.

17. Sylvester CM, Corbetta M, Raichle ME, Rodebaugh TL, Schlaggar BL, Sheline YI, et al. Functional network dysfunction in anxiety and anxiety disorders. Trends in Neurosciences. 2012 Sep;35(9):527–35. doi:10.1016/j.tins.2012.04.012

18. Etkin A, Wager TD. Functional Neuroimaging of Anxiety: A Meta-Analysis of Emotional Processing in PTSD, Social Anxiety Disorder, and Specific Phobia. AJP. 2007 Oct;164(10):1476–88. doi:10.1176/appi.ajp.2007.07030504

19. Disner SG, Beevers CG, Haigh EAP, Beck AT. Neural mechanisms of the cognitive model of depression. Nat Rev Neurosci. 2011 Aug;12(8):467–77. doi:10.1038/nrn3027

20. Hamilton JP, Etkin A, Furman DJ, Lemus MG, Johnson RF, Gotlib IH. Functional Neuroimaging of Major Depressive Disorder: A Meta-Analysis and New Integration of Baseline Activation and Neural Response Data. AJP. 2012 Jul;169(7):693–703. doi:10.1176/appi.ajp.2012.11071105

21. Sabatinelli D, Bradley MM, Fitzsimmons JR, Lang PJ. Parallel amygdala and inferotemporal activation reflect emotional intensity and fear relevance. NeuroImage. 2005 Feb;24(4):1265–70. doi:10.1016/j.neuroimage.2004.12.015

22. Straube T, Mentzel HJ, Miltner WHR. Common and Distinct Brain Activation to Threat and Safety Signals in Social Phobia. Neuropsychobiology. 2005;52(3):163–8. doi:10.1159/000087987

23. Koller K, Rafal RD, Platt A, Mitchell ND. Orienting toward threat: Contributions of a subcortical pathway transmitting retinal afferents to the amygdala via the superior colliculus and pulvinar. Neuropsychologia. 2019 May;128:78–86. doi:10.1016/j.neuropsychologia.2018.01.027

24. Benarroch EE. Pulvinar: Associative role in cortical function and clinical correlations. Neurology. 2015 Feb 17;84(7):738–47. doi:10.1212/WNL.0000000000001276

25. Cortes N, Ladret HJ, Abbas-Farishta R, Casanova C. The pulvinar as a hub of visual processing and cortical integration. Trends in Neurosciences. 2024 Feb;47(2):120–34. doi:10.1016/j.tins.2023.11.008

26. Brown EC, Clark DL, Hassel S, MacQueen G, Ramasubbu R. Thalamocortical connectivity in major depressive disorder. Journal of Affective Disorders. 2017 Aug;217:125–31. doi:10.1016/j.jad.2017.04.004

27. Feusner JD, Townsend J, Bystritsky A, Bookheimer S. Visual Information Processing of Faces in Body Dysmorphic Disorder. Arch Gen Psychiatry. 2007 Dec 1;64(12):1417. doi:10.1001/archpsyc.64.12.1417

28. Li W, Lai TM, Bohon C, Loo SK, McCurdy D, Strober M, et al. Anorexia nervosa and body dysmorphic disorder are associated with abnormalities in processing visual information. Psychol Med. 2015 Jul;45(10):2111–22. doi:10.1017/S0033291715000045

29. Bohon C, Hembacher E, Moller H, Moody TD, Feusner JD. Nonlinear relationships between anxiety and visual processing of own and others' faces in body dysmorphic disorder. Psychiatry Research: Neuroimaging. 2012 Nov;204(2–3):132–9. doi:10.1016/j.pscychresns.2012.09.003

30. Saygin ZM, Osher DE, Koldewyn K, Reynolds G, Gabrieli JDE, Saxe RR. Anatomical connectivity patterns predict face selectivity in the fusiform gyrus. Nat Neurosci. 2012 Feb;15(2):321–7. doi:10.1038/nn.3001

31. Amaral DG, Price JL. Amygdalo-cortical projections in the monkey ( *Macaca fascicularis* ). J of Comparative Neurology. 1984 Dec 20;230(4):465–96. doi:10.1002/cne.902300402

32. Moody TD, Sasaki MA, Bohon C, Strober MA, Bookheimer SY, Sheen CL, et al. Functional connectivity for face processing in individuals with body dysmorphic disorder and anorexia nervosa. Psychol Med. 2015 Dec;45(16):3491–503. doi:10.1017/S0033291715001397

33. Tadayonnejad R, Klumpp H, Ajilore O, Leow A, Phan KL. Aberrant pulvinar effective connectivity in generalized social anxiety disorder. Medicine. 2016 Nov;95(45):e5358. doi:10.1097/MD.0000000000005358

34. Pessoa L, Adolphs R. Emotion processing and the amygdala: from a “low road” to “many roads” of evaluating biological significance. Nat Rev Neurosci. 2010 Nov;11(11):773–82. doi:10.1038/nrn2920

35. Ghashghaei HT, Hilgetag CC, Barbas H. Sequence of information processing for emotions based on the anatomic dialogue between prefrontal cortex and amygdala. NeuroImage. 2007 Feb;34(3):905–23. doi:10.1016/j.neuroimage.2006.09.046

36. Croxson PL, Johansen-Berg H, Behrens TEJ, Robson MD, Pinsk MA, Gross CG, et al. Quantitative Investigation of Connections of the Prefrontal Cortex in the Human and Macaque using Probabilistic Diffusion Tractography. J Neurosci. 2005 Sep 28;25(39):8854–66. doi:10.1523/JNEUROSCI.1311-05.2005

37. Haber SN, Knutson B. The Reward Circuit: Linking Primate Anatomy and Human Imaging. Neuropsychopharmacol. 2010 Jan;35(1):4–26. doi:10.1038/npp.2009.129

38. Ahmari SE, Rauch SL. The prefrontal cortex and OCD. Neuropsychopharmacol. 2022 Jan;47(1):211–24. doi:10.1038/s41386-021-01130-2

39. Beucke JC, Sepulcre J, Talukdar T, Linnman C, Zschenderlein K, Endrass T, et al. Abnormally High Degree Connectivity of the Orbitofrontal Cortex in Obsessive-Compulsive Disorder. JAMA Psychiatry. 2013 Jun 1;70(6):619. doi:10.1001/jamapsychiatry.2013.173

40. Evans DW, Lewis MD, Iobst E. The role of the orbitofrontal cortex in normally developing compulsive-like behaviors and obsessive–compulsive disorder. Brain and Cognition. 2004 Jun;55(1):220–34. doi:10.1016/S0278-2626(03)00274-4

41. Frare F, Perugi G, Ruffolo G, Toni C. Obsessive–compulsive disorder and body dysmorphic disorder: a comparison of clinical features. Eur psychiatr. 2004 Aug;19(5):292–8. doi:10.1016/j.eurpsy.2004.04.014

42. Phillips KA, Pinto A, Menard W, Eisen JL, Mancebo M, Rasmussen SA. Obsessive–compulsive disorder versus body dysmorphic disorder: a comparison study of two possibly related disorders. Depress Anxiety. 2007;24(6):399–409. doi:10.1002/da.20232

43. Rotge JY, Guehl D, Dilharreguy B, Tignol J, Bioulac B, Allard M, et al. Meta-Analysis of Brain Volume Changes in Obsessive-Compulsive Disorder. Biological Psychiatry. 2009 Jan;65(1):75–83. doi:10.1016/j.biopsych.2008.06.019

44. Simon D, Kaufmann C, Müsch K, Kischkel E, Kathmann N. Fronto-striato-limbic hyperactivation in obsessive-compulsive disorder during individually tailored symptom provocation. Psychophysiology. 2010 Feb. doi:10.1111/j.1469-8986.2010.00980.x

45. Sun T, Song Z, Tian Y, Tian W, Zhu C, Ji G, et al. Basolateral amygdala input to the medial prefrontal cortex controls obsessive-compulsive disorder-like checking behavior. Proc Natl Acad Sci USA. 2019 Feb 26;116(9):3799–804. doi:10.1073/pnas.1814292116

46. Liang X, Zebrowitz LA, Aharon I. Effective connectivity between amygdala and orbitofrontal cortex differentiates the perception of facial expressions. Social Neuroscience. 2009 Apr;4(2):185–96. doi:10.1080/17470910802453105

47. Paul S, Beucke JC, Kaufmann C, Mersov A, Heinzel S, Kathmann N, et al. Amygdala–prefrontal connectivity during appraisal of symptom-related stimuli in obsessive–compulsive disorder. Psychol Med. 2019 Jan;49(2):278–86. doi:10.1017/S003329171800079X

48. Szeszko PR, Robinson D, Alvir JMaJ, Bilder RM, Lencz T, Ashtari M, et al. Orbital Frontal and Amygdala Volume Reductions in Obsessive-compulsive Disorder. Arch Gen Psychiatry. 1999 Oct 1;56(10):913. doi:10.1001/archpsyc.56.10.913

49. Feusner JD, Moody T, Hembacher E, Townsend J, McKinley M, Moller H, et al. Abnormalities of Visual Processing and Frontostriatal Systems in Body Dysmorphic Disorder. Arch Gen Psychiatry. 2010 Feb 1;67(2):197. doi:10.1001/archgenpsychiatry.2009.190

50. Fairhall SL, Ishai A. Effective Connectivity within the Distributed Cortical Network for Face Perception. Cerebral Cortex. 2007 Oct;17(10):2400–6. doi:10.1093/cercor/bhl148

51. Haist F, Anzures G. Functional development of the brain's face-processing system. WIRES Cognitive Science. 2017 Jan;8(1–2):e1423. doi:10.1002/wcs.1423

52. Palermo R, Rhodes G. Are you always on my mind? A review of how face perception and attention interact. Neuropsychologia. 2007;45(1):75–92. doi:10.1016/j.neuropsychologia.2006.04.025

53. Morris JS, Öhman A, Dolan RJ. A subcortical pathway to the right amygdala mediating "unseen" fear. Proc Natl Acad Sci USA. 1999 Feb 16;96(4):1680–5. doi:10.1073/pnas.96.4.1680

54. Gu YQ, Zhu Y. A randomized controlled trial of mindfulness-based cognitive therapy for body dysmorphic disorder: Impact on core symptoms, emotion dysregulation, and executive functioning. Journal of Behavior Therapy and Experimental Psychiatry. 2023 Dec;81:101869. doi:10.1016/j.jbtep.2023.101869

55. Lavell CH, Webb HJ, Zimmer-Gembeck MJ, Farrell LJ. A prospective study of adolescents' body dysmorphic symptoms: Peer victimization and the direct and protective roles of emotion regulation and mindfulness. Body Image. 2018 Mar;24:17–25. doi:10.1016/j.bodyim.2017.11.006

56. Minkova L, Sladky R, Kranz GS, Woletz M, Geissberger N, Kraus C, et al. Task-dependent modulation of amygdala connectivity in social anxiety disorder. Psychiatry Research: Neuroimaging. 2017 Apr;262:39–46. doi:10.1016/j.pscychresns.2016.12.016

57. Sladky R, Höflich A, Küblböck M, Kraus C, Baldinger P, Moser E, et al. Disrupted Effective Connectivity Between the Amygdala and Orbitofrontal Cortex in Social Anxiety Disorder During Emotion Discrimination Revealed by Dynamic Causal Modeling for fMRI. Cerebral Cortex. 2015 Apr;25(4):895–903. doi:10.1093/cercor/bht279

58. Framorando D, Moses E, Legrand L, Seeck M, Pegna AJ. Rapid processing of fearful faces relies on the right amygdala: evidence from individuals undergoing unilateral temporal lobectomy. Sci Rep. 2021 Jan 11;11(1):426. doi:10.1038/s41598-020-80054-1

59. Oldfield RC. The assessment and analysis of handedness: The Edinburgh inventory. Neuropsychologia. 1971 Mar;9(1):97–113. doi:10.1016/0028-3932(71)90067-4

60. Sheehan DV, Lecrubier Y, Sheehan KH, Amorim P, Janavs J, Weiller E, et al. The Mini-International Neuropsychiatric Interview (M.I.N.I.): the development and validation of a structured diagnostic psychiatric interview for DSM-IV and ICD-10. J Clin Psychiatry. 1998;59 Suppl 20:22-33;quiz 34-57. PubMed PMID: 9881538.

61. Phillips K, Atala K, Pope H. Diagnostic instruments for body dysmorphic disorder. 1995.

62. Hamilton M. THE ASSESSMENT OF ANXIETY STATES BY RATING. British Journal of Medical Psychology. 1959 Mar;32(1):50–5. doi:10.1111/j.2044-8341.1959.tb00467.x

63. Montgomery SA, Åsberg M. A New Depression Scale Designed to be Sensitive to Change. Br J Psychiatry. 1979 Apr;134(4):382–9. doi:10.1192/bjp.134.4.382

64. Eisen JL, Phillips KA, Baer L, Beer DA, Atala KD, Rasmussen SA. The Brown Assessment of Beliefs Scale: Reliability and Validity. AJP. 1998 Jan;155(1):102–8. doi:10.1176/ajp.155.1.102

65. Phillips KA, Hollander E, Rasmussen SA, Aronowitz BR, DeCaria C, Goodman WK. A severity rating scale for body dysmorphic disorder: development, reliability, and validity of a modified version of the Yale-Brown Obsessive Compulsive Scale. Psychopharmacol Bull. 1997;33(1):17–22. PubMed PMID: 9133747.

66. Power JD, Barnes KA, Snyder AZ, Schlaggar BL, Petersen SE. Spurious but systematic correlations in functional connectivity MRI networks arise from subject motion. NeuroImage. 2012 Feb;59(3):2142–54. doi:10.1016/j.neuroimage.2011.10.018

67. Lieberman MD, Eisenberger NI, Crockett MJ, Tom SM, Pfeifer JH, Way BM. Putting Feelings Into Words. Psychol Sci. 2007 May;18(5):421–8. doi:10.1111/j.1467-9280.2007.01916.x

68. Tottenham N, Tanaka JW, Leon AC, McCarry T, Nurse M, Hare TA, et al. The NimStim set of facial expressions: Judgments from untrained research participants. Psychiatry Research. 2009 Aug;168(3):242–9. doi:10.1016/j.psychres.2008.05.006

69. Diaz-Fong JP, Feusner JD. Visual Perceptual Processing Abnormalities in Body Dysmorphic Disorder. In. Berlin, Heidelberg: Springer Berlin Heidelberg; 2024 [cited 2024 Aug 29]. (Current Topics in Behavioral Neurosciences). Available from: https://link.springer.com/10.1007/7854_2024_472 doi:10.1007/7854_2024_472

70. Haxby JV, Hoffman EA, Gobbini MI. The distributed human neural system for face perception. Trends in Cognitive Sciences. 2000 Jun;4(6):223–33. doi:10.1016/S1364-6613(00)01482-0

71. Kim MJ, Whalen PJ. The Structural Integrity of an Amygdala–Prefrontal Pathway Predicts Trait Anxiety. J Neurosci. 2009 Sep 16;29(37):11614–8. doi:10.1523/JNEUROSCI.2335-09.2009

72. Craddock RC, James GA, Holtzheimer PE, Hu XP, Mayberg HS. A whole brain fMRI atlas generated via spatially constrained spectral clustering. Human Brain Mapping. 2012 Aug;33(8):1914–28. doi:10.1002/hbm.21333

73. Tzourio-Mazoyer N, Landeau B, Papathanassiou D, Crivello F, Etard O, Delcroix N, et al. Automated Anatomical Labeling of Activations in SPM Using a Macroscopic Anatomical Parcellation of the MNI MRI Single-Subject Brain. NeuroImage. 2002 Jan;15(1):273–89. doi:10.1006/nimg.2001.0978

74. Yarkoni T, Poldrack RA, Nichols TE, Van Essen DC, Wager TD. Large-scale automated synthesis of human functional neuroimaging data. Nat Methods. 2011 Aug;8(8):665–70. doi:10.1038/nmeth.1635

75. Julian JB, Fedorenko E, Webster J, Kanwisher N. An algorithmic method for functionally defining regions of interest in the ventral visual pathway. NeuroImage. 2012 May;60(4):2357–64. doi:10.1016/j.neuroimage.2012.02.055

76. Stephan KE, Penny WD, Moran RJ, Den Ouden HEM, Daunizeau J, Friston KJ. Ten simple rules for dynamic causal modeling. NeuroImage. 2010 Feb;49(4):3099–109. doi:10.1016/j.neuroimage.2009.11.015

77. Grace SA, Labuschagne I, Kaplan RA, Rossell SL. The neurobiology of body dysmorphic disorder: A systematic review and theoretical model. Neuroscience & Biobehavioral Reviews. 2017 Dec;83:83–96. doi:10.1016/j.neubiorev.2017.10.003

78. Sergerie K, Chochol C, Armony JL. The role of the amygdala in emotional processing: A quantitative meta-analysis of functional neuroimaging studies. Neuroscience & Biobehavioral Reviews. 2008 Jan;32(4):811–30. doi:10.1016/j.neubiorev.2007.12.002

79. Stephan KE, Harrison LM, Kiebel SJ, David O, Penny WD, Friston KJ. Dynamic causal models of neural system dynamics: current state and future extensions. J Biosci. 2007 Jan;32(1):129–44. doi:10.1007/s12038-007-0012-5

80. Friston KJ, Harrison L, Penny W. Dynamic causal modelling. NeuroImage. 2003 Aug;19(4):1273–302. doi:10.1016/S1053-8119(03)00202-7

81. Gobbini MI, Haxby JV. Neural systems for recognition of familiar faces. Neuropsychologia. 2007;45(1):32–41. doi:10.1016/j.neuropsychologia.2006.04.015

82. Unger A, Alm KH, Collins JA, O'Leary JM, Olson IR. Variation in White Matter Connectivity Predicts the Ability to Remember Faces and Discriminate Their Emotions. J Int Neuropsychol Soc. 2016 Feb;22(2):180–90. doi:10.1017/S1355617715001009

83. Wang Y, Metoki A, Alm KH, Olson IR. White matter pathways and social cognition. Neuroscience & Biobehavioral Reviews. 2018 Jul;90:350–70. doi:10.1016/j.neubiorev.2018.04.015

84. Abivardi A, Bach DR. Deconstructing white matter connectivity of human amygdala nuclei with thalamus and cortex subdivisions in vivo. Human Brain Mapping. 2017 Aug;38(8):3927–40. doi:10.1002/hbm.23639

85. Stephan KE, Penny WD, Daunizeau J, Moran RJ, Friston KJ. Bayesian model selection for group studies. NeuroImage. 2009 Jul;46(4):1004–17. doi:10.1016/j.neuroimage.2009.03.025

86. Prat CS, Stocco A, Neuhaus E, Kleinhans NM. Basal ganglia impairments in autism spectrum disorder are related to abnormal signal gating to prefrontal cortex. Neuropsychologia. 2016 Oct;91:268–81. doi:10.1016/j.neuropsychologia.2016.08.007

87. Stocco A, Prat CS, Graham LK. Individual Differences in Reward-Based Learning Predict Fluid Reasoning Abilities. Cognitive Science. 2021 Feb;45(2):e12941. doi:10.1111/cogs.12941

88. Friston KJ, Litvak V, Oswal A, Razi A, Stephan KE, Van Wijk BCM, et al. Bayesian model reduction and empirical Bayes for group (DCM) studies. NeuroImage. 2016 Mar;128:413–31. doi:10.1016/j.neuroimage.2015.11.015

89. Zeidman P, Jafarian A, Corbin N, Seghier ML, Razi A, Price CJ, et al. A guide to group effective connectivity analysis, part 1: First level analysis with DCM for fMRI. NeuroImage. 2019 Oct;200:174–90. doi:10.1016/j.neuroimage.2019.06.031

90. Zeidman P, Jafarian A, Seghier ML, Litvak V, Cagnan H, Price CJ, et al. A guide to group effective connectivity analysis, part 2: Second level analysis with PEB. NeuroImage. 2019 Oct;200:12–25. doi:10.1016/j.neuroimage.2019.06.032

91. Baas D, Aleman A, Kahn RS. Lateralization of amygdala activation: a systematic review of functional neuroimaging studies. Brain Research Reviews. 2004 May;45(2):96–103. doi:10.1016/j.brainresrev.2004.02.004

92. Gläscher J, Adolphs R. Processing of the Arousal of Subliminal and Supraliminal Emotional Stimuli by the Human Amygdala. J Neurosci. 2003 Nov 12;23(32):10274–82. doi:10.1523/JNEUROSCI.23-32-10274.2003

93. Wright CI, Fischer H, Whalen PJ, McInerney SC, Shin LM, Rauch SL. Differential prefrontal cortex and amygdala habituation to repeatedly presented emotional stimuli: Neuroreport. 2001 Feb;12(2):379–83. doi:10.1097/00001756-200102120-00039

94. Grace SA, Labuschagne I, Castle DJ, Rossell SL. Intranasal oxytocin alters amygdala-temporal resting-state functional connectivity in body dysmorphic disorder: A double-blind placebo-controlled randomized trial. Psychoneuroendocrinology. 2019 Sep;107:179–86. doi:10.1016/j.psyneuen.2019.05.022

95. Mao Y, Zuo XN, Ding C, Qiu J. OFC and its connectivity with amygdala as predictors for future social anxiety in adolescents. Developmental Cognitive Neuroscience. 2020 Aug;44:100804. doi:10.1016/j.dcn.2020.100804

96. Buhlmann U, McNally RJ, Wilhelm S, Florin I. Selective processing of emotional information in body dysmorphic disorder. Journal of Anxiety Disorders. 2002 Jan;16(3):289–98. doi:10.1016/S0887-6185(02)00100-7

97. Kelly MM, Didie ER, Phillips KA. Personal and appearance-based rejection sensitivity in body dysmorphic disorder. Body Image. 2014 Jun;11(3):260–5. doi:10.1016/j.bodyim.2014.03.004

98. Park LE, Calogero RM, Young AF, Diraddo AM. Appearance-Based Rejection Sensitivity Predicts Body Dysmorphic Disorder Symptoms and Cosmetic Surgery Acceptance. Journal of Social and Clinical Psychology. 2010 May;29(5):489–509. doi:10.1521/jscp.2010.29.5.489

99. Fang A, Baran B, Beatty CC, Mosley J, Feusner JD, Phan KL, et al. Maladaptive self-focused attention and default mode network connectivity: a transdiagnostic investigation across social anxiety and body dysmorphic disorders. Social Cognitive and Affective Neuroscience. 2022 Jul 2;17(7):645–54. doi:10.1093/scan/nsab130

100. Thorsen AL, Hagland P, Radua J, Mataix-Cols D, Kvale G, Hansen B, et al. Emotional Processing in Obsessive-Compulsive Disorder: A Systematic Review and Meta-analysis of 25 Functional Neuroimaging Studies. Biological Psychiatry: Cognitive Neuroscience and Neuroimaging. 2018 Jun;3(6):563–71. doi:10.1016/j.bpsc.2018.01.009

101. Kwon H, Ha M, Choi S, Park S, Jang M, Kim M, et al. Resting-state functional connectivity of amygdala subregions across different symptom subtypes of obsessive–

compulsive disorder patients. NeuroImage: Clinical. 2024;43:103644. doi:10.1016/j.nicl.2024.103644

102. Greenberg JL, Reuman L, Hartmann AS, Kasarskis I, Wilhelm S. Visual hot spots: An eye tracking study of attention bias in body dysmorphic disorder. Journal of Psychiatric Research. 2014 Oct;57:125–32. doi:10.1016/j.jpsychires.2014.06.015

103. Grocholewski A, Kliem S, Heinrichs N. Selective attention to imagined facial ugliness is specific to body dysmorphic disorder. Body Image. 2012 Mar;9(2):261–9. doi:10.1016/j.bodyim.2012.01.002

104. Kollei I, Horndasch S, Erim Y, Martin A. Visual selective attention in body dysmorphic disorder, bulimia nervosa and healthy controls. Journal of Psychosomatic Research. 2017 Jan;92:26–33. doi:10.1016/j.jpsychores.2016.11.008

105. Aguado L, Serrano-Pedraza I, Rodríguez S, Román FJ. Effects of Spatial Frequency Content on Classification of Face Gender and Expression. Span j psychol. 2010 Nov;13(2):525–37. doi:10.1017/S1138741600002225

106. Dima D, Stephan KE, Roiser JP, Friston KJ, Frangou S. Effective Connectivity during Processing of Facial Affect: Evidence for Multiple Parallel Pathways. J Neurosci. 2011 Oct 5;31(40):14378–85. doi:10.1523/JNEUROSCI.2400-11.2011

107. Herrington JD, Taylor JM, Grupe DW, Curby KM, Schultz RT. Bidirectional communication between amygdala and fusiform gyrus during facial recognition. NeuroImage. 2011 Jun;56(4):2348–55. doi:10.1016/j.neuroimage.2011.03.072

108. Willinger D, Karipidis II, Beltrani S, Di Pietro SV, Sladky R, Walitza S, et al. Valence-Dependent Coupling of Prefrontal-Amygdala Effective Connectivity during Facial Affect

Processing. eNeuro. 2019 Jul;6(4):ENEURO.0079-19.2019. doi:10.1523/ENEURO.0079-19.2019

109. Rosenblatt M, Tejavibulya L, Sun H, Camp CC, Khaitova M, Adkinson BD, et al. Power and reproducibility in the external validation of brain-phenotype predictions. Nat Hum Behav. 2024 Jul 31;8(10):2018–33. doi:10.1038/s41562-024-01931-7

110. Woo CW, Chang LJ, Lindquist MA, Wager TD. Building better biomarkers: brain models in translational neuroimaging. Nat Neurosci. 2017 Mar;20(3):365–77. doi:10.1038/nn.4478

111. Haller SP, Kircanski K, Stoddard J, White LK, Chen G, Sharif-Askary B, et al. Reliability of neural activation and connectivity during implicit face emotion processing in youth. Developmental Cognitive Neuroscience. 2018 Jun;31:67–73. doi:10.1016/j.dcn.2018.03.010

112. Plichta MM, Schwarz AJ, Grimm O, Morgen K, Mier D, Haddad L, et al. Test–retest reliability of evoked BOLD signals from a cognitive–emotive fMRI test battery. NeuroImage. 2012 Apr;60(3):1746–58. doi:10.1016/j.neuroimage.2012.01.129

113. Sauder CL, Hajcak G, Angstadt M, Phan KL. Test-retest reliability of amygdala response to emotional faces. Psychophysiology. 2013 Nov;50(11):1147–56. doi:10.1111/psyp.12129

114. Van Den Bulk BG, Koolschijn PCMP, Meens PHF, Van Lang NDJ, Van Der Wee NJA, Rombouts SARB, et al. How stable is activation in the amygdala and prefrontal cortex in adolescence? A study of emotional face processing across three measurements. Developmental Cognitive Neuroscience. 2013 Apr;4:65–76. doi:10.1016/j.dcn.2012.09.005

115. White LK, Britton JC, Sequeira S, Ronkin EG, Chen G, Bar-Haim Y, et al. Behavioral and neural stability of attention bias to threat in healthy adolescents. NeuroImage. 2016 Aug;136:84–93. doi:10.1016/j.neuroimage.2016.04.058

116. Eskander N, Limbana T, Khan F. Psychiatric Comorbidities and the Risk of Suicide in Obsessive-Compulsive and Body Dysmorphic Disorder. Cureus. 2020 Aug 17. doi:10.7759/cureus.9805

117. Gunstad J, Phillips KA. Axis I comorbidity in body dysmorphic disorder. Comprehensive Psychiatry. 2003 Jul;44(4):270–6. doi:10.1016/S0010-440X(03)00088-9

Supplementary Materials

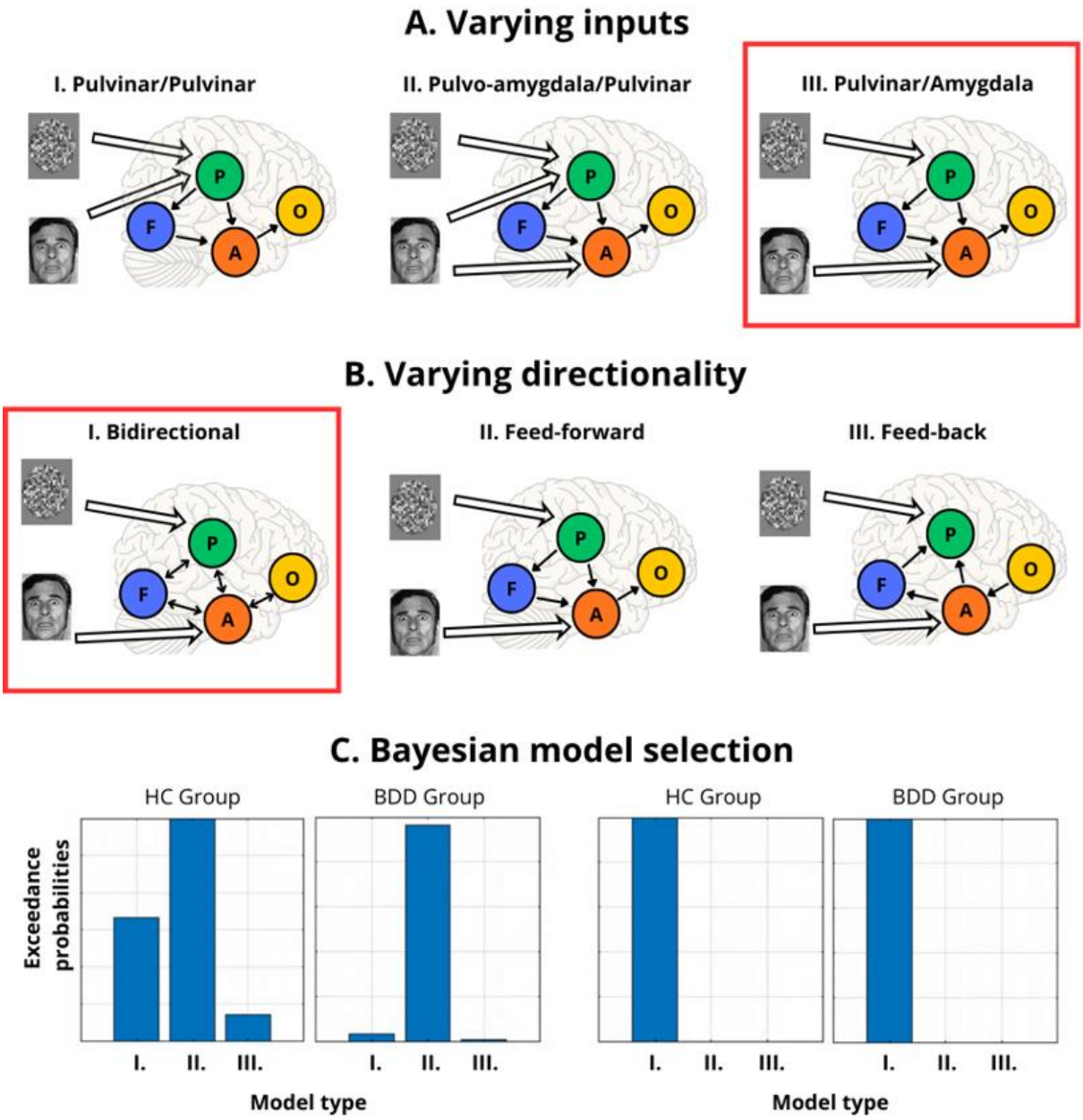


**Supplementary Figure 1.** Depiction of the Bayesian model selection process for models including *a priori* regions of bilateral pulvinar (P), amygdala (A), FFA (F), and mOFC (O) specifically testing A) models of varying stimulus input region and B) models of varying directionality and their C) corresponding exceedance probabilities calculated separately for each

group. We verified that both groups were fit by a model that allowed for stimulus input region to vary based on stimulus type, with fearful faces driving activity in both the bilateral pulvinar and amygdala and scrambled faces driving activity in just the bilateral pulvinar. We took that model structure to test optimal directionality between regions and verified bidirectional connections between all regions as the model with best fit for both groups. FFA = fusiform face area; mOFC = medial orbitofrontal cortex

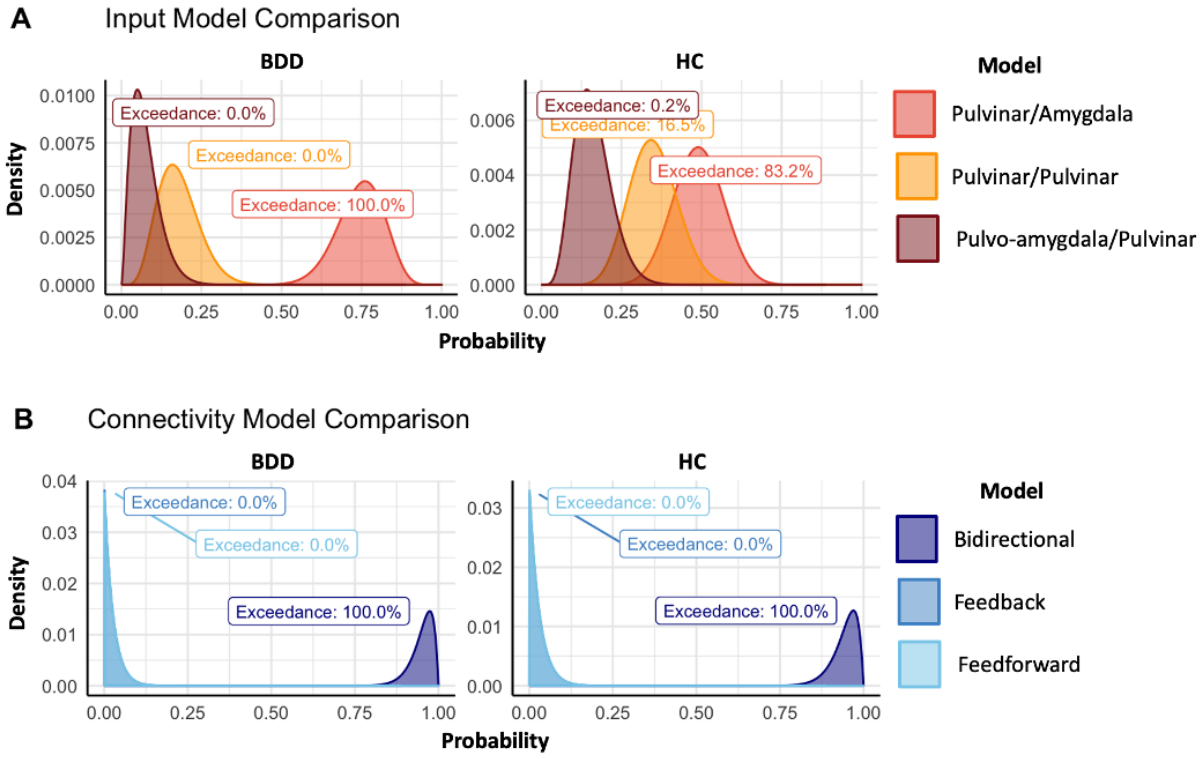


**Supplementary Figure 2.** Depiction of the exceedance probabilities for A) models of varying stimulus input region and B) models of varying directionality in both individuals with BDD (right) and healthy controls (left). The bell curves depicted in the figure represent the estimated densities of the probabilities that a given model would fit an individual in our sample; the areas of all distributions sum up to one. Distributions that are farther to the right imply that the associated model has a greater probability of accurate fit. Exceedance probabilities can be seen

for each distribution on the figure. The pulvinar/amygdala inputs with bidirectional connectivities between each connected node yielded the highest exceedance probabilities in both healthy control and BDD groups.

| **Connectivity** | **BDD (n=32)** Mean (SEM) | **HC (n=37)** Mean (SEM) | **Beta (SE)** | **Pp** |
|---|---|---|---|---|
| Left Amygdala – Left Amygdala | -0.070 (0.019) | -0.061 (0.015) | 0.01 (0.06) | 0.17 |
| Left Amygdala – Left FFA | 0.103 (0.051) | 0.164 (0.033) | -0.06 (0.04) | 0.81 |
| **Left Amygdala – Left mOFC** | 0.241 (0.042) | 0.111 (0.040) | 0.09 (0.04) | **0.96** |
| Left Amygdala – Left Pulvinar | 0.037 (0.039) | 0.003 (0.029) | 0.03 (0.05) | 0.42 |
| Right Amygdala – Right Amygdala | -0.035 (0.019) | -0.061 (0.013) | 0.02 (0.06) | 0.32 |
| Right Amygdala – Right FFA | 0.157 (0.048) | 0.200 (0.040) | -0.04 (0.04) | 0.65 |
| Right Amygdala – Right mOFC | 0.106 (0.049) | 0.087 (0.043) | 0.01 (0.04) | 0.27 |
| **Right Amygdala – Right Pulvinar** | -0.033 (0.031) | 0.050 (0.026) | -0.11 (0.05) | **0.98** |
| Left FFA – Left Amygdala | -0.113 (0.041) | -0.016 (0.034) | -0.03 (0.04) | 0.56 |
| **Left FFA – Left FFA** | -0.193 (0.020) | -0.145 (0.018) | 0.12 (0.06) | **0.96** |
| Left FFA – Left Pulvinar | -0.024 (0.037) | -0.003 (0.038) | -0.02 (0.04) | 0.33 |
| Right FFA – Right Amygdala | -0.044 (0.033) | -0.029 (0.030) | -0.02 (0.05) | 0.30 |
| Right FFA – Right FFA | -0.157 (0.020) | -0.159 (0.015) | -0.004 (0.06) | 0.05 |
| Right FFA – Right Pulvinar | 0.019 (0.037) | 0.013 (0.032) | 0.01 (0.05) | 0.26 |
| Left mOFC – Left Amygdala | 0.080 (0.031) | 0.044 (0.016) | 0.06 (0.05) | 0.75 |
| Left mOFC – Left mOFC | -0.066 (0.014) | -0.058 (0.016) | 0.06 (0.06) | 0.70 |

| | | | | |
|---|---|---|---|---|
| Right mOFC – Right Amygdala | 0.022 (0.023) | 0.047 (0.023) | -0.04 (0.05) | 0.53 |
| Right mOFC – Right mOFC | -0.061 (0.011) | -0.070 (0.016) | 0.04 (0.06) | 0.52 |
| Left Pulvinar – Left Amygdala | 0.040 (0.031) | 0.071 (0.034) | -0.03 (0.04) | 0.48 |
| Left Pulvinar – Left FFA | 0.227 (0.054) | 0.161 (0.054) | 0.05 (0.04) | 0.78 |
| Left Pulvinar – Left Pulvinar | -0.018 (0.018) | -0.053 (0.012) | -0.07 (0.05) | 0.81 |
| Right Pulvinar – Right Amygdala | 0.028 (0.031) | 0.099 (0.032) | -0.05 (0.05) | 0.75 |
| Right Pulvinar – Right FFA | 0.224 (0.047) | 0.192 (0.042) | 0.03 (0.04) | 0.50 |
| Right Pulvinar – Right Pulvinar | -0.033 (0.017) | -0.039 (0.009) | -0.01 (0.05) | 0.10 |

**Supplementary Table 1. Effective connectivity estimates between-group differences.**

Contains statistics (beta and standard error (SE), Posterior probabilities (Pp)) from group comparison using Parametric Empirical Bayes looking at connectivity differences between participants with BDD and healthy controls for each effective connectivity estimate (24 total). Connectivities with $Pp > 0.95$ indicate strong evidence for differences between individuals with BDD and healthy controls.

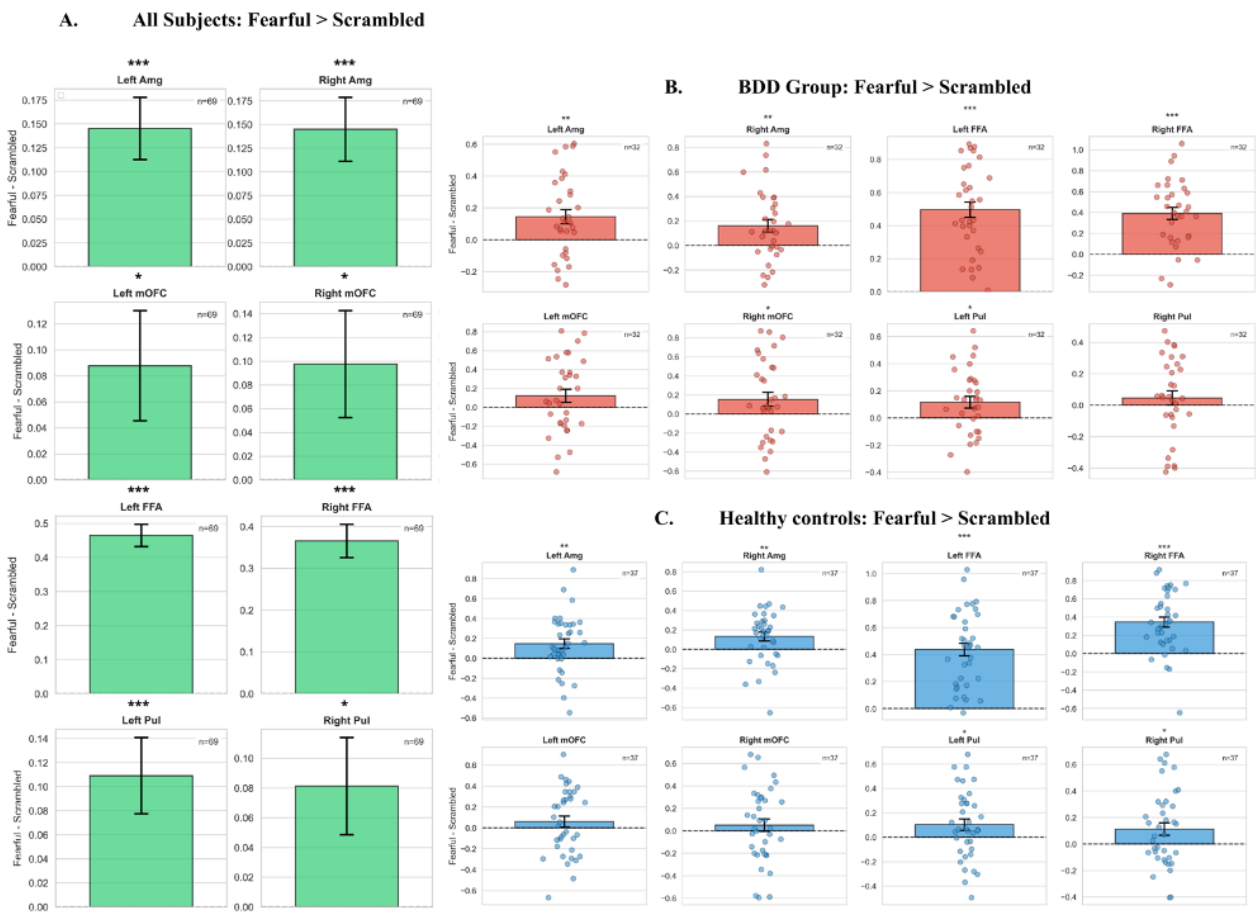


**Supplementary Figure 3.** Second-level GLM estimates of all ROIs used in the effective connectivity analysis A) across all subjects and within B) the BDD group and C) healthy controls. Of note, across all subjects and across all ROIs, participants showed greater fMRI BOLD responses to fearful compared to scrambled stimuli, indicating significant activity in the regions used within the DCM (* uncorrected $p < 0.05$; ** uncorrected $p < 0.01$, ** uncorrected $p < 0.001$).

| **Connectivity** | **All subjects (n=69)** | **BDD (n=32)** Mean (SE) | **HC (n=37)** Mean (SE) | **t-stat (p)** |
|---|---|---|---|---|

| | Mean (SE) | | | |
|---|---|---|---|---|
| Left Amygdala | 0.15 (0.03) | 0.15 (0.05) | 0.14 (0.04) | 4.45 (<0.001) |
| Right Amygdala | 0.14 (0.03) | 0.13 (0.05) | 0.16 (0.05) | 4.30 (<0.001) |
| Left FFA | 0.46 (0.03) | 0.44 (0.05) | 0.50 (0.05) | 14.26 (<0.001) |
| Right FFA | 0.37 (0.04) | 0.34 (0.06) | 0.39 (0.06) | 9.21 (<0.001) |
| Left mOFC | 0.09 (0.04) | 0.06 (0.05) | 0.12 (0.07) | 2.07 (0.04) |
| Right mOFC | 0.10 (0.05) | 0.05 (0.05) | 0.15 (0.07) | 2.16 (0.03) |
| Left Pulvinar | 0.11 (0.03) | 0.10 (0.05) | 0.12 (0.04) | 3.45 (<0.001) |
| Right Pulvinar | 0.08 (0.03) | 0.11 (0.05) | 0.05 (0.05) | 2.49 (0.02) |

**Supplementary Table 2.** Second-level GLM beta estimates of ROIs used in the effective connectivity analysis shown for all subjects as well as within-each group (BDD and HC). Means and standard error (SE) are provided for all subjects combined as well as within-each group. We performed univariate t-tests across all subjects (combined across BDD and HC groups) to confirm non-zero activation across all ROIs; test statistics and p-values are reported. Of note, all p-values are uncorrected.

# Aberrant visual processing in body dysmorphic disorder

Gillian Grennan[1], Scott Murray[1], Angela Fang[1]

1. University of Washington Department of Psychology

**Individuals with BDD display disruptions in visual processing. Specifically, clinical, behavioral, and neuroimaging evidence converge to show that individuals with BDD display an overreliance on high-spatial frequency, or fine-detail image information and an underreliance on low-spatial frequency, or broad image information. Despite this evidence, researchers have yet to investigate whether there is an early visual processing deficit in individuals with BDD. To probe this phenomenon, we recruited individuals with BDD (n=30) and healthy controls (n=30) to participate in a multimodal study probing both early and higher-order visual processing. A psychophysics paradigm measuring contrast sensitivity across a range of spatial frequencies revealed individuals with BDD to show reduced contrast sensitivity to low-spatial frequency. Further, individuals with BDD showed reduced activation in the bilateral middle temporal (MT) region in response to low-spatial frequency stimuli at low contrast, an effect that was significantly associated with behavioral measures of reduced low-spatial frequency contrast sensitivity. While our findings point towards an early visual processing deficit underlying perceptual distortion in BDD, our findings did not correlate with symptom severity in individuals with BDD. Further, we were unable to replicate prior work showing higher-order visual processing deficits in response to images of faces, houses, and bodies. Despite these limitations, our study has pioneered methods to examine aberrant early visual processing in BDD,**

**contributing novel findings of dysfunctional low-spatial frequency processing that could have profound effects on how we understand and treat this disorder.**

# Introduction

BDD is a relatively common and debilitating psychiatric disorder characterized by perceptual dysfunction (American Psychiatric Association 2013; Rück et al. 2024; Grace et al. 2017). BDD is marked by distorted perception of one's physical appearance, particularly facial features such as the skin, hair, or nose; notably these perceived flaws in their appearance are not noticeable to others (American Psychiatric Association 2013). This preoccupation can cause extreme distress and functional impairment (Phillips et al. 2005). BDD is associated with significant morbidity and mortality, with approximately 25% of patients attempting suicide in their lifetime (Phillips 2007; Phillips and Menard 2006). Despite the risks associated with this disorder, research into its neural contributions remains sparse.

Evidence from behavioral, eye-tracking, and neuroimaging studies converge to show abnormalities in visual processing and visuospatial organization that may give rise to these perceptual disturbances. Behaviorally, studies have shown that individuals with BDD display increased performance integrating local/high-detail, or high-spatial frequency, image information, compared to integrating low-spatial frequency, or holistic, image information (Jamie D. Feusner, Moller, et al. 2010). This has been shown in increased discrimination ability during object or facial recognition tasks (Stangier et al. 2008) as well as by selective recall of details compared to global image information (Deckersbach et al., 2000) providing evidence for disturbances in visuospatial integration of holistic information and a prioritization of high-detail information. Neuroimaging studies have confirmed that neural mechanisms underlying visual processing are perturbed in individuals with BDD: when viewing images filtered to selectively convey low-spatial frequency/holistic information, individuals with BDD have shown hypoactivity in early visual processing areas within V1 and V2 compared to healthy controls (HCS) (Jamie D. Feusner,

Moody, et al. 2010; J. D. Feusner et al. 2011; Li et al. 2015), indicating potential processing deficits in low-spatial frequency channels in the primary and secondary visual cortices.

Notably, hypoactivity in early visual cortices such as V1 and V2 and subsequent performance deficits during low-spatial frequency (LSF) image processing have been shown in object stimuli that are not relevant to BDD, such as in response to pictures of houses (Feusner et al., 2011). This pervasiveness of perceptual distortions may reflect a fundamental deficit in integrating LSF information in individuals with BDD. Dysfunction may therefore arise at stages in visual processing prior to object-integration and stimulus-specific attention modulatory mechanisms, indicating deviant low-level/early-stage visual, LSF processing abilities in individuals with BDD compared to HCs.

However, studies of perceptual differences in BDD have focused on late stages of visual processing rather than early visual processing, which leaves open the question of more fundamental perceptual mechanisms that break down in BDD. To date, perceptual processing in BDD has been studied in the context of complex stimuli, such as with faces and/or houses. The visual processing of stimuli such as these are considered high-level within the hierarchy of visual processing (Jennings and Martinovic 2014) and are subject to top-down modulatory influences that can affect cognitive processes. Conversely, low-level visual processes tend to be automatic and resistant to influence by higher-level processes (Firestone and Scholl 2016). Low-level visual processing/psychophysical tasks that utilize primitive images such as Gabor patches (Gaussian-enveloped sinusoidal gratings) minimize opportunities for disorder-specific/stimuli-related interference, such as selective attention to faces, perception of attractiveness of stimuli, or engagement of higher-level brain regions that produce stimulus-specific effects (Firestone & Sholl, 2016; Gabor, 1946). Gabor patches activate the primary visual cortex and varying their spatial

frequencies allow us to directly examine aberrant low-level visual perception (Daugman 1980; Gabor 1946). Characterizing dysfunction at early stages of visual processing could have profound implications for identification of risk markers for BDD, as well as identifying novel treatment targets for standalone or augmentative interventions that mitigate perceptual biases. Despite the implications of this research, no study to date has isolated low-level perceptual processes in individuals with BDD.

There is substantial evidence of perceptual distortion in individuals with BDD, reflected both in neural and behavioral studies showing imbalances in global/local processing. These visual processing imbalances are present in the presentation of stimuli of clinical significance, such as faces or bodies, but notably, persist to even non-appearance-related stimuli, such as houses. Further, individuals with BDD show hypoactivity during LSF image viewing, spanning beyond disorder-relevant stimuli, suggesting further evidence for a general deficit in low- versus high-spatial frequency processing. It is yet to be understood at what stage in the visual processing hierarchy these deficits arise, as no study to date has studied low-level perception in individuals with BDD. Toward this end, we leveraged techniques from basic vision neuroscience to probe low-level spatial frequency processing perturbations in individuals with BDD to understand how functional activity within the visual cortex during low spatial frequency processing relates to clinical and behavioral measures of BDD. Specifically, we hypothesized that individuals with BDD would show reduced sensitivity to low-spatial frequency stimuli in early visual cortices, with these deficits extending to higher-order stimuli. Further, we predicted visual differences will be present at the behavioral level, as evidenced by lower contrast sensitivity to low-spatial frequency stimuli in individuals with BDD. Finally, we hypothesized that aberrant low-spatial frequency processing at the behavioral and neural level would be associated with BDD symptom severity.

# Methods and Materials

## Participants

We recruited participants with BDD (n=32) and healthy controls (n=30); both groups were comprised of young individuals (aged 18-45 years old). The study was approved by the UW Institutional Review Board and all research was performed in accordance with relevant guidelines and regulations. Informed consent from all participants was obtained prior to study procedures. Participants were recruited from the community through flyers in the greater Seattle area. Participants with BDD were excluded if BDD was determined to not be their primary diagnosis, if they met diagnostic criteria for any serious mental illness (SMI) that may confound neural findings such as lifetime psychotic or bipolar disorder, current moderate-severe substance use disorder, and/or if they had active suicidal or homicidal ideation or self-injurious behavior. Two BDD participants were excluded during screening for a lack of primary BDD diagnosis (final BDD n=30).

Participants were excluded if they had a lifetime neurological disorder, current pregnancy, any medical illness that could affect cerebral metabolism or a positive MRI contraindication. Healthy controls were excluded if they had a lifetime psychiatric diagnosis and/or if they were currently taking psychotropic medications. BDD participants were required to be on stable psychoactive medications such as antidepressants or stimulants for ADHD for at least 8 weeks prior to the study. To enhance generalizability, we allowed current DSM-IV diagnoses that fell outside the scope of SMI such as major depression, OCD, panic disorder, generalized anxiety disorder, social anxiety disorder, agoraphobia, ADHD, PTSD, and trichotillomania. Comorbid diagnoses as well as psychotropic medication use in the BDD group can be found in Table 1.

## Measures

**Clinical Measures**. Participants were telephone screened, followed by a clinical interview (performed by either GG or EI). Diagnostic assessments included the Mini International Psychiatric Interview (MINI; (Sheehan et al., 1998)) and the BDD Diagnostic Module based on the DSM-IV. Delusionality in the BDD participants was assessed using the Brown Assessment of Beliefs Scale (BABS; Eisen et al., 1998) and BDD symptom severity was assessed using the Yale-Brown Obsessive Compulsive Scale Modified for BDD (BDD-YBOCS; Phillips et al., 1997). All participants also completed self-report versions of the State-Trait Anxiety Inventory (STAI; Spielberger, 2012), Quick Inventory of Depressive Symptomology (QIDS; Rush et al., 2003) and Body Dysmorphic Disorder Symptom Severity Scale (BDD-SS; Wilhelm et al., 2016).

**Face Inversion Task.** Holistic face processing was assessed using a delayed match-to-sample face inversion task (Farah et al., 1995; Feusner, Moller, et al., 2010; Leder & Bruce, 2000; Valentine, 1988). We used a ViewSonic PH790 CRT monitor (120 Hz) using a chin rest to standardize distance from the screen (66cm). We presented stimuli for this task through Psychopy Version XX (Peirce et al., 2019), which also recorded the response time (RT) and keyboard responses for accuracy calculations. This delayed matching-to-sample task required participants to match a briefly presented target face to one of two subsequently presented probe faces. On each trial, a single target face was presented for either 500ms (short encoding duration) or 5000ms (long encoding duration), followed by a 1000ms blank interstimulus interval and then a probe display for 3000ms containing two faces side by side: the correct match and a morphed foil. Probe faces appeared in either an upright or inverted orientation, yielding four stimulus conditions: upright-short, upright-long, inverted-short, and inverted-long. Participants indicated

their selection using the left or right arrow keys and were instructed to respond as rapidly and accurately as possible. The left/right position of the correct probe was randomized across trials. Conditions were presented block-wise with 28 trials per block; block order was pseudo-randomized across participants. Prior to the experimental blocks, participants completed a set of practice trials to familiarize themselves with the task structure and response mappings. The face inversion effect (FIE) was operationally defined as the mean difference in response time (RT) and accuracy between inverted and upright trials within each encoding duration condition. Slower RTs and lower accuracy for inverted relative to upright faces reflect intact holistic face processing.

**Psychophysics contrast sensitivity task.** We used a ViewSonic PH790 CRT monitor (120 Hz) using a chin rest to standardize distance from the screen (66cm) and Bits# stimulus processor (Cambridge Research Systems, Kent, UK). Stimuli were created and displayed in MATLAB (MathWorks, Natick, MA) and PsychToolbox. Viewing distance for all experiments was 66cm, and luminance was linearized using a PR650 spectrophotometer (Photo Research, Chatsworth, CA). Stimuli were sinusoidally modulated luminance gratings presented on a mean luminance background. Gratings were either oriented to the left or right. Participants were instructed to discriminate the orientation of the briefly presented gratings (whether the top of the lines were pointing to the left or to the right). Contrast sensitivity and was estimated using the quick Contrast Sensitivity Function (qCSF) method (Lesmes, 2010), an adaptive Bayesian procedure that efficiently estimates the full contrast sensitivity function (CSF) across spatial frequencies by selecting stimuli on each trial to maximally reduce uncertainty about the underlying CSF parameters. The stimulus space consisted of 60 contrast levels sampled logarithmically between

0.1% and 100%, and 12 spatial frequency levels sampled logarithmically between 0.25 and 36 cycles per degree (cpd). On each trial, the qCSF algorithm selected the grating contrast and spatial frequency from this 60x12 stimulus space predicted to be most informative given the current posterior distribution over CSF parameters. Each participant completed two runs of the task.

The CSF was parameterized using a four-parameter truncated log-parabola model describing peak gain (range: 2-2000), peak spatial frequency (0.2-20 cpd), bandwidth (1-9 octaves), and low-spatial frequency truncation (0.02-2). The task used a 2-alternative forced-choice design with a guessing rate of 0.50 and an estimated lapse rate of 0.05. Each participant completed 120 experimental trials, after which the qCSF algorithm returned the maximum a posteriori estimates of the four CSF parameters for each participant as well as contrast sensitivity for each spatial frequency. Each participant also completed 10 practice trials prior to beginning the experiment. Given our focus on low-spatial frequency processing, we focused on contrast sensitivity at low-spatial frequency (~1 cpd) and high-spatial frequency (~16 cpd).

**Imaging data acquisition.** Functional MRI data were acquired on a Siemens Prisma 3T scanner with a 64-channel head coil using a T1*weighted EPI sequence (TR=1000ms, TE= 30ms; flip angle = 64; field-of-view= 222mm; in-plane voxel-size = $3mm^3$; Phase partial Fourier = 7/8). A high-resolution anatomical scan was also acquired for coregistration using a T1-weighted 3D magnetization-prepared rf-spoiled rapid gradient-echo (MEMPRAGE) sequence (TR=2530ms; TE=1.69ms; flip angle=7°; field-of-view=256mm; in-plane voxel size=$1mm^3$) with EPI-based volumetric navigators for prospective motion correction and selective reacquisition.

**Spatial-frequency (SF) processing task.** The fMRI measurements were designed to assess individual differences in neural responsiveness to stimuli varying in spatial frequency and contrast within both early and higher-order visual cortex regions. Two versions of the task were administered: a low-level task intended to drive early visual cortex utilizing basic stimuli (gabor patches) and a high-level task intended to drive higher-order visual areas which utilized images of faces, houses, and bodies as the stimuli presented. *Low-level task:* A block-design was used that varied stimulus contrasts (50% and 4%) and spatial-frequencies (1 cycles per degree (cpd) and 16 cpd) across blocks, creating four conditions in a 2x2 factorial design: low-SF/high-contrast, high-SF/high-contrast, low-SF/low-contrast, high-SF/low-contrast). The scans began with fixation block in which only a fixation cross was presented on a mean gray background. Blocks of sinusoidal gratings were then presented centrally in an alternating order, each followed by a fixation block to permit the fMRI response to return to baseline. During a stimulus block, gratings were presented for 400ms followed by a fixation cross for 100ms, lasting for 10 seconds total; each fixation block was 10 seconds. Each run consisted of 4 low-contrast low-SF blocks (4% contrast; 1 cpd), 4 high-contrast low-SF blocks (50% contrast; 1 cpd), 4 low-contrast high-SF blocks (4% contrast; 16 cpd), 4 high-contrast high-SF blocks (50% contrast, 16 cpd). Subjects each completed 3 runs of the experiment, each lasting around 6 minutes. Throughout all blocks in all functional scans, participants were engaged in an oddball detection task in the center of the screen to encourage fixation and maintain engagement and wakefulness; participants were instructed to press a button when the fixation crosshair turned from white to green. Oddballs occurred in 10% of all trials. If a subject had an accuracy hit rate <70% in the oddball task, the

whole run was excluded. *High-level task:* Participants completed a categorical perception task designed to probe visual responses to ecologically relevant visual stimuli varying in spatial frequency content. The task consisted of three functional runs, each lasting around 6 minutes. Stimuli were images from three semantic categories: faces, bodies, and houses. Each stimulus category contained images with no filter applied (normal spatial frequency: NSF), and versions filtered to contain only low-spatial frequency (LSF) or high spatial frequency (HSF), creating a 3x3 factorial design with 9 conditions total. To control for potential order effects, each run presented stimuli from only one category, with category-run order randomized across participants. Within each run, the spatial frequency conditions (NSF, LSF, HSF) for that category were presented in 10-second blocks, with 5 blocks per spatial frequency condition per category. Order of spatial frequency block presentation was randomized across subjects but within each subject kept consistent across the 3 different category runs. As in the low-level task, participants performed an oddball detection task to maintain attention.

**Functional localizer.** To identify higher-level category-selective visual regions for each participant, we administered a functional localizer task following a prior-established protocol (Stigliani et al., 2015). Stimuli consisted of grayscale images drawn from four categories: faces, bodies, houses, and scrambled images. Scrambled images were created by phase-scrambling intact exemplars and served as a visual baseline. Images were presented in a block-design in which participants viewed sequential images from a single category per block; there were 14 trials, or stimulus presentations, per block. To maintain attention and encourage fixation throughout the task, participants performed a one-back repetition detection task, pressing a button whenever the same image appeared twice consecutively. Percent accuracy was calculated

for each subject; all subjects performed the task with high accuracy (all accuracy > 91.5%). Each category was presented across three blocks and block order was pseudo-randomized with order consistent across subjects. Participants completed one run which lasted around 5 minutes.

## Data preparation

**fMRI data preprocessing.** Results included in this manuscript come from preprocessing performed using rMRIPrep version 20.2.0(Esteban et al. 2019), a Nipype based tool (K. Gorgolewski et al. 2011; K. J. Gorgolewski et al. 2017). Each T1w (T1-weighted) volume was corrected for INU (intensity non-uniformity) using N4BiasFieldCorrection v2.1.0 (Tustison et al. 2010) and skull-stripped using antsBrainExtraction.sh v2.1.0 (using the OASIS template). Brain surfaces were reconstructed using recon-all from FreeSurfer v6.0.1(Dale et al. 1999), and the brain mask estimated previously was refined with a custom variation of the method to reconcile ANTs-derived and FreeSurfer-derived segmentations of the cortical gray-matter of Mindboggle (Klein et al. 2017). Spatial normalization to the ICBM 152 Nonlinear Asymmetrical template version 2009c (Fonov et al. 2009) was performed through nonlinear registration with the antsRegistration tool of ANTs v2.1.0 (Avants et al. 2008), using brain-extracted versions of both T1w volume and template. Brain tissue segmentation of cerebrospinal fluid (CSF), white-matter (WM) and gray-matter (GM) was performed on the brain-extracted T1w using FSL v5.0.9 (Zhang et al. 2001). Functional data were slice time corrected using 3dTshift from AFNI v16.2.07 (Cox 1996) and motion corrected using mcflirt (Jenkinson et al. 2002). This was followed by co-registration to the corresponding T1w using boundary-based registration (Greve and Fischl 2009) with six degrees of freedom, using bbregister (FreeSurfer v6.0.1). Motion

correcting transformations, BOLD-to-T1w transformation and T1w-to-template (MNI) warp were concatenated and applied in a single step using antsApplyTransforms (ANTs v2.1.0) using Lanczos interpolation. Physiological noise regressors were extracted applying CompCor (Behzadi et al. 2007). Principal components were estimated for the two CompCor variants: temporal (tCompCor) and anatomical (aCompCor). A mask to exclude signal with cortical origin was obtained by eroding the brain mask, ensuring it only contained subcortical structures. Six tCompCor components were then calculated including only the top 5% variable voxels within that subcortical mask. For aCompCor, six components were calculated within the intersection of the subcortical mask and the union of CSF and WM masks calculated in T1w space, after their projection to the native space of each functional run. Frame-wise displacement (Power et al. 2011) was calculated for each functional run using the implementation of Nipype. Many internal operations of fMRIPrep use Nilearn (Abraham et al. 2014), principally within the BOLD-processing workflow. For more details of the pipeline see https://fmriprep.readthedocs.io/en/20.2.0/workflows.html. All preprocessed outputs were visually inspected to ensure quality, and the summary reports generated by fMRIPrep were reviewed to confirm the accuracy of the preprocessing steps.

**Region of interest (ROI) parcellation.** We isolated regions within regions within both early and higher-level visual cortex to examine differences in visual processing in individuals with BDD. *V1:* To identify visually responsive voxels within the anatomical V1, we performed a retinotopic localizer analysis. A first-level GLM was implemented using Nilearn (Abraham et al., 2014) with the following specifications: a HRF modeled using the SPM canonical HRF, high-pass filtering at 0.01 Hz to remove slow drifts, a drift correction using third-order polynomial

regressors. Confound regression included 24 motion parameters (6 rigid-body parameters, their temporal derivatives, and squared terms), as well as mean signals from white matter and cerebrospinal fluid compartments (with temporal derivatives and squared terms). The retinotopic localizer contrast summed activity across all four experimental conditions within the low-level task (low-SF/high-contrast, high-SF/high-contrast, low-SF/low-contrast, high-SF/low-contrast) to identify voxels responsive to visual stimulation regardless of stimulus properties. The resulting statistical map was thresholded at $z > 2.3$ (uncorrected-$p < 0.01$) to define the functional V1 for each participant. We further masked the functional V1 via an individually-tailored V1 atlas derived using the visual-autolabel package (Ribeiro et al., 2025). This package utilizes a convoluted neural network trained on the Young Adult Human Connectome project (HCP) and the HCP 7 Tesla Retinotopy Dataset to predict the boundaries of the early visual cortex areas such as V1, V2, and V3. The intersection of our individually-tailored anatomical V1 atlas and supra-threshold voxels from the retinotopic localizer defined the final functional V1 ROI for each participant. *Category-selective ROIs:* Category-selective functional ROIs within higher-order visual areas were derived using the functional localizer task (fLoc; Stigliani et al., 2015). All participants performed the task with high accuracy (all accuracies > 91.5%) and therefore all participants were included in functional **ROI extraction.** A first-level GLM was fitted to the preprocessed BOLD time series of the functional localizer task, modeling each stimulus category (faces, bodies, houses, scrambled) as a separate regressor convolved with a canonical HRF, with the same nuisance regressors (32 motion parameters) described above. Functional ROIs were defined individually for each participant using an anatomically constrained peak-activation approach. For each ROI, a bilateral anatomical search space was derived from the Harvard-Oxford Cortical Atlas at 25% probability threshold, 2mm resolution

(Desikan et al., 2006). The search spaces used for each ROI were as follows: For face-selective regions, the fusiform face area (FFA) was localized within the fusiform gyrus (Harvard-Oxford atlas). For body-selective regions, the extrastriatal body area (EBA) was localized within the inferior division of the lateral occipital cortex (Harvard-Oxford atlas). For house or scene-selective regions, the parahippocampal place area (PPA) was localized within the posterior parahippocampal gyrus and (Harvard-Oxford atlas). Within each anatomical search space, the voxel with the peak z-score from the relevant functional contrast was identified separately for the left and right hemispheres. ROIs were then defined as 8mm radius spheres centered on each hemispheric peak, constrained to remain within the anatomical search region. A minimum of 5 suprathreshold voxels ($z > 2.1$, uncorrected $p < 0.05$) within the search mask was required for an ROI to be defined. This procedure yielded 3 functionally defined ROIs per participant to be used for analysis of the high-level task.

**ROI analyses.** *Low-level task:* For each participant, a GLM was fitted to the preprocessed BOLD time series using nilearn. Each stimulus condition (low-contrast low-SF, high-contrast low-SF, low-contrast high-SF, high-contrast high-SF) were modeled block-wise as separate regressors and then convolved with a canonical hemodynamic response function (HRF). Twenty-four motion parameters (6 rigid-body parameters, their temporal derivatives, and squared terms), as well as mean signals from white matter and cerebrospinal fluid compartments (with temporal derivatives and squared terms) were included as nuisance regressors to reduce motion-related signal variance; run-wise intercepts were likewise included to account for drift across runs. Trials with framewise displacement > 0.5mm were removed prior to first-level fitting (1.83%); there were no observed group differences in number of frames excluded for motion (BDD group %

frames removed = 2.22%, HC group % frames removed = 1.40%; $p = 0.70$). Runs with < 80% accuracy on the oddball task were excluded (runs excluded=17, 9.9%). Parameter estimates reflecting average-BOLD response magnitude were extracted for each condition within the V1. *High-level task:* A first-level GLM was similarly fitted to the preprocessed BOLD time series of the high-level task using nilearn. Each of the nine stimulus conditions, corresponding to the factorial combination of stimulus category (faces, bodies, houses) and spatial frequency (NSF, LSF, HSF), was modeled block-wise as separate regressors convolved with a canonical HRF. The same confound regressors described above were included: 24 motion parameters, mean white matter and CSF signals (with temporal derivatives and squared terms), and run-wise intercepts. Trials with framewise displacement > 0.5mm were removed prior to first-level fitting. Runs with < 80% accuracy on the oddball task were excluded. Condition-specific beta estimates were extracted within the category-selective ROIs (see category-selective ROI derivation details above) for use in subsequent group-level analysis. Given that each run presented stimuli from only one stimulus category, run-wise intercepts additionally served to absorb any between-category differences in baseline signal unrelated to the experimental manipulations.

**Whole-brain fMRI.** Whole-brain analyses were conducted in BrainVoyager 22.4 (Brain Innovation, Maastricht). *Low-level:* For each subject*run, a single-study GLM was fit using a design matrix with the four task conditions (low-contrast low-SF, high-contrast low-SF, low-contrast high-SF, high-contrast high-SF) as predictors of interest; task predictors were convolved with a SPM canonical two-gamma hemodynamic response function prior to GLM fitting. Nuisance regressors of the six rigid-body motion parameters, framewise displacement, the top six aCompCor components, all cosine drift regressors, and motion outlier spike regressors were

included in the design matrix as confounds. An ANCOVA random effects analysis was conducted on the combined multi-subject GLM with a between-subjects factor of group (BDD or HC), a within-subjects factor of trial type (low-contrast low-SF, high-contrast low-SF, low-contrast high-SF, high-contrast high-SF), as well as a group*condition interaction; a random intercept of run/subject was also included to account for run-wise variance. *High-level*: We followed identical procedures as for the low-level task (i.e., same nuisance regressors), adapted for the high-level task design. For this task, as each run consisted of a different category (faces, houses, bodies), runs were analyzed separately each with task predictors of the different spatial frequency conditions (NSF, HSF, LSF). An ANCOVA random effects analysis was conducted separately for each run/category on the combined multi-subject GLM with a between-subjects factor of group (BDD or HC), a within-subjects factor of trial type (LSF, NSF, HSF), as well as a group*condition interaction. ANCOVAs for each task yielded omnibus F-tests for the main effects of each factor/interaction with each F-statistic computed voxelwise across the whole brain. Post-hoc targeted hypothesis tests of group and condition differences were conducted using t-tests. For both tasks, whole-brain statistical maps were thresholded at $p<0.001$ uncorrected at the voxel level, then cluster-extent corrected to a family-wise error rate of $p<0.05$ using Monte Carlo simulation as implemented in BrainVoyager's cluster-level statistical threshold estimator (n=1000 iterations). Clusters surviving the resulting minimum cluster-extent threshold were reported.

**Statistical analysis**

All statistical analyses were performed in Python. Linear mixed models (LMMs) were fitted using statsmodels in Python and p-values for fixed effects were estimated using Satterthwaite-

approximated degrees of freedom. The threshold for statistical significance was set at $\alpha = 0.05$. Where normality of residuals was violated (assessed via Q-Q plot inspection and Shapiro-Wilk test), outcomes were log-transformed prior to analysis. Multiple comparisons were corrected using the false-discovery rate (FDR) procedure (Benjamini and Hochberg, 1995) unless otherwise specified.

**Behavioral analyses.** *Face inversion task:* Our primary hypothesis concerned differences in the FIE between individuals with BDD and HCs. We applied linear mixed effects models to response times and accuracy, respectively, with a random intercept for subject to account for the correlation induced by obtaining multiple measurements per participant, thereby increasing power to test hypotheses about fixed effects as well as providing flexibility with respect to missing data and complex covariance structures. Models were fit using restricted maximum likelihood (REML) estimation. Response times were analyzed on the log10 scale. Trials with RT beyond 3 standard deviations of the conditioned mean for each participant were excluded as outliers prior to analysis (2.93% of trials excluded). Accuracy was analyzed using a linear probability model applied to trial-level binary outcomes. To test the hypotheses of interest, the models fit separate means to each condition (group, orientation, encoding duration). A fixed effect of within-session trial number (standardized within subjects) was included in all models to account for learning/practice effects across the experiment. Effect sizes are reported as unstandardized regression coefficients ($\beta$) with a 95% confidence interval. *Psychophysics contrast sensitivity task:* Contrast sensitivity was measured across 12 spatial frequencies (0.25, 0.39, 0.62, 0.97, 1.52, 2.39, 3.76, 5.91, 9.28, 14.58, 22.91, 36 cpd). Where participants completed two runs (n=57/60 participants), contrast sensitivity values for each spatial frequency

were averaged across sessions prior to analysis to reduce measurement noise. Test-retest reliability across runs was assessed using pearson correlations and intraclass correlation coefficients (ICC) at each spatial frequency prior to averaging (ICC across spatial frequencies = 0.08-0.71) To identify participants with anomalous run-to-run variability, we computed each participant's mean absolute difference between sessions across all spatial frequencies. Participants with both runs available whose mean absolute difference exceeded the 75$^{th}$ percentile plus 1.5 times the interquartile range of this distribution were excluded from all analyses (n=3/60, 5.0%); participants with only a single run were retained regardless of their values. Group differences in contrast sensitivity (BDD vs. HC) were examined using separate linear mixed models (LMMs) at each spatial frequency (12 models total). In each model, run-averaged contrast sensitivity served as the outcome variable, patient group was entered as a fixed effect, and participant was included as a random intercept to account for between-subject variance. Models were estimated using restricted maximum likelihood (REML). Group fixed effects for each model were corrected using FDR to account for comparisons across the multiple tests. Effect sizes are reported as unstandardized regression coefficients ($\beta$) with a 95% confidence interval.

**fMRI group-level analyses.** *Low-level task:* To examine group differences in early visual cortex responses to spatial frequency and contrast, V1 beta estimates were entered as the outcome variable in an LMM with spatial frequency (low- versus high-spatial frequency), contrast (low versus high contrast), and group (BDD, HC) as fixed effects, along with all two- and three-way interactions. Participant was included as a random intercept to account for the repeated-measures structure of the data. A significant group x spatial frequency interaction would indicate that BDD

and HC participants differ in their early visual cortex sensitivity to spatial frequency content, independent of contrast. Significant interactions involving group were followed up with pairwise t-tests with FDR correction for multiple comparisons. *High-level task:* To examine group differences in higher-order visual cortex responses to spatial frequency content across stimulus categories, beta estimates from each category-selective ROI (FFA, EBA, PPA) as well as the V1 were analyzed in separate LMMs. Each model included spatial frequency (NSF, LSF, HSF), category (faces, bodies, houses), and group (BDD, HC) as fixed effects, along with all two- and three-way interactions, with participant as a random intercept. Analyses were conducted separately for each ROI to preserve the specificity of category-selective responses; FDR-correction was applied across ROIs to account for the multiple tests. A significant group x SF interaction within a given ROI would indicate that the BDD participants show atypical SF-tuned responses in that region. Significant interactions were decomposed by condition/group and followed up with pairwise contrasts with FDR correction.

**Associations with behavioral and clinical measures.** To examine relationships between neural and behavioral outcomes of contrast sensitivity, Pearson correlations were conducted across all participants to test associations between areas responsible for low-spatial frequency processing in the brain (derived from the low-level fMRI task) and behavioral measures of contrast sensitivity to low-spatial frequency stimuli (derived from the psychophysics behavioral task). Correlations were conducted across all participants as well as separately between groups. Further, to examine the relationships between measures of low-spatial frequency processing and clinical symptoms, Pearson correlations were conducted within the BDD group only, to examine relationships between 1) behavioral measures of contrast sensitivity to low-spatial frequency

stimuli and 2) neural measures of contrast sensitivity to low-spatial frequency stimuli with symptom severity measures. Symptom severity measures included both the clinician-rated BDD-YBOCS and BABS scales.

# Results

## Demographics

| Characteristic | BDD group (n = 30) | Control group (n = 30) | P-value |
|---|---|---|---|
| Age | 24.57 ± 5.66 | 23.14 ± 4.53 | 0.29 |
| Gender (n, %) | | | 0.71 |
| Women | 21 (70.0) | 21 (70.0) | |
| Men | 7 (23.33) | 7 (23.33) | |
| Non-binary/trans | 2 (6.67) | 2 (6.67) | |
| Sex at birth (n, %) | | | 0.61 |
| Female | 21 (70.0) | 23 (76.67) | |
| Male | 9 (30.0) | 7 (23.33) | |
| Race/ethnicity (n, %) | | | 0.40 |
| Asian | 11 (36.67) | 11 (36.67) | |
| African American/Black | 0 (0.0) | 0 (0.0) | |
| Hispanic | 2 (6.67) | 2 (6.67) | |

| | | | |
|---|---|---|---|
| Mixed race | 0 (0.0) | 2 (6.67) | |
| Native American | 2 (6.67) | 0 (0.0) | |
| White | 15 (50.0) | 15 (50.0) | |
| Education (years) | | | 0.53 |
| BDD-SS | 33.30 ± 10.31 | 2.22 ± 2.24 | **<0.0001** |
| QIDS | 11.07 ± 6.11 | 3.41 ± 3.36 | **<0.0001** |
| STAI | 56.23 ± 10.64 | 29.04 ± 7.92 | **<0.0001** |
| BDD-YBOCS | 28.67 ± 0.79 | NA | - |
| BABS | 14.97 ± 0.88 | NA | - |
| Comorbid diagnoses (n, %) | | | - |
| Major depressive disorder | 11 (36.67%) | | |
| Social anxiety disorder | 10 (33.33%) | | |
| OCD | 7 (23.33%) | | |
| Generalized anxiety disorder | 7 (23.33%) | | |
| Panic disorder | 2 (6.67%) | | |
| PTSD | 1 (3.33%) | | |
| Illness anxiety disorder | 1 (3.33%) | | |
| Trichotillomania | 1 (3.33%) | | |
| Medications (n, %) | | | |

| | | | |
|---|---|---|---|
| Bupropion | 2 (6.67%) | | |
| Escitalopram | 1 (3.33%) | | |
| Venlafaxine | 1 (3.33%) | | |
| Fluvoxamine | 1 (3.33%) | | |
| Aripiprazole | 1 (3.33%) | | |
| Viloxazine | 1 (3.33%) | | |
| Amphetamine/Dextroamphetamine | 1 (3.33%) | | |

**Table 1. Demographic and clinical characteristics of the sample.** P-values are derived from between-groups t-tests or chi-square. Comorbidities of the BDD group are also listed here. To enhance generalizability, we allowed current DSM-IV diagnoses of major depression, social anxiety disorder, OCD, generalized anxiety disorder, panic disorder, PTSD, illness anxiety disorder, and trichotillomania. Of note, 22/30 (73.33%) participants in the BDD group were assessed as having a comorbid diagnosis; 12/30 (40.0%) of participants in the BDD group had at least 2 comorbidities. Medications on a stable dose for at least 8 weeks prior to study procedures were also allowed. Specifically, medications used to treat anxiety, depression, OCD, or ADHD symptoms were allowed to increase generalizability; 6/30 (20.0%) participants reported medication use with 2/30 (6.67%) taking two medications.

## Behavioral results

**Face inversion task.** Both groups showed a robust face inversion effect across both encoding duration conditions, evidenced by slower RTs and reduced accuracy in response to inverted compared to upright trials. In the RT model, participants across groups responded slower when the stimuli were inverted versus upright (all $p < 0.001$, see Table 3). Across groups, the FIE was significant for both the long encoding ($\beta = 0.07 \pm 0.01$, $p < 0.001$) and short encoding ($\beta = 0.05 \pm 0.01$, $p < 0.001$), corresponding to approximately 18% and 12% slower responses for inverted versus upright trials, respectively. The accuracy model likewise showed significantly lower accuracy for inverted versus upright trials across groups and encoding durations (all $p < 0.001$).

Of note, we observed a significant learning/practice effect in the RT model as evidenced by faster RT across the sessions ($\beta$ = -0.05 $\pm$ 0.01, $p < 0.001$); no learning/practice effect was evident in the accuracy model ($p = 0.58$). Across both RT and accuracy, we found that encoding duration significantly modulated the magnitude of the face inversion effect. Collapsed across groups, the FIE was significantly larger following long versus short encoding for both RT ($\beta$ = 0.02 $\pm$ 0.01, $p = 0.01$) and accuracy ($\beta$ = 0.05 $\pm$ 0.02, $p = 0.001$), replicating the established finding that holistic face processing is enhanced with longer encoding time (Feusner et al., 2010). Of note, we observed a marginal three-way interaction of encoding duration*group*orientation ($\beta$ = -0.03 $\pm$ 0.01, $p = 0.06$), driven by increased FIE in the short encoding condition in the BDD group compared to HCs (HC-BDD $\Delta$ = 0.02, 95% CI [-0.07, 0.11]) and reduced FIE in the long encoding duration in BDD versus HCs (HC-BDD $\Delta$ = -0.03, 95% CI [-0.12, 0.05]). Given this, we explored group differences within each encoding duration separately. Our primary hypothesis was that individuals with BDD would show a reduced FIE relative to HCs. We did not observe a significant group*orientation interaction within either encoding duration within the accuracy model (both $p > 0.14$), however controls showed smaller odds ratio, or larger FIE, compared to BDD during long encoding trials (see Table 4). Of note, the group*orientation interaction was marginal within the long encoding duration in the RT model (Figure 1B; $\beta$ = -0.02 $\pm$ 0.01, $p = 0.08$) but was not significant in the short encoding condition ($p = 0.37$).

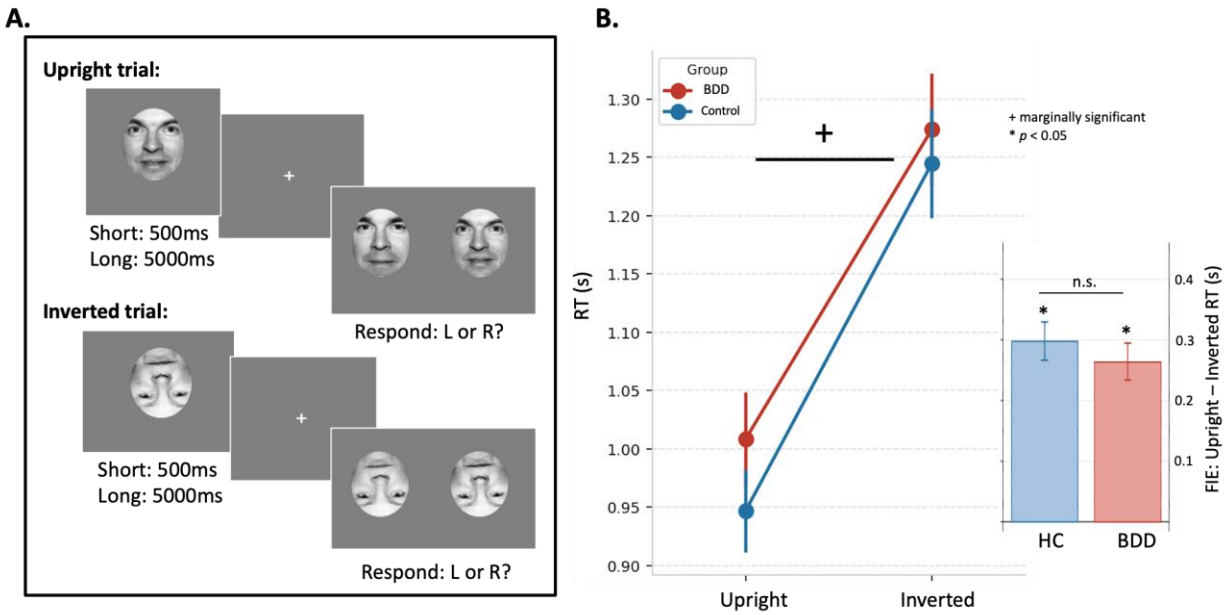


**Figure 1.** A) Face inversion task depiction. The task included both upright and inverted trials each with short (500ms) and long (5000ms) target encoding duration conditions. B) Reaction times (in seconds) for both upright and inverted trials in individuals with BDD (red) versus HCs (blue) during the long (5000ms) target encoding duration. We observed significant face inversion effects (FIEs) across both groups (see bar graph). Of note, we observed a marginal group*orientation interaction, driven by trending higher reaction times in the BDD group compared to controls during upright trials.

| Group | Orientation | Encoding | RT (s) | Accuracy |
|---|---|---|---|---|
| Control | Upright | Long | 0.95 ± 0.34 | 0.97 ± 0.18 |
| | Upright | Short | 0.91 ± 0.31 | 0.92 ± 0.28 |
| | Inverted | Long | 1.24 ± 0.50 | 0.90 ± 0.30 |
| | Inverted | Short | 1.11 ± 0.42 | 0.79 ± 0.41 |
| Patient | Upright | Long | 1.01 ± 0.39 | 0.96 ± 0.19 |
| | Upright | Short | 0.94 ± 0.35 | 0.93 ± 0.26 |
| | Inverted | Long | 1.27 ± 0.51 | 0.91 ± 0.29 |

| | | | | |
|---|---|---|---|---|
| | Inverted | Short | 1.17 ± 0.44 | 0.83 ± 0.37 |

**Table 2.** Mean response times (RTs) in seconds and accuracy (proportion correct) by group, orientation, and encoding duration. RT includes all trials after ± 3 SD outlier removal.

| | Estimated % change | Estimated log change | Std error (log scale) | p-value |
|---|---|---|---|---|
| **a. Inversion effect** | | | | |
| BDD 5000 ms | +14% | +.057 | .0088 | <.001 |
| Control 5000 ms | +18% | +.073 | .0088 | <.001 |
| BDD 500 ms | +13% | +.051 | .0089 | <.001 |
| Control 500 ms | +10% | +.043 | .0088 | <.001 |
| **b. Inversion effect contrasts** | | | | |
| BDD – Control during 5000 ms | −4% | −.017 | .0095 | .077 |
| BDD – Control during 500 ms | +2% | +.008 | .0094 | .372 |
| Difference: BDD – Control 5000–500 ms | −6% | −.025 | .0134 | .060 |

**Table 3.** Estimated inversion effects on response times. Across groups and conditions, participants showed a robust FIE, indicated by significantly longer RT on inverted compared to upright trials (all $p < 0.001$). Participants with BDD showed a marginally smaller FIE compared to controls during the long encoding condition ($p = 0.08$).

| | Estimated odds ratio |
|---|---|
| BDD 5000 ms | 0.38 |

| | |
|---|---|
| Control 5000 ms | 0.29 |
| BDD 500 ms | 0.40 |
| Control 500 ms | 0.35 |

**Table 4.** Estimated inversion effects on accuracy. Odds ratios were computed from proportions as [P(correct|inverted) / (1 – (correct|inverted))] / [P(correct|upright) / (1 – P(correct|upright))]/ Values below 1.0 indicate lower odds of a correct response for inverted than upright faces (inversion effect in accuracy). Neither group comparison was statistically significant (all $p >$ 0.14).

**Psychophysics contrast sensitivity task.** Of the 60 participants who completed the contrast sensitivity task, 58 participants completed both test sessions. We excluded 3 participants due to anomalous session-to-session variability (mean absolute inter-session difference > 0.37), leaving a final sample of 57 participants (n=28 HC, n=29 BDD). For participants with both sessions available, contrast sensitivity values were averaged across sessions prior to analysis; the two participants with a single session contributed that session's value directly. LMMs were fitted separately across each of the 12 spatial frequencies with patient group as a fixed effect and participant as a random intercept. Following FDR-correction for comparison across multiple tests, we observed significantly lower contrast sensitivity in BDD participants compared to HCs across low-spatial frequencies (Figure 2: 0.25-1.52 cpd; all FDR-corrected $p < 0.001$). No significant group differences were observed at spatial frequencies above 1.52 cpd (Table 5: all FDR-corrected $p > 0.25$).

| Spatial frequency (cpd) | $\beta \pm$ SE | z | $p$ (raw) | $p$ (FDR) |
|---|---|---|---|---|
| **0.25** | -0.07 ± 0.02 | -4.05 | **<0.0001** | **<0.0001** |
| **0.39** | -0.07 ± 0.01 | -10.88 | **<0.0001** | **<0.0001** |
| **0.62** | -0.06 ± 0.01 | -7.08 | **<0.0001** | **<0.0001** |

| | | | | |
|---|---|---|---|---|
| **0.97** | -0.06 ± 0.01 | -8.21 | **<0.0001** | **<0.0001** |
| **1.52** | -0.05 ± 0.01 | -4.80 | **<0.0001** | **<0.0001** |
| 2.39 | -0.03 ± 0.02 | -1.55 | 0.12 | 0.25 |
| 3.76 | -0.01 ± 0.01 | -1.35 | 0.18 | 0.30 |
| 5.91 | -0.02 ± 0.04 | -0.45 | 0.66 | 0.79 |
| 9.28 | -0.02 ± 0.07 | -0.34 | 0.73 | 0.80 |
| 14.58 | -0.01 ± 0.07 | -0.08 | 0.94 | 0.94 |
| 22.91 | 0.07 ± 0.08 | 0.90 | 0.37 | 0.49 |
| 36 | 0.06 ± 0.06 | 0.91 | 0.36 | 0.49 |

**Table 5. Group differences in contrast sensitivity to varying spatial frequencies.** We tested group differences across the 12 spatial frequencies ranging from 0.25-36 cycles per degree. We found that individuals with BDD show significantly lower contrast sensitivity to low-spatial frequency stimuli (0.25-1.52), an effect that is absent for intermediary-high spatial frequencies.

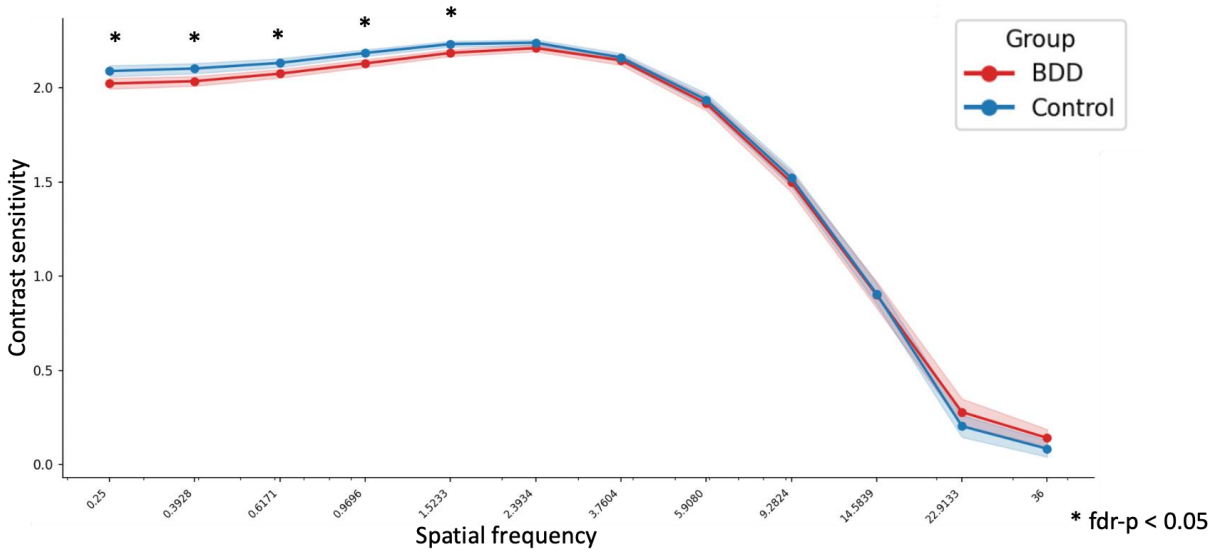


**Figure 2.** Contrast sensitivity task results. Individuals with BDD (in red) showed significantly lower contrast sensitivity to low-spatial frequency stimuli compared to controls (in blue). Specifically, we observed a main effect of group within the spatial frequencies ranging from 0.25-1.52 cycles per degree (cpd) (all fdr-$p$ < 0.001). Of note, this effect was absent in intermediary-high spatial frequencies (2.40–36 cpd).

## fMRI results

**Low-level task.** To first explore underlying spatial frequency processing differences in BDD, we extracted average BOLD activation to all four task conditions (low-contrast low-SF, high-contrast low-SF, low-contrast high-SF, high-contrast high-SF) within individualized ROIs for each subject in the primary visual cortex, or V1 (see ROI parcellation: V1). We hypothesized that individuals with BDD would display lower activation in early visual cortices to low spatial frequency stimuli compared to healthy controls. We explored this using a linear mixed model in which group (BDD vs. HC), spatial frequency (high-SF, low-SF) and contrast (high-contrast, low-contrast) were entered as fixed effects along with all two- and three-way interactions; participant was included as a random intercept to account for repeated measures. As expected, we observed a main effect of contrast across groups and spatial frequency conditions ($\beta$ = -84.46, $p < 0.0001$), driven by higher responses to high-contrast versus low-contrast stimuli (t(59)=14.38, fdr-$p$ <0.0001). Contrary to our hypothesis, we did not observe a significant main effect of group, significant group*spatial frequency interaction, or a group*spatial frequency*contrast interaction (all $p > 0.15$). However, we did observe a significant effect of spatial frequency ($\beta$ = -86.56, $p < 0.0001$), driven by higher responses to high spatial frequency compared to low spatial frequency, across groups and across contrast conditions (t(59)=17.34, fdr-$p$ <0.0001).

As the V1 showed preferential responses to high-spatial frequency stimuli in this paradigm, we expanded our ROI search space to locate regions showing strong responses to low-spatial frequency. We employed a whole-brain multi-subject GLM and found four regions preferentially responding to low- versus high-spatial frequency including the bilateral middle temporal visual area (MT), inferior parietal lobule (IPL), superior frontal gyrus (SFG), and the

V3A; we also confirmed preferential activation in the V1 to high- versus low-spatial frequency stimuli (see Table 6). As these ROIs were defined from a contrast that pooled across both groups, the subsequent between-groups comparison is orthogonal to the contrast that defined the ROIs and therefore does not bias the group test. We reran our ROI analysis including the functionally-derived bilateral MT, IPL, SFG, and V3A, extracting average BOLD-signal within each stimulus condition. Given the stimulus-dependent regional responses, we analyzed low- versus high-spatial frequency processing separately within relevant ROIs testing for differences in responses to low-contrast conditions of the relevant spatial frequency. Within the V1, in which we tested group differences to high-spatial frequency low-contrast, we found that individuals with BDD showed lower responses to high-spatial frequency low-contrast stimuli compared to healthy controls ($t(59) = -2.43$, $p = 0.02$), indicating lower contrast sensitivity to high-spatial frequency stimuli.

Within the low-spatial frequency ROIs (bilateral MT, IPL, SFG, V3A), we tested group differences to low-spatial frequency low-contrast. Notably, we observed significantly reduced activation to low-spatial frequency low-contrast stimuli in individuals with BDD compared to healthy controls within the bilateral MT [Figure 3A: $t(59) = -2.54$, $p = 0.01$]. The directionality and selectivity of the effect to MT specifically is consistent with the predicted impairment in early magnocellular processing. No other ROI showed significant differences between groups (all $p > 0.77$).

| Region (at peak) | Hemi | Peak [x,y,z] | Spatial frequency preference | Peak t | Peak p | Voxels |
|---|---|---|---|---|---|---|

| | | | | | | |
|---|---|---|---|---|---|---|
| hMT+/V5 | R | [49, -68, 7] | LSF > HSF | 6.75 | <0.001 | 3,563 |
| hMT+/V5 | L | [-47, -68, 13] | LSF > HSF | 6.25 | <0.001 | 1,089 |
| Supramarginal gyrus / TPJ | R | [61, -32, 28] | LSF > HSF | 5.23 | <0.001 | 1,433 |
| Precentral gyrus/ frontal eye field | R | [40, -2, 46] | LSF > HSF | 6.93 | <0.001 | 870 |
| V3A | L | [-11, -92, 28] | LSF > HSF | 6.56 | <0.001 | 1,073 |
| Calcarine/V1, Occipital Pole, V2 | B | [13, -98, -2] | HSF > LSF | -11.46 | <0.001 | 30,144 |

**Table 6.** Cluster summary table for whole-brain GLM across subjects. We isolated regions that preferentially respond to either low-spatial frequency (LSF) or high-spatial frequency (HSF) stimuli to test group differences to spatial frequency processing. We observed higher responses to LSF stimuli in the bilateral MT, TPJ, precentral gyrus, and V3A. We observed higher responses to HSF stimuli in the bilateral early visual cortex, identified as the V1 but extends to V2 and extends bilaterally (indicated by the B in the Hemi column).

To test whether bilateral MT activation tracks with individual differences in behavioral contrast sensitivity to low-spatial frequency stimuli, we computed pearson correlations between contrast sensitivity behavioral measures at 1 cycle per degree (to match the spatial frequency used in the fMRI stimuli) and bilateral MT activation to low-spatial frequency high-contrast–low-contrast stimuli. For this contrast, higher differences between high- and low-contrast indicate lower contrast sensitivity, or reduced neural responses to low-contrast stimuli. Across all subjects, we saw a significant association between MT activation and behavioral contrast sensitivity (Figure 3B: r = -0.32, $p$ = 0.01) such that lower behavioral contrast sensitivity correlated with lower contrast sensitivity to low-SF low-contrast stimuli in the MT. Interestingly, this effect was driven by a significant association within the BDD group only (r = -0.41, $p$ = 0.02), an association that was absent in the control group (r = 0.08, $p$ = 0.69).

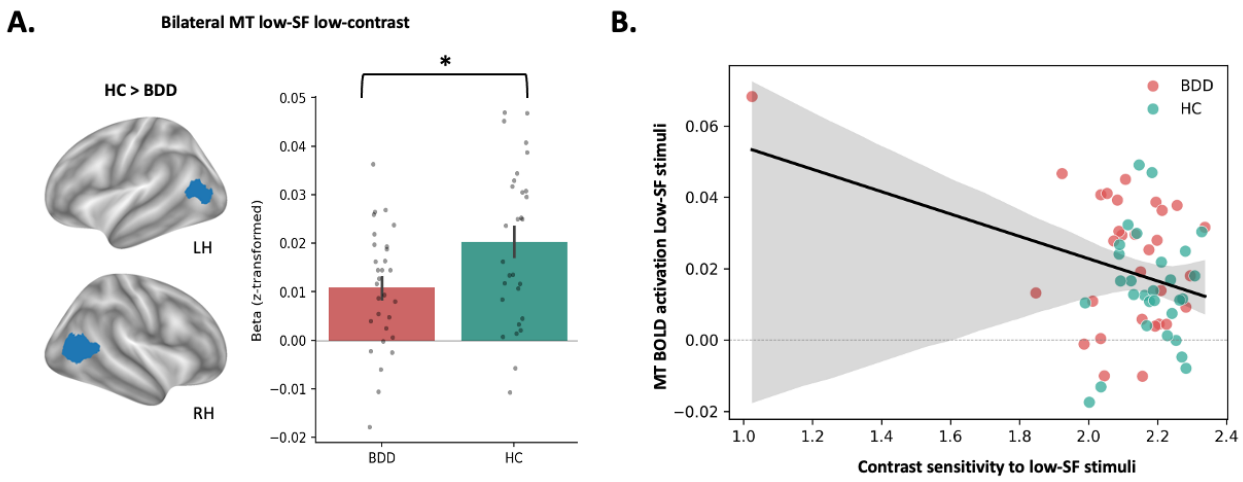


**Figure 3.** A) Individuals with BDD showed lower responses in the bilateral middle temporal area (MT) in response to low-spatial frequency low-contrast stimuli compared to healthy controls ($p$ = 0.01). B) Neural activation to low-SF stimuli in the bilateral MT was significantly correlated with behavioral measures of contrast sensitivity to low-spatial frequency (r = -0.32, $p$ = 0.01).

Within the BDD group, we examined the relationship between aberrant low-spatial frequency processing in the MT and symptom severity, using both the BDD-YBOCS and BABS severity measures. However, no significant correlations emerged with either symptom-severity measure (both $p$ > 0.12).

**High-level task.**

To investigate cortical activation differences to ethnologically-relevant stimuli such as faces, houses, and bodies, we first conducted ROI analyses targeting category-specific visual regions identified by the separate functional localizer (fLoc) task: parahippocampal place area (PPA), fusiform face area (FFA), extrastriate body area (EBA). For each subject, we extracted per-category responses from the individually-derived functional ROIs for the corresponding stimulus category (houses: PPA, faces: FFA, bodies: EBA) as well as in the V1. To test for differential group and spatial frequency activation, within each ROI/category we ran separate

linear mixed models including a main effect of group (BDD vs. control), spatial frequency (low-spatial frequency versus normal; high-spatial frequency versus normal), as well as group*spatial frequency interactions. However, across all stimulus categories, we did not observe any significant main effects of group or spatial frequency, nor interactions between group*spatial frequency in the category-specific ROIs (all $p > 0.16$) or V1 (all $p > 0.14$).

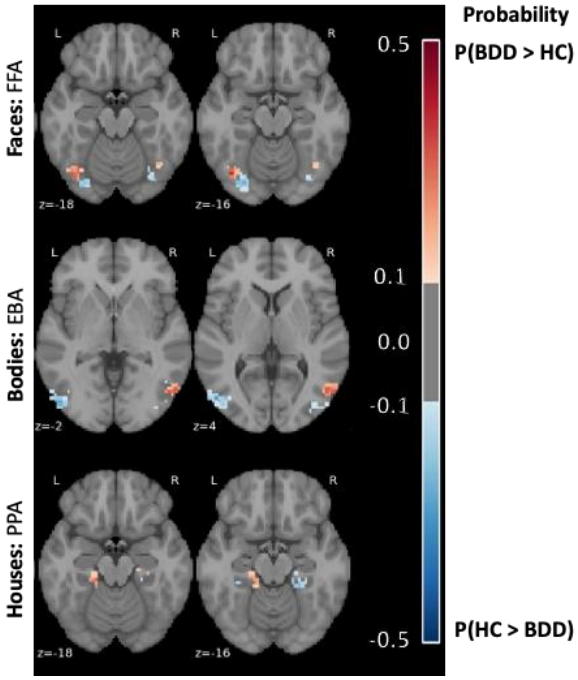


**Figure 4.** Probability map of fLoc-derived category-specific to faces (top), bodies (middle) and houses (bottom). Clusters in red represent areas with higher probability to be activated in individuals with BDD compared to healthy controls while clusters in blue represent areas more likely to be activated in healthy controls. Based on visual inspection of the probability map, there are some group-wise dissociations in the locations and lateralizations of ROIs derived via the functional localizer fLoc task.

However, visual inspection of the localizer-defined ROI locations suggested possible group differences in the spatial localization of category-selective regions themselves rather than in their response amplitude (Figure 4). To assess whether overly individualized ROI definitions

might be masking group-level differences in regional response patterns, we conducted complementary exploratory whole-brain analyses. As described in the methods, we analyzed responses to houses, bodies, and faces separately and all statistical maps were thresholded at $p<0.001$ uncorrected at the voxel level and cluster-corrected to a family-wise error rate of $p<0.05$. Across all three categories, we observed a robust effect of spatial frequency: within the faces condition we observed significantly higher activation to high-spatial frequency images compared to low- and normal images in the primary visual cortex with the significant cluster extending into the FFA (peak-MNI: [16, -92, -2]; $t(59) = 11.81$, $p < 0.0001$; n voxels = 60,272); within the bodies condition we observed the same pattern in the primary visual cortex (peak-MNI: [-11, -101, -2]; $t(59) = 10.25$, $p < 0.0001$; n voxels = 50,681) and the EBA (peak-MNI: [49, -53, -5]; $t(59) = 6.26$, $p < 0.0001$; n voxels = 1,723); and within houses we observed the same effects in the primary visual cortex (peak-MNI: [-14, -95, -2]; $t(59) = 10.33$, $p < 0.0001$; n voxels = 11,911). For each category, we tested our specific hypotheses that differential responses to low-spatial frequency–normal spatial frequency images would be lower in individuals with BDD compared to HCs. However, we did not find significant group differences in low-spatial frequency processing in response to any stimulus category.

## Discussion

In the present study, we examined whether body dysmorphic disorder is associated with altered spatial frequency processing across multiple levels of the visual hierarchy. By combining behavioral psychophysics, a face inversion paradigm, and whole-brain fMRI with both simple and complex visual stimuli, we tested whether previously reported differences in BDD's visual processing reflect deficits in early sensory mechanisms or impaired feedback processing in

response to higher-level category-specific stimulus processing. Notably, we found that at both the level of behavior and neurally, individuals with BDD show an early-stage visual processing deficit in response to low-spatial frequency stimuli, indicating that altered visual perception in BDD may be due to bottom-up sensory processing differences.

Consistent with prior work, we observed a marginally reduced face inversion effect in BDD participants compared to healthy controls (Feusner, Moller, et al., 2010; Jefferies et al., 2012; Monzani et al., 2013). Although the magnitude of this effect was modest, the directionality replicates earlier findings of altered configural face processing and selective recall of fine-detail versus global image information in BDD (Deckersbach et al., 2000; Feusner, Moller, et al., 2010; Hanes, 1998; Jefferies et al., 2012; Monzani et al., 2013).

In the psychophysics behavioral task, participants with BDD exhibited significantly reduced contrast sensitivity for low-SF stimuli compared to healthy controls. This finding contributes a novel, behaviorally measurable index of early visual processing dysfunction in BDD, complementing prior emphases of perceptual deficits to complex stimuli (Feusner et al., 2011; Feusner, Moody, et al., 2010). Prior research has shown an overreliance of high-detail, or high-spatial frequency information and an underutilization to broad image or low-spatial frequency information in individuals with BDD (Feusner et al., 2011; Feusner, Moody, et al., 2010; Grace et al., 2017; Li et al., 2015; Virgili et al., 2024). The present findings extend this literature by suggesting that the local-versus-global imbalance observed in BDD may have an early sensory basis, not solely a top-down attentional one.

The whole-brain fMRI analysis identified bilateral middle temporal area (MT) as a region preferentially responding to low-spatial frequency stimuli across participants. This is consistent with prior work showing preferential tuning to low-spatial frequency stimuli in both humans and

non-human primates (Gaglianese et al., 2023; Lui et al., 2007; Priebe et al., 2006). Within the functionally-defined MT, individuals with BDD showed significantly reduced activation to low-spatial frequency at low-contrast compared to healthy controls. Critically, MT activation to low-spatial frequency was correlated with participant's behavioral contrast sensitivity to low-spatial frequency, such that reduced activation within the MT correlated with lower behavioral contrast sensitivity. This provides functional validation that the neural response in MT reflects perceptually relevant low-spatial frequency processing.

Together, the behavioral and neural findings converge to show that BDD is associated with reduced sensitivity to low-spatial frequency visual input at both the perceptual and neural levels, localized in part to the MT. This provides evidence for a bottom-up visual deficit underlying perceptual imbalances observed in BDD.

Interestingly, we observed a topographical dissociation within early visual processing across subjects with high-spatial frequency stimuli preferentially engaging the primary visual cortex (V1) while low-spatial frequency processing preferentially engaged MT and higher-order regions such as the V3A, inferior parietal lobule, and superior frontal gyrus. This dissociation is consistent with the proposed division of labor between the parvocellular and magnocellular streams, where parvocellular processing remains largely localized to V1 and its immediate cortical neighbors, while magnocellular processing reaches MT through more direct ascending projections (Livingstone & Hubel, 1987; Merigan & Maunsell, 1993). The present findings suggest that BDD's perceptual differences are most pronounced specifically within the magnocellular stream, and future research is needed to fully characterize the deficits underlying BDD within this pathway.

The identification of specific early-visual mechanisms associated with BDD has implications for emerging and current perceptual-retraining interventions (Beilharz et al., 2018; Wilhelm et al., 2013). These programs typically aim to shift patients' attention from local to global features of stimuli, with the implicit assumption that the local-versus-global imbalance is primarily an attentional deficit. The present results suggest that, in addition to such top-down retraining, interventions targeting bottom-up low-spatial frequency processing itself may be useful. For example, training tasks that explicitly require detection or discrimination of low-spatial frequency, could complement existing approaches by addressing the sensory contribution to perceptual bias.

In contrast to the robust low-level effects, we found no significant group differences in category-selective visual areas or in the early visual cortex in response to higher-order stimuli of houses, faces, bodies. Null results were consistent across both ROI-based and exploratory whole-brain analyses. The present design was likely insufficiently powered to detect subtle group differences in category-selective regions. With only 5-blocks per condition per category, individual-level beta estimates have high-within subject noise, and detecting between-group differences requires either substantially more trials or larger sample sizes. The present design was optimized for within-subject spatial-frequency comparisons rather than between-group comparisons which limits inferences about the absence of category-specific effects. In addition, prior reports of category-specific abnormalities in BDD have used designs that emphasize repeated presentation of personally relevant stimuli (i.e., own-face) or emotionally salient categories, both of which may better elicit BDD-specific responses. Taken together, we argue that the absence of category-specific findings is not strong evidence against BDD-related

differences in face/body/scene processing, but rather due to constraints from the present design in its ability to detect differences.

In addition to the design constraints above, several limitations bear mentioning. First, our spatial frequency fMRI manipulation, while well-controlled at the stimulus level, sampled only two spatial frequency levels (1 and 16 cpd). Future studies would benefit from sampling across the full spatial frequency spectrum to fully characterize perceptual differences. Secondly and importantly, both behavioral and neural measures of low-spatial frequency processing did not show significant associations with BDD symptom severity or measures of clinical insight in the BDD group, which complicates a straightforward interpretation of the present findings as a direct neural correlate of BDD pathology. However, observed low-spatial frequency processing differences may represent a trait-level vulnerability factor rather than a state-dependent marker of symptom expression. This pattern, of early sensory differences indexing disorder status but not current severity, has been observed in neurodevelopmental disorders such as autism (Balasco et al., 2020). Further, it is possible that the symptom measures used, while psychometrically sound, may not capture specific symptom dimensions most theoretically linked with perceptual deficits. The BDD-YBOCS (Phillips et al., 1997) aggregates across multiple symptom domains (preoccupation, behaviors, insight, avoidance) and the BABS (Eisen et al., 1998)focuses on belief-related insight; neither was designed to specifically index the perceptual or attentional symptoms that might better relate to early sensory differences. Future studies incorporating perceptually-focused measures may reveal symptom-brain relationships that broader severity measures miss.

The present results converge on a novel account of altered bottom-up low-spatial frequency processing in BDD, supported by findings of reduced contrast sensitivity for low-

spatial frequency stimuli at the behavioral level which was corroborated by reduced activation in the bilateral MT in response to low-spatial frequency stimuli at the neural level. These findings extend our understanding of BDD beyond top-down attentional and emotional accounts of perceptual disturbances, pointing instead to an early-stage sensory contribution that may be a fruitful target for clinical intervention and future research.

# References


Abraham, A., Pedregosa, F., Eickenberg, M., Gervais, P., Mueller, A., Kossaifi, J., Gramfort, A., Thirion, B., & Varoquaux, G. (2014). Machine learning for neuroimaging with scikit-learn. *Frontiers in Neuroinformatics*, *8*. https://doi.org/10.3389/fninf.2014.00014

American Psychiatric Association. (2013). *Diagnostic and Statistical Manual of Mental Disorders* (Fifth Edition). American Psychiatric Association. https://doi.org/10.1176/appi.books.9780890425596

Avants, B., Epstein, C., Grossman, M., & Gee, J. (2008). Symmetric diffeomorphic image registration with cross-correlation: Evaluating automated labeling of elderly and neurodegenerative brain. *Medical Image Analysis*, *12*(1), 26–41. https://doi.org/10.1016/j.media.2007.06.004

Balasco, L., Provenzano, G., & Bozzi, Y. (2020). Sensory Abnormalities in Autism Spectrum Disorders: A Focus on the Tactile Domain, From Genetic Mouse Models to the Clinic. *Frontiers in Psychiatry*, *10*, 1016. https://doi.org/10.3389/fpsyt.2019.01016

Behzadi, Y., Restom, K., Liau, J., & Liu, T. T. (2007). A component based noise correction method (CompCor) for BOLD and perfusion based fMRI. *NeuroImage*, *37*(1), 90–101. https://doi.org/10.1016/j.neuroimage.2007.04.042

Beilharz, F., Castle, D. J., Phillipou, A., & Rossell, S. L. (2018). Visual training program for body dysmorphic disorder: Protocol for a novel intervention pilot and feasibility trial. *Pilot and Feasibility Studies*, *4*(1), 189. https://doi.org/10.1186/s40814-018-0384-3

Cox, R. W. (1996). AFNI: Software for Analysis and Visualization of Functional Magnetic Resonance Neuroimages. *Computers and Biomedical Research*, *29*(3), 162–173. https://doi.org/10.1006/cbmr.1996.0014

Dale, A. M., Fischl, B., & Sereno, M. I. (1999). Cortical Surface-Based Analysis. *NeuroImage*, *9*(2), 179–194. https://doi.org/10.1006/nimg.1998.0395

Daugman, J. G. (1980). Two-dimensional spectral analysis of cortical receptive field profiles. *Vision Research*, *20*(10), 847–856. https://doi.org/10.1016/0042-6989(80)90065-6

Deckersbach, T., Savage, C. R., Phillips, K. A., Wilhelm, S., Buhlmann, U., Rauch, S. L., Baer, L., & Jenike, M. A. (2000). Characteristics of memory dysfunction in body dysmorphic disorder. *Journal of the International Neuropsychological Society*, *6*(6), 673–681. https://doi.org/10.1017/S1355617700666055

Desikan, R. S., Ségonne, F., Fischl, B., Quinn, B. T., Dickerson, B. C., Blacker, D., Buckner, R. L., Dale, A. M., Maguire, R. P., Hyman, B. T., Albert, M. S., & Killiany, R. J. (2006). An automated labeling system for subdividing the human cerebral cortex on MRI scans into gyral based regions of interest. *NeuroImage*, *31*(3), 968–980. https://doi.org/10.1016/j.neuroimage.2006.01.021

Eisen, J. L., Phillips, K. A., Baer, L., Beer, D. A., Atala, K. D., & Rasmussen, S. A. (1998). The Brown Assessment of Beliefs Scale: Reliability and Validity. *American Journal of Psychiatry*, *155*(1), 102–108. https://doi.org/10.1176/ajp.155.1.102

Esteban, O., Markiewicz, C. J., Blair, R. W., Moodie, C. A., Isik, A. I., Erramuzpe, A., Kent, J. D., Goncalves, M., DuPre, E., Snyder, M., Oya, H., Ghosh, S. S., Wright, J., Durnez, J., Poldrack, R. A., & Gorgolewski, K. J. (2019). fMRIPrep: A robust preprocessing pipeline for functional MRI. *Nature Methods*, *16*(1), 111–116. https://doi.org/10.1038/s41592-018-0235-4

Farah, M. J., Wilson, K. D., Maxwell Drain, H., & Tanaka, J. R. (1995). The inverted face inversion effect in prosopagnosia: Evidence for mandatory, face-specific perceptual

mechanisms. *Vision Research*, *35*(14), 2089–2093. https://doi.org/10.1016/0042-6989(94)00273-O

Feusner, J. D., Hembacher, E., Moller, H., & Moody, T. D. (2011). Abnormalities of object visual processing in body dysmorphic disorder. *Psychological Medicine*, *41*(11), 2385–2397. https://doi.org/10.1017/S0033291711000572

Feusner, J. D., Moller, H., Altstein, L., Sugar, C., Bookheimer, S., Yoon, J., & Hembacher, E. (2010). Inverted face processing in body dysmorphic disorder. *Journal of Psychiatric Research*, *44*(15), 1088–1094. https://doi.org/10.1016/j.jpsychires.2010.03.015

Feusner, J. D., Moody, T., Hembacher, E., Townsend, J., McKinley, M., Moller, H., & Bookheimer, S. (2010). Abnormalities of Visual Processing and Frontostriatal Systems in Body Dysmorphic Disorder. *Archives of General Psychiatry*, *67*(2), 197. https://doi.org/10.1001/archgenpsychiatry.2009.190

Feusner, J. D., Townsend, J., Bystritsky, A., & Bookheimer, S. (2007). Visual Information Processing of Faces in Body Dysmorphic Disorder. *Archives of General Psychiatry*, *64*(12), 1417. https://doi.org/10.1001/archpsyc.64.12.1417

Firestone, C., & Scholl, B. J. (2016). Cognition does not affect perception: Evaluating the evidence for "top-down" effects. *Behavioral and Brain Sciences*, *39*, e229. https://doi.org/10.1017/S0140525X15000965

Fonov, V., Evans, A., McKinstry, R., Almli, C., & Collins, D. (2009). Unbiased nonlinear average age-appropriate brain templates from birth to adulthood. *NeuroImage*, *47*, S102. https://doi.org/10.1016/S1053-8119(09)70884-5

Gabor, D. (1946). Theory of communication. Part 1: The analysis of information. *Journal of the Institution of Electrical Engineers - Part III: Radio and Communication Engineering*, *93*(26), 429–441. https://doi.org/10.1049/ji-3-2.1946.0074

Gaglianese, A., Fracasso, A., Fernandes, F. G., Harvey, B., Dumoulin, S. O., & Petridou, N. (2023). Mechanisms of speed encoding in the human middle temporal cortex measured by 7T FMRI. *Human Brain Mapping*, *44*(5), 2050–2061. https://doi.org/10.1002/hbm.26193

Gorgolewski, K., Burns, C. D., Madison, C., Clark, D., Halchenko, Y. O., Waskom, M. L., & Ghosh, S. S. (2011). Nipype: A Flexible, Lightweight and Extensible Neuroimaging Data Processing Framework in Python. *Frontiers in Neuroinformatics*, *5*. https://doi.org/10.3389/fninf.2011.00013

Gorgolewski, K. J., Esteban, O., Ellis, D. G., Notter, M. P., Ziegler, E., Johnson, H., Hamalainen, C., Yvernault, B., Burns, C., Manhães-Savio, A., Jarecka, D., Markiewicz, C. J., Salo, T., Clark, D., Waskom, M., Wong, J., Modat, M., Dewey, B. E., Clark, M. G., … Ghosh, S. (2017). *Nipype: A flexible, lightweight and extensible neuroimaging data processing framework in Python. 0.13.1* (Version 0.13.1) [Computer software]. Zenodo. https://doi.org/10.5281/ZENODO.581704

Grace, S. A., Labuschagne, I., Kaplan, R. A., & Rossell, S. L. (2017). The neurobiology of body dysmorphic disorder: A systematic review and theoretical model. *Neuroscience & Biobehavioral Reviews*, *83*, 83–96. https://doi.org/10.1016/j.neubiorev.2017.10.003

Greenberg, J. L., Weingarden, H., Reuman, L., Abrams, D., Mothi, S. S., & Wilhelm, S. (2018). Set shifting and visuospatial organization deficits in body dysmorphic disorder. *Psychiatry Research*, *260*, 182–186. https://doi.org/10.1016/j.psychres.2017.11.062

Greve, D. N., & Fischl, B. (2009). Accurate and robust brain image alignment using boundary-based registration. *NeuroImage*, *48*(1), 63–72. https://doi.org/10.1016/j.neuroimage.2009.06.060

Hanes, K. R. (1998). Neuropsychological performance in body dysmorphic disorder. *Journal of the International Neuropsychological Society*, *4*(2), 167–171. https://doi.org/10.1017/S1355617798001672

Jefferies, K., Laws, K. R., & Fineberg, N. A. (2012). Superior face recognition in Body Dysmorphic Disorder. *Journal of Obsessive-Compulsive and Related Disorders*, *1*(3), 175–179. https://doi.org/10.1016/j.jocrd.2012.03.002

Jenkinson, M., Bannister, P., Brady, M., & Smith, S. (2002). Improved Optimization for the Robust and Accurate Linear Registration and Motion Correction of Brain Images. *NeuroImage*, *17*(2), 825–841. https://doi.org/10.1006/nimg.2002.1132

Jennings, B. J., & Martinovic, J. (2014). Luminance and color inputs to mid-level and high-level vision. *Journal of Vision*, *14*(2), 9–9. https://doi.org/10.1167/14.2.9

Klein, A., Ghosh, S. S., Bao, F. S., Giard, J., Häme, Y., Stavsky, E., Lee, N., Rossa, B., Reuter, M., Chaibub Neto, E., & Keshavan, A. (2017). Mindboggling morphometry of human brains. *PLOS Computational Biology*, *13*(2), e1005350. https://doi.org/10.1371/journal.pcbi.1005350

Leder, H., & Bruce, V. (2000). When Inverted Faces are Recognized: The Role of Configural Information in Face Recognition. *The Quarterly Journal of Experimental Psychology Section A*, *53*(2), 513–536. https://doi.org/10.1080/713755889

Lesmes, L. A. (2010). Bayesian adaptive estimation of the contrast sensitivity function: The quick CSF method. *Journal of Vision*, *10*(3), 1–21. https://doi.org/10.1167/10.3.17

Li, W., Lai, T. M., Bohon, C., Loo, S. K., McCurdy, D., Strober, M., Bookheimer, S., & Feusner, J. (2015). Anorexia nervosa and body dysmorphic disorder are associated with abnormalities in processing visual information. *Psychological Medicine*, *45*(10), 2111–2122. https://doi.org/10.1017/S0033291715000045

Livingstone, M., & Hubel, D. (1987). Psychophysical evidence for separate channels for the perception of form, color, movement, and depth. *The Journal of Neuroscience*, *7*(11), 3416–3468. https://doi.org/10.1523/JNEUROSCI.07-11-03416.1987

Lui, L. L., Bourne, J. A., & Rosa, M. G. P. (2007). Spatial and temporal frequency selectivity of neurons in the middle temporal visual area of new world monkeys ( *Callithrix jacchus* ). *European Journal of Neuroscience*, *25*(6), 1780–1792. https://doi.org/10.1111/j.1460-9568.2007.05453.x

Merigan, W. H., & Maunsell, J. H. R. (1993). How Parallel are the Primate Visual Pathways? *Annual Review of Neuroscience*, *16*(1), 369–402. https://doi.org/10.1146/annurev.ne.16.030193.002101

Monzani, B., Krebs, G., Anson, M., Veale, D., & Mataix-Cols, D. (2013). Holistic versus detailed visual processing in body dysmorphic disorder: Testing the inversion, composite and global precedence effects. *Psychiatry Research*, *210*(3), 994–999. https://doi.org/10.1016/j.psychres.2013.08.009

Peirce, J., Gray, J. R., Simpson, S., MacAskill, M., Höchenberger, R., Sogo, H., Kastman, E., & Lindeløv, J. K. (2019). PsychoPy2: Experiments in behavior made easy. *Behavior Research Methods*, *51*(1), 195–203. https://doi.org/10.3758/s13428-018-01193-y

Phillips, K. A. (2007). Suicidality in Body Dysmorphic Disorder. *Primary Psychiatry*, *14*(12), 58–66.

Phillips, K. A., Hollander, E., Rasmussen, S. A., Aronowitz, B. R., DeCaria, C., & Goodman, W. K. (1997). A severity rating scale for body dysmorphic disorder: Development, reliability, and validity of a modified version of the Yale-Brown Obsessive Compulsive Scale. *Psychopharmacology Bulletin*, *33*(1), 17–22.

Phillips, K. A., & Menard, W. (2006). Suicidality in Body Dysmorphic Disorder: A Prospective Study. *American Journal of Psychiatry*, *163*(7), 1280–1282. https://doi.org/10.1176/ajp.2006.163.7.1280

Phillips, K. A., Menard, W., Fay, C., & Weisberg, R. (2005). Demographic Characteristics, Phenomenology, Comorbidity, and Family History in 200 Individuals With Body Dysmorphic Disorder. *Psychosomatics*, *46*(4), 317–325. https://doi.org/10.1176/appi.psy.46.4.317

Power, J. D., Cohen, A. L., Nelson, S. M., Wig, G. S., Barnes, K. A., Church, J. A., Vogel, A. C., Laumann, T. O., Miezin, F. M., Schlaggar, B. L., & Petersen, S. E. (2011). Functional Network Organization of the Human Brain. *Neuron*, *72*(4), 665–678. https://doi.org/10.1016/j.neuron.2011.09.006

Priebe, N. J., Lisberger, S. G., & Movshon, J. A. (2006). Tuning for Spatiotemporal Frequency and Speed in Directionally Selective Neurons of Macaque Striate Cortex. *The Journal of Neuroscience*, *26*(11), 2941–2950. https://doi.org/10.1523/JNEUROSCI.3936-05.2006

Ribeiro, F. L., Satzger, R., Hoffstaedter, F., Bürger, C., Herholz, P., Linhardt, D., Benson, N. C., Schwarzkopf, D. S., Puckett, A. M., Bollmann, S., & Hebart, M. N. (2025). *Predicting functional topography of the human visual cortex from cortical anatomy at scale*. https://doi.org/10.1101/2025.11.27.690210

Rück, C., Mataix-Cols, D., Feusner, J. D., Shavitt, R. G., Veale, D., Krebs, G., & Fernández De La Cruz, L. (2024). Body dysmorphic disorder. *Nature Reviews Disease Primers*, *10*(1), 92. https://doi.org/10.1038/s41572-024-00577-z

Rush, A. J., Trivedi, M. H., Ibrahim, H. M., Carmody, T. J., Arnow, B., Klein, D. N., Markowitz, J. C., Ninan, P. T., Kornstein, S., Manber, R., Thase, M. E., Kocsis, J. H., & Keller, M. B. (2003). The 16-Item quick inventory of depressive symptomatology (QIDS), clinician rating (QIDS-C), and self-report (QIDS-SR): A psychometric evaluation in patients with chronic major depression. *Biological Psychiatry*, *54*(5), 573–583. https://doi.org/10.1016/S0006-3223(02)01866-8

Sheehan, D. V., Lecrubier, Y., Sheehan, K. H., Amorim, P., Janavs, J., Weiller, E., Hergueta, T., Baker, R., & Dunbar, G. C. (1998). The Mini-International Neuropsychiatric Interview (M.I.N.I.): The development and validation of a structured diagnostic psychiatric interview for DSM-IV and ICD-10. *The Journal of Clinical Psychiatry*, *59 Suppl 20*, 22-33;quiz 34-57.

Spielberger, C. D. (2012). *State-Trait Anxiety Inventory for Adults* [Dataset]. https://doi.org/10.1037/t06496-000

Stangier, U., Adam-Schwebe, S., Müller, T., & Wolter, M. (2008). Discrimination of facial appearance stimuli in body dysmorphic disorder. *Journal of Abnormal Psychology*, *117*(2), 435–443. https://doi.org/10.1037/0021-843X.117.2.435

Stigliani, A., Weiner, K. S., & Grill-Spector, K. (2015). Temporal Processing Capacity in High-Level Visual Cortex Is Domain Specific. *Journal of Neuroscience*, *35*(36), 12412–12424. https://doi.org/10.1523/JNEUROSCI.4822-14.2015

Tustison, N. J., Avants, B. B., Cook, P. A., Yuanjie Zheng, Egan, A., Yushkevich, P. A., & Gee, J. C. (2010). N4ITK: Improved N3 Bias Correction. *IEEE Transactions on Medical Imaging*, *29*(6), 1310–1320. https://doi.org/10.1109/TMI.2010.2046908

Valentine, T. (1988). Upside-down faces: A review of the effect of inversion upon face recognition. *British Journal of Psychology*, *79*(4), 471–491. https://doi.org/10.1111/j.2044-8295.1988.tb02747.x

Virgili, G., Neill, E., Enticott, P., Castle, D., & Rossell, S. L. (2024). A systematic review of visual processing in body dysmorphic disorder (BDD). *Psychiatry Research*, *339*, 116013. https://doi.org/10.1016/j.psychres.2024.116013

Wilhelm, S., Greenberg, J. L., Rosenfield, E., Kasarskis, I., & Blashill, A. J. (2016). The Body Dysmorphic Disorder Symptom Scale: Development and preliminary validation of a self-report scale of symptom specific dysfunction. *Body Image*, *17*, 82–87. https://doi.org/10.1016/j.bodyim.2016.02.006

Wilhelm, S., Phillips, K. A., & Steketee, G. (2013). *Cognitive-behavioral therapy for body dysmorphic disorder: A treatment manual.* The Guilford Press.

Zhang, Y., Brady, M., & Smith, S. (2001). Segmentation of brain MR images through a hidden Markov random field model and the expectation-maximization algorithm. *IEEE Transactions on Medical Imaging*, *20*(1), 45–57. https://doi.org/10.1109/42.906424

# Conclusion

## 1. Summary of empirical findings

The present dissertation set out to advance the neurobiological model of body dysmorphic disorder (BDD) by investigating three mechanistically distinct but theoretically interrelated neurocognitive processes: the attentional biases that selectively direct processing resources toward threatening cues and their susceptibility to oxytonergic modulation; the effective connectivity architecture of cortical and subcortical networks engaged during fearful face processing; and the low- versus high-level spatial frequency (SF) processing differences that underlie BDD's characteristic perceptual distortions. Across these levels of analysis, the dissertation sought to move beyond phenomenological description toward a mechanistic account of how distorted attention, perception, and threat sensitivity arise and are sustained in this disorder.

### 1.1 Chapter one: attentional bias and oxytocinergic modulation

The first empirical chapter examined attentional biases in BDD using a drift diffusion model (DDM) applied to a Modified Posner Task, allowing decomposition of behavior into latent cognitive parameters. Most critical of these, was the non-decision time parameter t0, which captures attention orienting independently of decision-related processes (Ratcliff & McKoon, 2008). In the placebo condition, a significant group difference in t0 emerged, whereas healthy controls showed a preferential attentional orientation toward neutral relative to disgust stimuli, individuals with BDD displayed the opposite pattern, orienting preferentially toward disgust

faces. This dissociation provides computational evidence that BDD is characterized by attentional bias toward threat-congruent social stimuli. An exploratory finding of lower decisional boundary separation in BDD for disgust versus neutral trials further suggests that individuals with BDD require less information to initiate a response in the presence of disgust cues, a form of decisional impulsivity that warrants further investigation given BDD's elevated rates of suicidal ideation.

Contrary to the a priori hypothesis, intranasal oxytocin did not selectively normalize attentional biases in BDD. Instead, oxytocin produced a main effect across both groups, increasing t0 bias toward disgust faces in both BDD participants and controls. This effect is consistent with emerging evidence that oxytocin may amplify social salience or emotional reactivity regardless of valence rather than selectively attenuating threat responses and that its effects may be context- and population dependent (Bartz et al., 2011; Olff et al., 2013). Although this finding should be interpreted with caution given the small sample size, it converges with prior work in BDD showing that oxytocin did not reduce symptom severity (Fang et al., 2019). The potential relevance of endogenous oxytocin is further highlighted by evidence that serum oxytocin levels are elevated in BDD and associated with symptom severity, suggesting that the oxytocinergic system may already be dysregulated in this population in ways that modulate, and potentially limit, the therapeutic effects of exogenous administration.

### 1.2 Chapter two: effective connectivity in visual fear-processing networks

The second empirical chapter characterized effective connectivity within cortical and subcortical networks engaged during fearful face viewing in BDD using dynamic causal modeling (DCM). We identified higher feedforward connectivity from the left amygdala to the

medial orbitofrontal cortex (mOFC) in BDD relative to controls. The left amygdala's role in detailed stimulus evaluation during sustained arousal, rather than the right amygdala's rapid threat detection, may implicate a secondary-process emotional appraisal deficit in BDD: one in which the ruminative evaluation of socially relevant stimuli, such as threatening facial expressions, is amplified via elevated amygdala-OFC connectivity. We similarly observed reduced connectivity from the right amygdala to the right pulvinar in BDD compared to controls. With the pulvinar's role in integrating multimodal cortical feedback and redirecting processing resources toward salient stimuli (Pessoa & Adolphs, 2010), reduced amygdala-pulvinar feedback may therefore reflect impaired attention modulation in response to threat, potentially contributing to attention dysregulation observed in Chapter one and documented in prior BDD studies (Grace et al., 2017, 2019; Greenberg et al., 2014). Finally, we observed elevated within-region connectivity of the left fusiform face area (FFA) in BDD, converging with prior reports of FFA hyperactivity and consistent with an overreliance on the ventral visual stream for high-detail face processing (Feusner et al., 2007; Li et al., 2015). These circuit-level findings extend and specify the neurobiological model of BDD, localizing the disorder's threat-processing abnormalities within identifiable and potentially modifiable network dynamics.

### 1.3 Chapter three: low-spatial frequency processing deficits and their significance

The third empirical chapter investigated SF processing differences in BDD across behavioral and neural levels, employing psychophysical contrast sensitivity measurement, a face inversion paradigm, and an fMRI paradigm probing both early and higher-order visual processing. A convergent and novel finding emerged across both levels of analysis: individuals with BDD showed reduced sensitivity to low-SF visual information compared to healthy controls. Behaviorally, BDD participants exhibited significantly lower contrast sensitivity for

low-SF stimuli. At the neural level, this was mirrored by reduced bilateral activation in the middle temporal area (MT) in response to low-SF stimuli at low contrast, a region with well-established preferential tuning for LSF input via the magnocellular visual pathway. Critically, MT activation to LSF stimuli was correlated with behavioral contrast sensitivity scores, providing functional validation that the neural response in MT indexes perceptually relevant LSF processing. These findings extend the existing BDD visual processing literature in an important direction. Prior work established that individuals over-rely on high-SF information and underutilize global, low-SF image information (Feusner et al., 2007, 2011; Li et al., 2015). The present results reframe this not solely as an attentional preference for detail but as an early-stage sensory deficit in magnocellular stream processing, a bottom-up contribution to the perceptual imbalance that has previously been attributed to top-down attentional accounts.

## 2. Toward an integrated neurocognitive model of BDD

Considered together, the three empirical chapters converge on a multi-level neurocognitive model of BDD in which bottom-up sensory deficit and dysregulated fear-processing circuit may interact to produce and sustain some of the disorder's defining features. Our findings suggest that at the most fundamental sensory level, BDD is characterized by reduced magnocellular stream sensitivity, which limits processing of global visual information on which accurate appearance judgements and social perception depend.

At the circuit level, the fearful face viewing DCM findings reveal that this perceptual deficit unfolds within a network characterized by heightened amygdala-OFC feedforward drive and reduced amygdala-pulvinar feedback connectivity, a configuration with amplified secondary affective appraisal of threatening social stimuli and impaired attentional reorientation away from

them. Elevated within-FFA connectivity further suggests that the ventral visual stream is over-engaged during face processing in BDD, consistent with the overreliance on high-detail, parvocellular-mediated processing documented throughout this dissertation.

3. Clinical implications

The mechanistic findings of this dissertation carry several implications for BDD treatment. The identification of reduced LSF/magnocellular processing as a bottom-up sensory deficit has direct consequences for how perceptual retraining interventions are conceptualized and delivered. Current perceptual retraining approaches in BDD operate on the implicit assumption that local-versus-global imbalance is primarily top-down attention driven (Beilharz et al., 2018; Wilhelm et al., 2013). However, our findings suggest that this is insufficient and that interventions explicitly targeting bottom-up low-SF detection and discrimination will be a needed complement to existing approaches.

Further, the circuit-level findings from the DCM chapter provide a more precise neurobiological rationale for neuromodulatory interventions such as transcranial magnetic stimulation (TMS) or neurofeedback targeting the amygdala-OFC or amygdala-pulvinar circuit. Heightened amygdala-to-mOFC feedforward connectivity in BDD is a potentially modifiable network parameter, one that in principle could be attenuated through repetitive TMS or through real time neurofeedback training.

## 4. Limitations and future directions

Several limitations across the three chapters merit acknowledgement. All three studies employed relatively modest sample sizes, reflecting the practical challenges of recruiting clinical-BDD samples with additional constraints imposed by pharmacological and neuroimaging protocols. Group differences in all chapters show modest effect sizes and behavioral/neural measures across all three chapters were not significantly associated with BDD symptom severity. Additionally, cross-sectional designs across all three studies preclude causal inference about the developmental trajectory of BDD's neurocognitive profile. Longitudinal studies tracking SF sensitivity, fear network connectivity, and attentional parameters, will be essential for determining whether the identified deficits are antecedent vulnerability factors, state-dependent correlates of active psychopathology, or consequences of chronic symptom burden. Mechanistic treatment studies incorporating pre- and post-CBT neuroimaging and psychophysical assessment, with and without adjunctive pharmacological and neuromodulatory interventions, would directly test the translational application of the present findings. Finally, direct transdiagnostic comparisons, deploying identical paradigms across BDD, OCD, autism spectrum, anorexia nervosa, would constitute a major advance in characterizing the shared and disorder-specific neurocognitive vulnerabilities that contribute to psychopathology across these conditions.

## 5. Concluding remarks

Body dysmorphic disorder remains a relatively severe psychiatric disorder with debilitating effects on patient wellbeing. Its core phenomenology, intrusive, ego-dystonic

preoccupation with appearance driving compulsive behavior and profound functional impairment, has been long recognized but its neurocognitive mechanisms only partially characterized. The present dissertation has advanced this understanding through three empirical contributions that, taken together, delineate a multi-level mechanistic account of the disorder. Taken together, these findings support a model of BDD in which bottom-up sensory impairment, circuit-level dysregulation, and attentional biases form a mutually reinforcing system that may generate and sustain distorted appearance perception. By grounding this model in mechanistic evidence, spanning sensory psychophysics, computational modeling of behavior, and connectivity neuroimaging, this dissertation contributes to a more empirically tractable and therapeutically actionable account of the neurobiology underlying BDD. It is hoped that the elucidation of these mechanisms will help lay the groundwork for the development of more effective and accessible interventions for a disorder that exacts an extraordinary toll on those it affects.

# References


Bartz, J. A., Zaki, J., Bolger, N., & Ochsner, K. N. (2011). Social effects of oxytocin in humans: Context and person matter. *Trends in Cognitive Sciences*, S1364661311000830. https://doi.org/10.1016/j.tics.2011.05.002

Beilharz, F., Castle, D. J., Phillipou, A., & Rossell, S. L. (2018). Visual training program for body dysmorphic disorder: Protocol for a novel intervention pilot and feasibility trial. *Pilot and Feasibility Studies*, *4*(1), 189. https://doi.org/10.1186/s40814-018-0384-3

Fang, A., Lawson, E. A., & Wilhelm, S. (2019). Intranasal oxytocin modulates higher order social cognition in body dysmorphic disorder. *Depression and Anxiety*, *36*(2), 153–161. https://doi.org/10.1002/da.22876

Feusner, J. D., Hembacher, E., Moller, H., & Moody, T. D. (2011). Abnormalities of object visual processing in body dysmorphic disorder. *Psychological Medicine*, *41*(11), 2385–2397. https://doi.org/10.1017/S0033291711000572

Feusner, J. D., Townsend, J., Bystritsky, A., & Bookheimer, S. (2007). Visual Information Processing of Faces in Body Dysmorphic Disorder. *Archives of General Psychiatry*, *64*(12), 1417. https://doi.org/10.1001/archpsyc.64.12.1417

Grace, S. A., Labuschagne, I., Kaplan, R. A., & Rossell, S. L. (2017). The neurobiology of body dysmorphic disorder: A systematic review and theoretical model. *Neuroscience & Biobehavioral Reviews*, *83*, 83–96. https://doi.org/10.1016/j.neubiorev.2017.10.003

Grace, S. A., Toh, W. L., Buchanan, B., Castle, D. J., & Rossell, S. L. (2019). Impaired Recognition of Negative Facial Emotions in Body Dysmorphic Disorder. *Journal of the International Neuropsychological Society*, *25*(08), 884–889. https://doi.org/10.1017/S1355617719000419

Greenberg, J. L., Reuman, L., Hartmann, A. S., Kasarskis, I., & Wilhelm, S. (2014). Visual hot spots: An eye tracking study of attention bias in body dysmorphic disorder. *Journal of Psychiatric Research*, *57*, 125–132. https://doi.org/10.1016/j.jpsychires.2014.06.015

Li, W., Lai, T. M., Bohon, C., Loo, S. K., McCurdy, D., Strober, M., Bookheimer, S., & Feusner, J. (2015). Anorexia nervosa and body dysmorphic disorder are associated with abnormalities in processing visual information. *Psychological Medicine*, *45*(10), 2111–2122. https://doi.org/10.1017/S0033291715000045

Livingstone, M., & Hubel, D. (1987). Psychophysical evidence for separate channels for the perception of form, color, movement, and depth. *The Journal of Neuroscience*, *7*(11), 3416–3468. https://doi.org/10.1523/JNEUROSCI.07-11-03416.1987

Merigan, W. H., & Maunsell, J. H. R. (1993). How Parallel are the Primate Visual Pathways? *Annual Review of Neuroscience*, *16*(1), 369–402. https://doi.org/10.1146/annurev.ne.16.030193.002101

Olff, M., Frijling, J. L., Kubzansky, L. D., Bradley, B., Ellenbogen, M. A., Cardoso, C., Bartz, J. A., Yee, J. R., & Van Zuiden, M. (2013). The role of oxytocin in social bonding, stress regulation and mental health: An update on the moderating effects of context and interindividual differences. *Psychoneuroendocrinology*, *38*(9), 1883–1894. https://doi.org/10.1016/j.psyneuen.2013.06.019

Pessoa, L., & Adolphs, R. (2010). Emotion processing and the amygdala: From a “low road” to “many roads” of evaluating biological significance. *Nature Reviews Neuroscience*, *11*(11), 773–782. https://doi.org/10.1038/nrn2920

Ratcliff, R., & McKoon, G. (2008). The Diffusion Decision Model: Theory and Data for Two-Choice Decision Tasks. *Neural Computation*, *20*(4), 873–922. https://doi.org/10.1162/neco.2008.12-06-420

Wilhelm, S., Phillips, K. A., & Steketee, G. (2013). *Cognitive-behavioral therapy for body dysmorphic disorder: A treatment manual.* The Guilford Press.